UNIVERSIDADE ESTADUAL DE CAMPINAS

INSTITUTO DE QUÍMICA

GISLÁINE CORRÊA DA SILVA

ESTUDO DA INTERAÇÃO ENTRE OS EXTRATOS DA SEMENTE DO MARACUJÁ (PASSIFLORA EDULIS) E DAS PARTES AÉREAS DE JAMBU (SPILANTHES ACMELLA) EM FORMULAÇÕES FOTOPROTETORAS TÓPICAS: ESTABILIDADE E PERMEAÇÃO CUTÂNEA

CAMPINAS
2023

GISLÁINE CORRÊA DA SILVA

ESTUDO DA INTERAÇÃO ENTRE OS EXTRATOS DA SEMENTE DO MARACUJÁ (PASSIFLORA EDULIS) E DAS PARTES AÉREAS DE JAMBU (SPILANTHES ACMELLA) EM FORMULAÇÕES FOTOPROTETORAS TÓPICAS: ESTABILIDADE E PERMEAÇÃO CUTÂNEA

Tese de Doutorado apresentada ao Instituto de Química da Universidade Estadual de Campinas como parte dos requisitos exigidos para a obtenção do título de Doutora em Ciências.

Orientadora: Profa. Dra. Carla Beatriz Grespan Bottoli

Coorientador: Prof. Dr. Rodney Alexandre Ferreira Rodrigues

O arquivo digital corresponde à versão final da Tese defendida pela aluna Gisláine Corrêa da Silva e orientada pela Profa. Dra. Carla Beatriz Grespan Bottoli.

CAMPINAS
2023

Ficha catalográfica
Universidade Estadual de Campinas
Biblioteca do Instituto de Química
Simone Luiz Alves - CRB 8/9094

Si38e

Silva, Gisláine Corrêa da, 1985-
Estudo da interação entre os extratos da semente do maracujá (*Passiflora edulis*) e das partes aéreas de jambu (*Spilanthes acmella*) em formulações fotoprotetoras tópicas : estabilidade e permeação cutânea / Gisláine Corrêa da Silva. – Campinas, SP : [s.n.], 2023.

Orientador: Carla Beatriz Grespan Bottoli.
Coorientador: Rodney Alexandre Ferreira Rodrigues.
Tese (doutorado) – Universidade Estadual de Campinas, Instituto de Química.

1. *Passiflora*. 2. *Spilanthes oleraceae*. 3. Fotoproteção. 4. Cosmetologia. 5. Cromatografia. I. Bottoli, Carla Beatriz Grespan, 1973-. II. Rodrigues, Rodney Alexandre Ferreira, 1964-. III. Universidade Estadual de Campinas. Instituto de Química. IV. Título.

Informações Complementares

Título em outro idioma: The interaction between passion fruit seeds (*Passiflora edulis*) and paracress aerial parts (*Spilanthes acmella*) extracts in topical sunscreen formulations : stability and cutaneous permeation
Palavras-chave em inglês:
Passiflora
Spilanthes oleracea
Photoprotection
Cosmetology
Chromatography
Área de concentração: Química Analítica
Titulação: Doutora em Ciências
Banca examinadora:
Rodney Alexandre Ferreira Rodrigues [Coorientador]
Ivo Milton Raimundo Junior
Alexandra Christine Helena Frankland Sawaya
André Rolim Baby
Verônica Santana de Freitas Blanco
Data de defesa: 05-10-2023
Programa de Pós-Graduação: Química

Identificação e informações acadêmicas do(a) aluno(a)
- ORCID do autor: https://orcid.org/0000-0002-1784-9268
- Currículo Lattes do autor: http://lattes.cnpq.br/0584270844095129

BANCA EXAMINADORA

Prof. Dr. Rodney Alexandre Ferreira Rodrigues (Coorientador)

Prof. Dr. Ivo Milton Raimundo Junior (Universidade Estadual de Campinas)

Prof. Dr. Alexandra Christine Helena Frankland Sawaya (Universidade Estadual de Campinas)

Prof. Dr. Andre Rolim Baby (Univerdidade de São Paulo)

Profa. Dra. Verônica Santana de Freitas Blanco (CRODA)

A Ata da defesa assinada pelos membros da Comissão Examinadora, consta no SIGA/Sistema de Fluxo de Dissertação/Tese e na Secretaria do Programa da Unidade.

Este exemplar corresponde à redação final da Tese de Doutorado defendida pela aluna **GISLÁINE CORRÊA DA SILVA**, aprovada pela Comissão Julgadora em 5 de outubro de 2023.

AGRADECIMENTO

À profa. Dra. Carla Beatriz Grespan Bottoli, do laboratório NovaCrom, pertencente ao Instituto de Química da Universidade Estadual de Campinas (IQ - UNICAMP);

Ao prof. Dr. Rodney Alexandre Ferreira Rodrigues, do Centro Pluridisciplinar de Pesquisas Químicas, Biológicas e Agrícolas da Universidade Estadual de Campinas (CPQBA – UNICAMP);

A Cleber Barros, da empresa Vinia Inovações Cosméticas, pelo estágio concedido;

À prof. Dra. Marcia Cristina Breitkreitz, por ceder espaço à execução deste trabalho no UHPLC-PAD Waters Acquity;

Ao Laboratório Nacional de Nanotecnologia, do Centro Nacional de Pesquisa em Energia e Materiais (LNNano – CNPEM);

Ao apoio técnico de Lucília Vilela de Melo, Paulo Ricardo Garcia, Manuela Sabino e Fabiana Amorim, do IQ – Unicamp, e de Carolina Pirogini Torres, do LNNano – CNPEM;

A todos os colegas de laboratório com os quais convivi e dos quais recebi o suporte necessário durante a realização deste trabalho;

Ao apoio do Instituto Nacional de Ciência e Tecnologia Bioanalítica - Brasil (INCTBio),

E à Fundação de Amparo à Pesquisa do Estado de São Paulo - Brasil (FAPESP) e ao Instituto de Química da Unicamp (IQ – Unicamp) pelo financiamento do equipamento multiusuário LUMiSizer por meio do projeto 2016/13926-7.

O presente trabalho foi realizado com apoio da Fundação de Amparo à Pesquisa do Estado de São Paulo - Brasil (FAPESP) - Códigos de Financiamento 2012/06642-1, 2014/50867-3, 2015/26300-6 e 2018/07234-0.

O presente trabalho também foi realizado com apoio do Conselho Nacional de Desenvolvimento Científico e Tecnológico - Brasil (CNPq) - Código de Financiamento 304415/2013-8, 465389/2014-7 e 311671/2015-2,

Ainda, o presente trabalho foi realizado com apoio da Coordenação de Aperfeiçoamento de Pessoal de Nível Superior – Brasil (CAPES) – Código de Financiamento 001.

RESUMO

Dentre os mais de 8.000 compostos fenólicos vegetais atualmente elucidados, o piceatanol apresenta-se como um potencial candidato a ativo dermocosmético, com propriedades fotoprotetoras e regenerativas da pele demonstradas *in vitro*. Uma fonte relevante de piceatanol é a semente do maracujá (*Passiflora edulis*), atualmente subaproveitada na cadeia agroindustrial desta fruta. A entrega desta molécula às camadas mais profundas da pele, no entanto, é desafiadora: enquanto a administração via oral incorre em intenso metabolismo e *clearance*, a administração tópica encontra, como impeditivo, a própria barreira cutânea. Nesse sentido, moléculas promotoras de permeação podem ser associadas ao piceatanol para auxiliá-lo a difundir para além do estrato córneo, e o espilantol, presente nas partes aéreas de jambu (*Spilanthes acmella*), além da sua reconhecida ação antirrugas, possui esta propriedade. Na proteção da pele contra os efeitos deletérios do ambiente, é fundamental o bloqueio da radiação solar por meio de filtros solares orgânicos e inorgânicos. Assim, este trabalho teve, por objetivo principal, avaliar a interação dos extratos de semente de maracujá e das partes aéreas do jambu quanto à estabilidade em formulação e à permeação cutânea *in vitro* sobre o modelo sintético Strat-M® (Merck Millipore). O CAPÍTULO 1 provê uma revisão sobre a permeação cutânea de fenólicos vegetais, mostrando que há dados sobre uma multiplicidade de veículos e de modelos de pele, dificultando o estabelecimento de correlações, mas permitindo obter algumas afirmações gerais. O CAPÍTULO 2 trata da obtenção de um extrato de sementes de maracujá assistida por micro-ondas (MAE), até então não descrito na literatura. Nas condições otimizadas de 87 °C, 30 min, EtOH 70 % e dois ciclos, obteve-se um extrato com características sensoriais mais adequadas para formulação e com o dobro do teor de piceatanol (27,17 ± 0,9 µg por mg de extrato) em relação a uma extração por Soxhlet, por 120 min, com EtOH 80 %. No CAPÍTULO 3 apresentam-se os resultados de um estudo de estabilidade dos extratos de maracujá e jambu em uma emulsão base (B_{em}), com filtros orgânicos (O_{em}) ou inorgânicos (I_{em}), no qual se observou que estes não afetaram a estabilidade física, mas ocorreram interações químicas em todas as formulações. O piceatanol foi encontrado apenas em B_{em} após 12 dias de ciclo de temperaturas (5 e 40 °C) e tanto ele quanto o espilantol foram incompatíveis com os filtros inorgânicos na emulsão proposta. Por fim, o CAPÍTULO 4 mostra o perfil de permeação *in vitro* do piceatanol pela membrana Strat-M®, revelando que, na formulação proposta, ele atingiu ao equivalente de derme, alcançando camadas mais profundas na presença do espilantol e dos filtros solares orgânicos. Para o desenvolvimento deste trabalho, as técnicas de HPLC-ESI-MS/MS, UPLC-DAD, espectrofotometria UV-vis, DSC, TGA e microscopia Raman confocal foram empregadas.

ABSTRACT

Among the more than 8,000 currently elucidated plant phenolic compounds, piceatannol is presented as a potential dermo cosmetic active ingredient candidate with *in vitro* demonstrated photoprotective and skin regenerative properties. Passion fruit seed (*Passiflora edulis*) is a relevant and currently agroindustry underused source of piceatannol. The delivery of this molecule to the deeper layers of the skin, however, is challenging. While the oral administration involves intense metabolism and clearance, the topical administration encounters, as an impediment, the skin barrier itself. In this sense, permeation-promoting molecules can be associated with piceatannol to help it diffuse beyond the stratum corneum, and spilanthol, present in the aerial parts of paracress (*Spilanthes acmella*), in addition to its recognized anti-wrinkle action, exhibits this property. In order to protect the skin against the deleterious effects of the environment, it is fundamental to block sun radiation through organic and inorganic sunscreens. Thus, the main objective of this work was to evaluate the interaction between passion fruit seed and paracress aerial parts extracts in terms of formulation stability and *in vitro* skin permeation on the Strat-M^{TM} (Merck Millipore) synthetic model. CHAPTER 1 provides a review on the cutaneous permeation of plant phenolics, showing the occurrence of data on a multiplicity of vehicles and skin models, what makes it difficult to establish correlations but allows the provision of some general statements. CHAPTER 2 reveals the obtention of a passion fruit seed extract by microwave assisted extraction (MAE), which had not been described in the literature so far. Under the optimized conditions of 87 °C, 30 min, 70% EtOH and two cycles, an extract with more suitable sensory features for formulation and with twice the piceatannol content (27.17 ± 0.9 µg per mg of extract) in relation to a Soxhlet extraction, for 120 min, with 80% EtOH, was provided. CHAPTER 3 presents the results of passion fruit and paracress extracts stability study in a base emulsion (B_{em}), added with organic (O_{em}) or inorganic (I_{em}) sunscreens, in which it was observed that they did not affect their physical stability, but chemical interactions occurred in all formulations. Piceatannol was only found in B_{em} after 12 days of temperature cycling (5 and 40 °C) and both it and spilanthol were incompatible with the inorganic sunscreens in the proposed emulsion. Finally, CHAPTER 4 shows the *in vitro* permeation profile of piceatannol through the Strat-M^{TM} membrane, revealing that, in the proposed formulation, it reached the dermis equivalent, hitting deeper layers in the presence of spilanthol and organic sunscreens. For the development of this work, HPLC-ESI-MS/MS, UPLC-DAD, UV-vis spectrophotometry, DSC, TGA and confocal Raman microscopy techniques were used.

SUMÁRIO

INTRODUÇÃO

Introdução

Os compostos fenólicos são uma das classes de moléculas mais difundidas pelo reino vegetal, havendo mais de 8.000 estruturas identificadas no presente momento. Classificadas em categorias como ácidos fenólicos, flavonoides, taninos, estilbenoides, cumarinas e lignanas, estes compostos estão, geralmente, envolvidos em fatores como cor, crescimento, defesa contra radiação ultravioleta (UV) ou patógenos, e em outros processos regulatórios para a sobrevivência das plantas (Figura 1) [1–3].

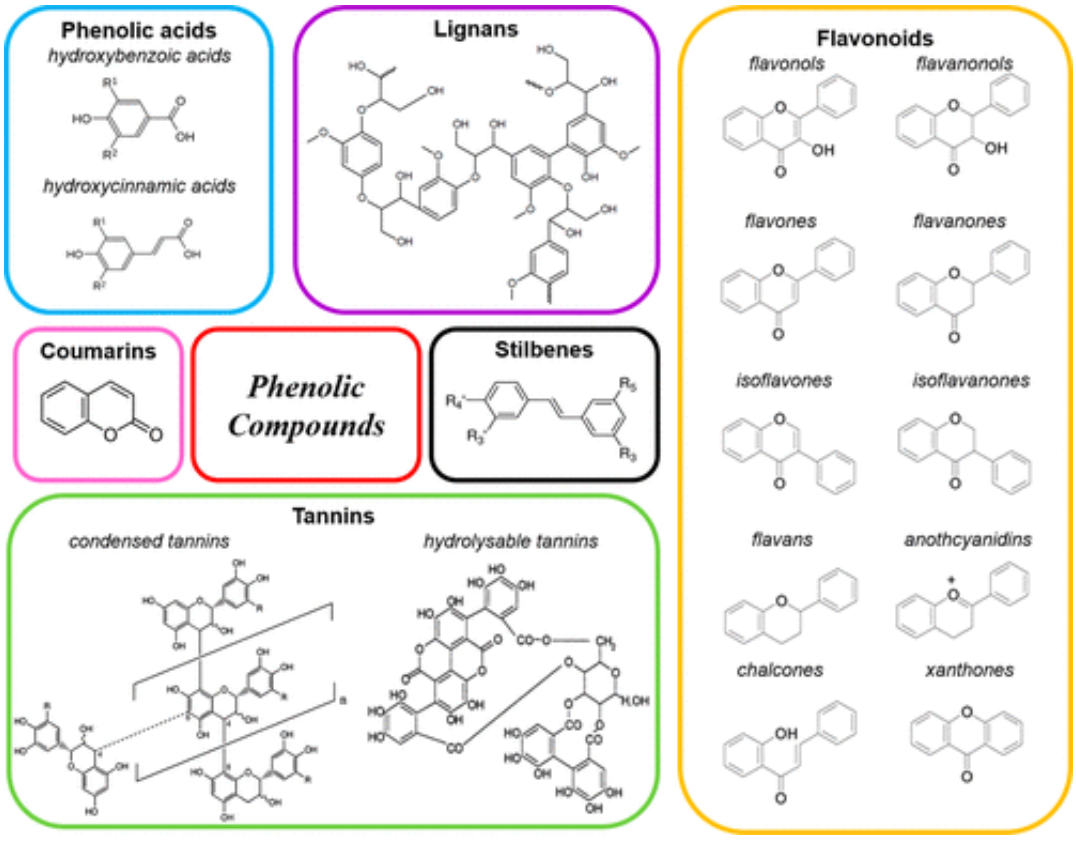

Figura 1: estruturas moleculares base dos compostos fenólicos vegetais. Reproduzido de [4], com permissão (Anexo 1).

Adquiridos principalmente por meio da dieta, estes compostos passam a exercer atividades biológicas sobre a fisiologia humana. Particularmente para a pele, suas propriedades antioxidante, antimutagênica, quelante e de eliminação de radicais livres são de grande importância. A pele contribui para a manutenção da temperatura corporal, é local de produção de vitamina D, promove a percepção sensorial, faz parte do sistema imunológico e atua como barreira contra a perda de água e eletrólitos do corpo. Uma vez em contato direto com os componentes do ar, poluentes e,

principalmente, com a luz UV, ela requer que seus mecanismos próprios de defesa e adaptação aos agentes externos esteja em pleno funcionamento para a manutenção de sua saúde e vitalidade [5–8].

Dentro do arsenal regulatório do equilíbrio redox cutâneo, encontram-se moléculas antioxidantes e enzimas endógenas que, em conjunto, formam uma rede intrincada de combate aos efeitos deletérios dos radicais livres, em geral oriundas de reações com espécies reativas de oxigênio (ROS) e de nitrogênio (RNS) formadas pela interação da pele com o ambiente externo ao corpo. O ubiquinol, também conhecido como coenzima Q10, age na eliminação de radicais livres lipossolúveis e inibe a expressão de algumas enzimas metaloproteinases, que agem degradando componentes como o colágeno, por exemplo. Já as diferentes isoformas de superóxido dismutase (SOD) catalisam conversão do ânion radical superóxido ($O_2^{\cdot -}$) em peróxido de hidrogênio (H_2O_2), que é reduzido a água por ação das catalases (Cat) e das glutationa peroxidases (GPXs). A glutationa (GSH), em si, é um tripeptídeo que se dimeriza com outra unidade de GSH ao ser oxidado por ROS e retorna a unidades monoméricas por ação da enzima glutationa redutase. Outra molécula relevante dentro desta rede é a vitamina E, que previne a peroxidação lipídica e a oxidação de ácidos graxos insaturados. Ela é altamente depletada por ação da radiação UV e, quando oxidada, é reparada pela vitamina C, que também atua na remoção de radicais livres e na síntese e reticulação do colágeno [9, 10].

Em geral, a capacidade antioxidante endógena da pele diminui com a idade, e a pele envelhecida torna-se ainda mais vulnerável aos agentes externos. A diminuição natural do metabolismo celular ao longo dos anos, bem como a exposição excessiva aos fatores ambientais, pode levar a pele a um desequilíbrio oxidativo, desencadeando processos inflamatórios, danos moleculares e celulares. Tais danos se traduzem em deficiências funcionais que originam rugas, ressecamento, flacidez, e, eventualmente, células tumorais. Assim sendo, torna-se imprescindível tomar medidas preventivas para limitar a exposição excessiva da pele aos fatores danosos. A Organização Mundial da Saúde recomenda procurar estar à sombra, utilizar chapéus, óculos escuros, e aplicar protetores solares nas partes expostas ao sol, mas fornecer à pele um aporte externo de antioxidantes e compostos capazes de reparar os danos causados pelo estresse oxidativo também é uma estratégia razoável para manter sua saúde [5, 6, 10, 11].

Para uma melhor compreensão sobre como aportar estes reforços ao arsenal antioxidante e reparador, cabe, neste ponto, apresentar uma visão geral sobre a anátomo-fisiologia da pele. Este órgão é composto pela epiderme, que é a camada mais externa e que fica em contato com o meio ambiente, e pela derme, intimamente ligada à camada mais profunda da epiderme e a camada de células adiposas que conectam a pele aos músculos. Atualmente, a camada adiposa é designada como tecido subcutâneo, em um entendimento de que esta camada se trata de um órgão à parte, ou hipoderme, que a classifica como parte integrante da pele. Embora, atualmente, não haja um consenso formal sobre sua classificação anatômica, é fato que ela envolve os nervos, vasos linfáticos e sanguíneos que nutrem a pele e, além de auxiliar na regulação da temperatura e nos tráfegos neurais e de fluidos, ela fornece suporte mecânico à pele como um todo (Figura 2) [12, 13].

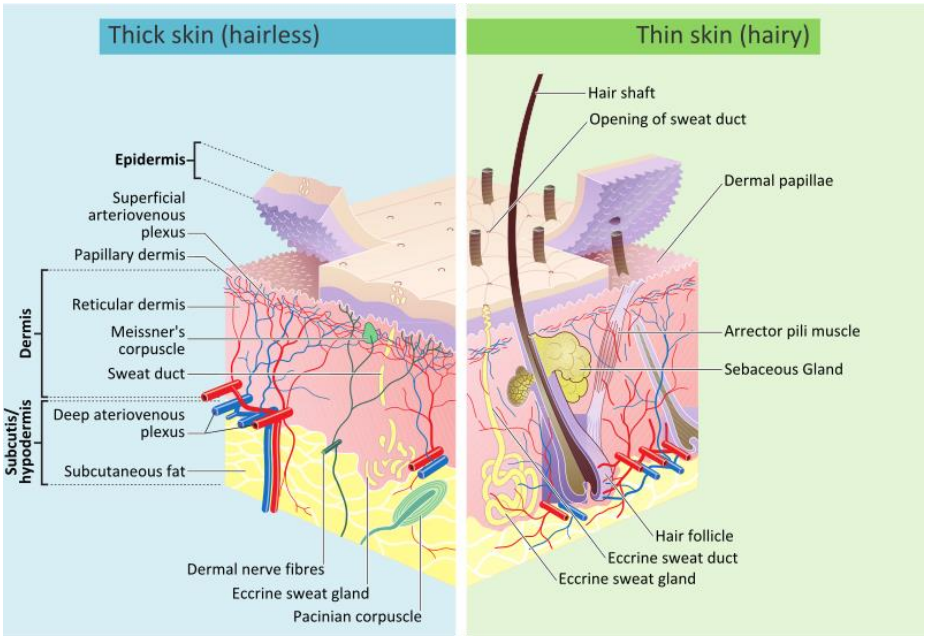

Figura 2: representação esquemática da estrutura da pele. Reproduzido de [14] com permissão. Madhero88 and M.Komorniczak, CC BY-SA 3.0 <https://creativecommons.org/licenses/by-sa/3.0>, via Wikimedia Commons.

A derme, por sua vez, é responsável pela flexibilidade e elasticidade. Ela pode ser subdividida em duas camadas:

- derme reticular, frouxa e em contato com o tecido subcutâneo,

- e derme papilar, densa, altamente vascularizada e em contato com a epiderme [12, 15].

Dentre as fibras conectivas que constituem esta camada da pele, o colágeno é o componente majoritário. Além dele, a derme também contém fibras de elastina, proteo e glicosaminoglicanos, especialmente ácido hialurônico. O principal componente dérmico, no entanto, é a água (cerca de 70%), o que a torna propensa a receber compostos hidrofílicos. Os vasos sanguíneos e linfáticos que alimentam a pele estão acomodados em sua estrutura, que também envolve os apêndices cutâneos (folículos pilosos, glândulas sebáceas e sudoríparas) e mecanorreceptores (terminações nervosas, corpúsculos de Pacini e de Meissner). Células com diferentes funções estão espalhadas dentro desta matriz. Os fibroblastos, por exemplo, atuam na renovação das fibras conectivas, enquanto os mastócitos, macrófagos e células dendríticas são responsáveis pela proteção imunológica [12, 15].

A epiderme, por sua vez, é um ambiente celular altamente organizado. Em geral, é formado por estratos celulares (queratinócitos) permeados pelos ductos das glândulas sudoríparas e sebáceas, estas últimas acopladas aos folículos pilosos (Figura 3) [12].

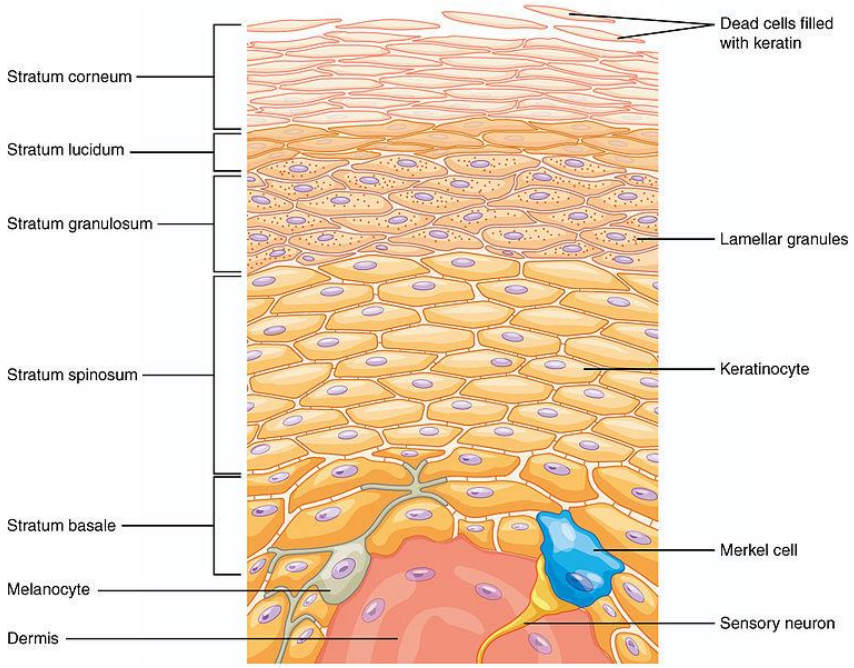

Figura 3: representação esquemática da estrutura da epiderme. Reproduzido de [16] com permissão. OpenStax College : J. Gordon Betts, Peter Desaix, Eddie Johnson., CC BY 3.0 <https://creativecommons.org/licenses/by/3.0>, via Wikimedia Commons.

Intimamente em contato com a derme papilar, o estrato basal é constituído por queratinócitos-tronco, que estão constantemente originando novos queratinócitos por meio de multiplicação celular. Além deles, melanócitos, responsáveis pela produção de melanina para proteção contra a luz UV, células de Merkel e de Langherhans, que fazem parte do sistema imunológico, estão presentes nesse estrato [17].

Sobre o estrato basal, há camadas contendo queratinócitos em diferentes estágios de maturidade. Em direção à camada mais externa, o estrato espinhoso possui células em estágios iniciais de diferenciação morfológica e histológica. O estrato granuloso compreende queratinócitos ainda mais maduros, que acumulam maiores quantidades de queratina e ceramidas. Juntamente com o estrato basal, essas camadas são chamadas coletivamente de epiderme viável e contém cerca de 50% de água. Como não são encontrados vasos sanguíneos na epiderme, a nutrição das células viáveis é feita por difusão a partir da junção derme-epidérmica [12, 17].

Acima da epiderme viável permanece a camada que está em contato direto com o meio ambiente: o estrato córneo (SC), contendo de 10 a 25 camadas de queratinócitos mortos, anucleados, densos e totalmente diferenciados, agora denominados corneócitos. Os corneócitos são células alongadas preenchidas com filamentos de queratina envoltos por filagrina, e estão embutidos em uma matriz lipídica contendo ácidos graxos, ceramidas e colesterol em uma estrutura do tipo “tijolo e argamassa”. O SC descama continuamente, exercendo sua função de protetor contra o estresse mecânico, e é substituído por novas células que emergem da epiderme viável [12].

Dependendo do nível de hidratação, a espessura da SC pode variar de cerca de 10 a 40 μm, mas o teor de água nessa camada sempre será o menor de toda a pele (cerca de 10%). Nas palmas das mãos e nas solas dos pés, uma camada denominada estrato lúcido é um estágio intermediário entre o estrato granuloso e o SC, o que torna a pele ainda mais espessa. Nesse sentido, o SC é considerado uma camada hidrofóbica, o que é crucial para a função de barreira e para evitar a perda de água do interior ao exterior do corpo [12].

Uma vez que a epiderme é a parte da pele que está mais exposta a estímulos externos, a carga de ROS é maior nesta parte em comparação com a

derme. Assim, o sistema protetor cutâneo está presente em concentrações mais altas na epiderme, particularmente nas camadas mais profundas do SC [10].

No entanto, a radiação UV não só atinge, como também ultrapassa as camadas onde a proteção contra o estresse oxidativo é mais relevante. É nesse sentido que os métodos que formem uma barreira à radiação, como os filtros solares e as vestimentas, atuam como importantes auxiliares na proteção da pele. Os filtros solares, em especial, são uma maneira físico-química de se bloquear ao menos parte da radiação incidente. Estes filtros são compostos ativos classificados entre orgânicos, que hoje são moléculas absorvedoras da radiação UV utilizadas em concentrações determinadas em cosméticos, perfumes e produtos de higiene pessoal, e inorgânicos, que são, essencialmente, formas de ZnO e TiO_2. A Tabela 1 apresenta os filtros orgânicos permitidos e suas concentrações-limite dentro de diferentes legislações [11, 18].

Os filtros orgânicos atuam, em geral, absorvendo a radiação que atinge a superfície onde eles estão presentes e devolvendo a energia recebida sob a forma de calor ao ambiente. Por sua vez, os filtros inorgânicos agem, primariamente, pela reflexão e pelo espalhamento da luz recebida, embora parte da luz também seja absorvida e emitida sob a forma de calor (Figura 4). No entanto, existem ingredientes orgânicos particulados, como o MBBT (methylene bis-benzotriazolyl tetramethylbutylphenol) e a TBPT (tris-biphenyl triazine), que possuem mecanismo de ação similar à dos filtros inorgânicos [19, 20].

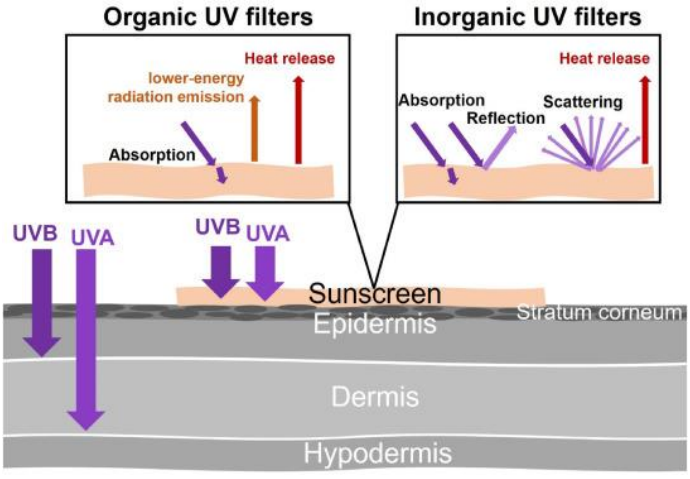

Figura 4: mecanismo de ação dos filtros solares orgânicos e inorgânicos. Reproduzido de [11] com permissão (Anexo 1).

Tabela 1: quantidades permitidas dos filtros solares orgânicos em formulação conforme as legislações dos diferentes países e regiões [21].

	EU (%)	CN (%)	US (%)	AU (%)	CA (%)	JP (%)	IN (%)	ZA (%)	ASEAN (%)	Mercosur (%)
PABA (and its esters – JP)	–*	5	15	–	15	4	5	15	–	15
Camphor benzalkonium methosulphate	6	6	–	6	–	–	6	6	6	6
Homosalate	10	10	15	15	15	10	10	10	10	15
Benzophenone-3	10	10	8	10	6	5	10	10	10	10
Phenylbenzimidazole sulphonic acid	8	8	4	4	4	3	8	8	8	8
Terephthalylidene dicamphor sulphonic acid	10	10	–	10	10	10	10	10	10	10
Butyl methoxydibenzoylmethane	5	5	3	5	3	10	5	5	5	5
Benzylidene camphor sulphonic acid	6	6	–	6	–	–	6	6	6	6
Octocrylene	10	10	10	10	10	10	10	10	10	10
Polyacrylamidomethyl benzylidene camphor	6	6	–	–	–	–	6	6	6	6
Ethylhexyl methoxycinnamate	10	10	7.5	10	7.5	20	10	10	10	10
PEG-25 PABA	10	10	–	10	–	–	10	10	10	10
Isoamyl p-methoxycinnamate	10	10	–	10	–	–	10	10	10	10
Ethylhexyl triazone	5	5	–	5	–	5	5	5	5	5
Drometrizole trisiloxane	15	15	–	15	15	15	15	15	15	15
Diethylhexyl butamido triazone	10	10	–	–	–	–	10	10	10	10
4-Methylbenzylidene camphor	4	4	–	4	6	–	4	4	4	4
3-Benzylidene camphor	2	2	–	–	–	–	2	2	2	2
Ethylhexyl salicylate	5	5	5	5	5	10	5	5	5	5
Ethylhexyl dimethyl PABA	8	8	8	8	8	10	8	8	8	8
Benzophenone-4	5**	5**	10	10	10	10	5**	10	5**	10
Benzophenone-5	–	–	–	10	–	10	–	5	–	5
MBBT	10	10	–	10	–	10	10	10	10	10
DPDT	10	10	–	10	–	–	10	10	10	10
BEMT	10	10	–	10	–	3	10	10	10	10
Polysilicone-15	10	10	–	10	–	10	10	10	10	10
DHHB	10	10	–	10	–	10	10	10	10	10
Tris-biphenyl triazine (nano)	10	–	–	–	–	–	–	–	–	–
Menthyl anthranilate	–	–	5	5	5	–	–	5	5	5
Cinoxate	–	–	3	6	3	5	–	5	–	3
Benzophenone-8	–	–	3	3	3	–	–	3	–	3

TEA salicylate	–	–	12	12	12	–	–	12	–	12
Diethanolamine methoxycinnamate	–	–		–	10	–	–	8	–	–
Benzophenone-1	–	–		–	–	10	–	10	–	–
Benzophenone-2	–	–		–	–	10	–	10	–	–
Benzophenone-6	–	–		–	–	10	–	5	–	–
Benzophenone-9	–	–		–	–	10	–	No limit	–	–
Methyl-2,5-diisopropylcinnamate	–	–		–	–	10	–	10	–	–
1-(3,4-Dimethoxyphenyl)4,4-dimethyl-3-pentadiene	–	–		–	–	7	–	7	–	–
Ethylhexyl dimethoxybenzylidene oxoimidazoline propionate	–	–		–	–	3	–	3	–	–
Ferulic acid	–	–		–	–	10	–	10	–	–
4-(2-Beta-Glucopyranosiloxy)propoxy-2-/hydroxybenzophenone	–	–		–	–	5	–	–	–	–
Glyceryl ethylhexanoate dimethoxycinnamate	–	–		–	–	10	–	10	–	–
Glyceryl PABA	–	–		–	–	4	–	5	–	–
Isopentyl trimethoxycinnamate trisiloxane	–	–		–	–	7.5	–	7.5	–	–
Mixture: Isopropyl *p*-methoxycinnamate + Ethyl	–	–		–	–	–	–		–	–
diisopropylcinnamate + Methyl-2,4-diisopropylcinnamate	–	–		–	–	10	–	10	–	–
Pentyl dimethyl PABA	–	–		–	–	10	–	–	–	–
Digalloyl trioleate	–	–		–	–	–	–	5	–	–
Ethyl dihydroxypropyl PABA	–	–		–	–	–	–	5	–	–

Ações distintas das de bloqueio, contudo, requerem que o composto ativo atinja as diferentes camadas que compõem a pele para que sua atividade seja exercida. Embora se entenda que os compostos fenólicos vegetais adquiridos pela dieta apresentem atividades relevantes para reforçar o sistema natural de equilíbrio redox e a manutenção dos componentes dérmicos, é preciso salientar que a sua absorção, distribuição, metabolismo e excreção sofrem grande variabilidade, inclusive a nível de indivíduo, a depender da estrutura química, da matriz alimentícia de onde ele é adquirido, da susceptibilidade às enzimas digestivas, do quanto eles são absorvidos para a corrente sanguínea e das reações sofridas em decorrência do metabolismo hepático. Atualmente se compreende, ainda, que parte dos compostos

fenólicos vegetais que chegam ao intestino sofre catabolismo pela microbiota local e que, ao serem absorvidos, parte é biotransformada pelo fígado e retornada ao intestino por meio da bile. Tais metabólitos podem exercer ação sobre a própria microbiota intestinal, eventualmente agindo como probióticos, e os benefícios gerados pelo consumo de compostos fenólicos à saúde seriam, portanto, uma combinação entre o efeito probiótico e a chegada direta dos compostos ao seu sítio de ação. E, como a variabilidade da própria microbiota depende de fatores e estilos de vida de cada pessoa, fala-se, também, em prescrição de suplementação individualizada de compostos fenólicos partindo-se do perfil de cada paciente, considerando-se, em conjunto, suas características genômicas e epigenômicas [22–26] .

De toda forma, a vulnerabilidade dos compostos fenólicos às condições gástricas pode incorrer em baixa biodisponibilidade para o efeito desejado na pele, limitando sua aplicação por via oral para o fim de reforço cutâneo. Neste sentido, a aplicação tópica de produtos que os contenham pode ser uma via mais efetiva de sua entrega nos sítios alvos de ação. Por esta razão, formulações contendo não só compostos fenólicos vegetais, como também as vitaminas C, E, peptídeos bioativos, oligossacarídeos e outros compostos estão disponíveis atualmente no mercado. O bom desempenho da maioria desses produtos, entretanto, está relacionado à capacidade de permeação cutânea dos princípios ativos às camadas mais profundas da pele, sendo desejável a menor absorção sistêmica possível [6, 27, 28].

A administração tópica ideal pode ser dificultada pela natureza da pele como uma interface semipermeável, e é condicionada por vários fatores. A própria estrutura e composição do SC limita a passagem de compostos para o interior da pele. Os compostos a traspõem por três vias distintas: (i) intercelular, que é a de maior contribuição, (ii) transcelular, que seria a menor contribuição, (iii) transapendicial, que ocorre pelas aberturas das glândulas sudoríparas, pela via das glândulas sebáceas, e por intermédio dos folículos pilosos (Figura 5) [29].

Uma vez vencida a barreira mais hidrofóbica, as moléculas encontram, ambientes cada vez mais hidratados à medida em que atingem maiores profundidades. Ao atingirem a derme, encontram um ambiente altamente vascularizado, e são susceptíveis a alcançarem a corrente sanguínea e serem distribuídas sistemicamente. As características estruturais gerais da pele são

somadas a outros fatores como a região do corpo, a etnia, a idade, o gênero e a presença de enfermidades e, a elas, se somam as propriedades das moléculas ativas, do veículo e da interação ativo-veículo para o comportamento de permeação apresentado [29, 30].

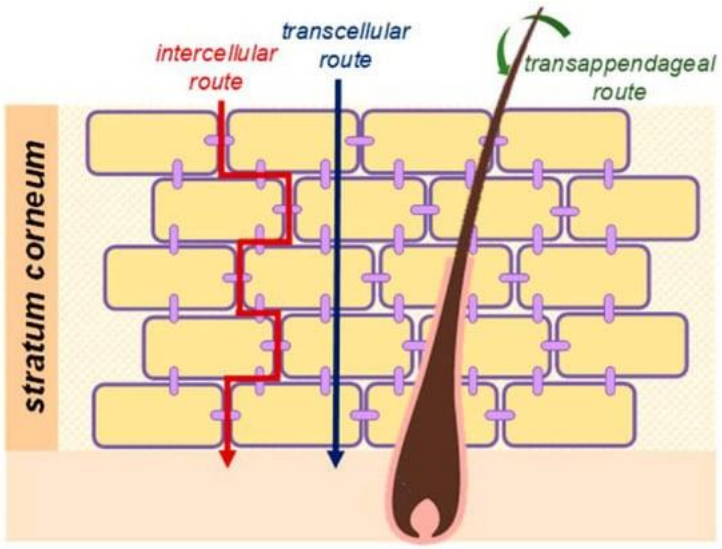

Figura 5: rotas de difusão de compostos pelo estrato córneo. Reproduzido de [31] com permissão (Anexo 1).

No que compete à molécula ativa em si, aquelas que preferencialmente possuam um valor de logP (o/w) entre 1 e 3, estejam na sua forma não iônica, possuam menos que 500 Da de massa molecular e ponto de fusão inferior a 200 °C são tidas como as que melhor particionam com os lipídeos da pele. Mas há outros critérios a serem atendidos para um determinado composto ser capaz de transpor a barreira cutânea, incluindo, no rol de características, aquelas ligadas à presença de determinados átomos e grupamentos químicos, ligações rotacionáveis e área de superfície polar topológica (Tabela 2) [29, 32, 33].

Tabela 2: conjuntos de critérios de predição de permeabilidade molecular à barreira cutânea. Adaptado de [33], com permissão (Anexo 1).

Autor	Critério	Valores
Lipinski	Massa molar	< 500
	Log P	< 4,15
	Número de átomos de N ou O	< 10
	Número de grupos N ou OH	< 5
Ghose	Massa molar	Entre 160 e 480

Veber	Log P	Entre -0,4 e 5,6
	Número de átomos	< 70
	Refratividade molar	Entre 40 e 130
	Número de ligações rotáveis	< 10
	Área de superfície polar topológica (TPSA)	< 140
Egan	Log P	< 5,88
	Área de superfície polar topológica (TPSA)	< 131,6
Muegge	Massa molar	Entre 200 e 600
	Log P	Entre -2 e 5
	Área de superfície polar topológica (TPSA)	< 150
	Número de anéis	< 7
	Número de carbonos	> 4
	Número de heteroátomos	> 1
	Número de ligações rotáveis	< 15
	Número de aceptores de hidrogênio (NHA)	< 10
	Número de doadores de hidrogênio (NHD)	< 5

A permeação de uma molécula, porém, pode ser modulada de acordo com o veículo. Um exemplo claro é o caso do ácido azeláico: em comparação com uma suspensão de sua forma não ionizada, uma solução da forma ionizada apresenta maior permeação na pele, indicando que a solubilidade do ativo no veículo compensa o fato de este ativo estar sob a forma da espécie iônica. No entanto, diferentemente do ácido azeláico, o ibuprofeno apresenta uma redução da permeação com o aumento da solubilidade, indicando que essa questão não é um comportamento universal [34].

Existem outras características inerentes aos veículos que afetam o padrão de permeação de um ativo. Conforme o tipo de agente emulsionante empregado em uma formulação, os ativos podem ser encapsulados pelo veículo, facilitando ou dificultando a sua translocação pela pele.

A carga dos emulsionantes (aniônico, catiônico ou não iônico) também interfere na permeação do ativo de forma variável, bem como a polaridade, a viscosidade e o pH. Embora filtros solares não devam permear a pele, mas sim, permanecer em sua superfície para exercer sua função de bloqueio, a oxibenzona, por exemplo, é um filtro solar orgânico hidrofóbico que exibe maior permeação quando

em petrolato e menor quando em gel de hidroxietilcelulose. Por outro lado, a sulizobenzona, um filtro orgânico hidrofílico, exibe o comportamento inverso estando nos mesmos veículos. Já com relação à viscosidade, a benzofenona-3, outro filtro solar orgânico, tem sua permeação impedida por formulações mais viscosas, porém este comportamento se altera quando se aplicam várias doses da mesma formulação uma sobre a outra, já que, devido a um efeito de oclusão, aumenta-se a hidratação cutânea e, por consequência, a difusibilidade do filtro também é aumentada [32, 35].

Esta variabilidade de circunstâncias afeta também o comportamento dos compostos fenólicos vegetais sobre a pele. No **CAPÍTULO 1** desta tese, apresenta-se uma revisão da literatura sobre o perfil de difusão destes compostos em modelos *in vitro*, no qual se observa que, apesar de alguns guias preditivos, não há uma regra geral a ser atendida para formular produtos tópicos a partir deles. Neste sentido, a determinação experimental do perfil de permeação cutânea torna-se uma grande aliada na concepção de produtos seguros e eficazes.

Dentre os mais de 8.000 fenólicos vegetais descritos, um dos que possui propriedades interessantes para a pele é o piceatanol (Figura 6), um sequestrador de radicais peróxido superior ao resveratrol, seu análogo, independentemente da polaridade do meio. Tanto o resveratrol quanto o piceatanol podem ser regenerados eficientemente em pH fisiológico, e sugere-se que ambos podem sequestrar mais que 2 radicais equivalentes sob esta condição [7]. Baseado na atividade antioxidante, Wang et al. [36] e Lu et al. [37] realizaram estudos teóricos sobre o mecanismo de ação do piceatanol frente a radicais livres, concluindo que o grupamento -OH em destaque na Figura 6 é fundamental para a atividade antioxidante do composto pela via de transferência de átomo de hidrogênio.

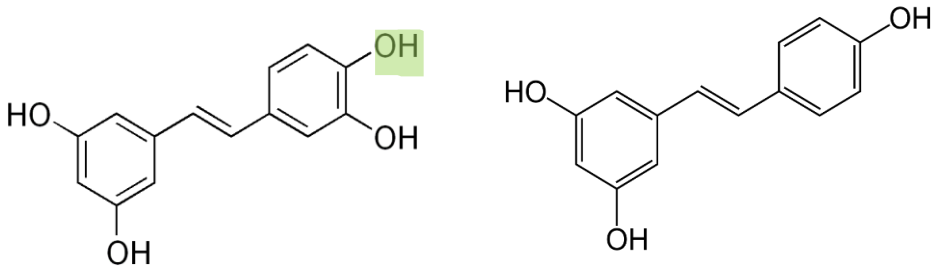

Figura 6: estruturas moleculares do piceatanol (esq.) e do resveratrol (dir.)

Hosoda et al. [38] avaliaram a proteção conferida pelo resveratrol e pelo piceatanol contra as ROS, comparando a citotoxicidade, a atividade antioxidante e os mecanismos de citoproteção destas moléculas. Como conclusão, os autores observaram que ambas as moléculas, embora análogas, apresentam atividades distintas, e o piceatanol confere maior proteção celular contra a apoptose induzida por ROS. À parte da atividade antioxidante, Matsui *et al.* [39] demonstraram que o piceatanol, é capaz de inibir a melanogênese em cultura de células de melanoma humano e de promover a síntese de colágeno em cultura de fibroblastos. O piceatanol também foi testado como um tratamento prévio à irradiação de raios UVB em células epidérmicas humanas *in vitro*, e os efeitos encontrados foram o da supressão da formação de espécies reativas de oxigênio UVB-induzidas e a redução da ação da enzima MMP-1, responsável pela degradação de colágeno [40]. Em testes sobre modelo celular e ratos, o piceatanol foi capaz de atenuar a dermatite atópica, reduzindo a migração de células e a incidência de marcadores inflamatórios [41]. Estes resultados mostram que o piceatanol possui potencial como ativo protetor e regenerador da pele contra fatores extrínsecos deletérios.

Na natureza, o piceatanol pode ser encontrado em uvas e vinhos (*Vittis* ssp.), estando presente também no mirtilo (*Vaccinium* ssp) e em espécies vegetais como *Polygonum cuspidatum*, *Melaleuca leucadendron*, *Cassia garrettiana*, *Cassia marginata*, *Rheum* spp., *Euphorbia lagascae*, *Mezoneuron cucullatum*, *Caragana tibetica*, *Rheum rhaponticum*, *Partneocissus tricuspidata*, *Aiphanes aculeata*, *Arachis hypogaea*, e *Ampelopsis brevipedunculaata* Recentemente, esta molécula foi encontrada também no fruto da “canjiqueira” (*Byrsonima cydoniifolia*), uma planta do cerrado brasileiro. Outra importante fonte natural de piceatanol é a semente do maracujá (*Passiflora edulis*), onde este é tido, inclusive, como o composto majoritário. Neste sentido, o Brasil é um país com grande potencial para a exploração deste fenólico, dado que este é o principal produtor mundial da fruta de acordo com o levantamento mais recente disponível na Food and Agriculture Organization (FAO). Entre os anos de 2019 e 2022, o Brasil produziu em torno de 600 mil toneladas por ano desta fruta [42–44].

Passiflora edulis Sims., popularmente conhecida como maracujá azedo no Brasil, é a espécie de maracujá mais economicamente relevante (Figura 7). Dentro da espécie, existem subespécies (var. Sims, roxo, e var. flavicarpa, amarelo), além de

aproximadamente 30 cultivares e híbridos, frutos de melhoramentos realizados por instituições como a Empresa Brasileira de Pesquisa Agropecuária – EMBRAPA, e o Instituto Agronômico – IAC. A maior agregação de valor ao fruto está, atualmente, no processamento para a fabricação de sucos e polpas, sendo este o destino de cerca de 40 % da produção do maracujá brasileiro. O volume de exportação dos produtos industrializados é bastante mais elevado que o do fruto para consumo *in natura* e vem crescendo nos últimos anos, tendo ultrapassado a casa das 1000 toneladas em 2022 (Figura 8) [44–46].

Figura 7: frutos de *Passiflora edulis* Sims. Imagem de jcomp no Freepik.

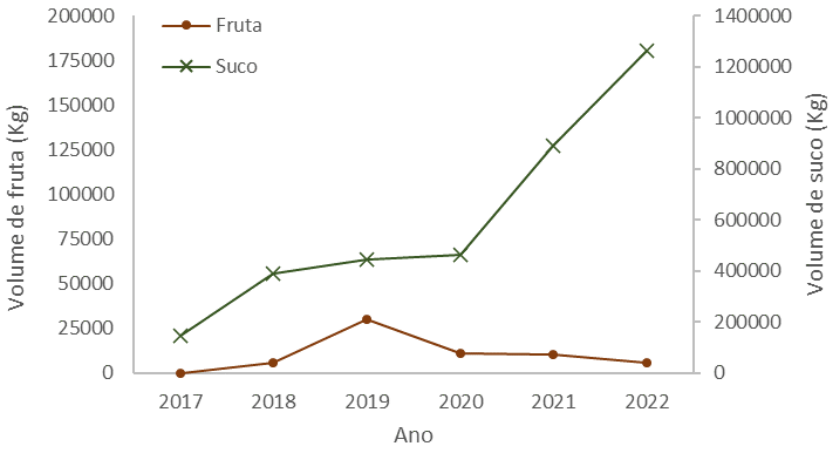

Figura 8: desempenho das exportações brasileiras do maracujá de 2017 a 2022. Dados de [46].

A casca e as sementes são um rejeito industrial geralmente descartado ou destinado ao uso como ração animal ou adubo orgânico. Das sementes, é possível também se obter um óleo com elevado teor de ácidos graxos insaturados e com espaço na alimentação animal, humana e em cosméticos. O resíduo da extração do óleo pode ser empregado como fonte de proteínas e fibras, ou como um esfoliante físico da pele em formulações. Contudo, este material poderia também ser aproveitado como fonte de piceatanol, agregando ainda mais valor à cadeia do maracujá [47, 48].

A Tabela 3 apresenta os métodos de preparo de extratos de semente de maracujá com foco na recuperação do piceatanol ou outros fenólicos. Na maioria dos casos, a extração se dá com uma mistura etanol:água (EtOH:H_2O). Há trabalhos com butilenoglicol, metanol:água (MeOH:H_2O) e CO_2 supercrítico (SC-CO_2). Em alguns casos, uma etapa prévia de desengorduramento do material com hexano é realizada. Dentre as técnicas de extração encontram-se as clássicas, como a maceração e o refluxo, e técnicas modernas além de SC-CO_2, como a extração por assistida por ultrassom (UAE, do inglês *ultrasound-assisted extraction*) e a extração por líquido pressurizado (PLE). Sobre a eficiência dos processos, alguns autores não apresentaram detalhes sobre a quantificação de moléculas alvo e utilizaram, como resposta, o teor de fenólicos totais ou a atividade antioxidante do extrato.

Esforços visando o isolamento do piceatanol também são encontrados na literatura. Pan et al. [49] conseguiram isolar o piceatanol e a scirpusina B de sementes de maracujá por cromatografia contracorrente de alta velocidade (HSCCC, do inglês *high-speed conter-current chromatography*), com purezas de 94,2 e 90,2 %, respectivamente. Estratégia similar já havia sido empregada por Liu et al.[50] no isolamento de compostos antioxidantes das raízes de *Polygonum multiflorum*, uma planta utilizada na medicina tradicional chinesa de onde foi possível obter o piceatanol com 96,85 % de pureza.

A extração assistida por micro-ondas (MAE, do inglês *microwave-assisted extraction*), por outro lado, é uma técnica moderna com possibilidade de emprego na produção de extratos em larga escala e para a qual não se encontravam relatos de aplicação na extração do piceatanol até o momento da execução deste trabalho. MAE opera por meio da indução da rotação molecular de dipolos, permitindo o aquecimento interno, rápido e seletivo dos conteúdos submetidos à extração. A técnica foi

introduzida na década de 1970, em nível de bancada, para a digestão ácida de amostras visando a análise de metais. Seu uso foi expandido para a extração de moléculas orgânicas na década de 1980 e, desde então, observa-se um aumento na aplicação de MAE para a extração de compostos bioativos de plantas e resíduos agroindustriais [51, 52].

O fenômeno do aquecimento em MAE ocorre pela interação entre a radiação micro-ondas incidente (109 a 1011 Hz) e moléculas dielétricas com um momento dipolar. Essa interação resulta em movimento molecular e, portanto, em elevação de temperatura. Apesar de ser uma técnica de extração baseada em aquecimento, seu mecanismo de ação de dissipação de calor de dentro para fora do material o torna único e diferente das extrações convencionais por aquecimento ou refluxo, nas quais o calor é dissipado de fora para dentro da amostra. Provavelmente, esta é a razão pela qual o aquecimento no MAE é mais rápido do que nas técnicas convencionais e, como resultado, alcançam-se curtos tempos de processamento e menores consumos de energia [51–53]

No caso de matrizes vegetais, o mecanismo de aquecimento de MAE permite que a água contida no interior do material seja aquecida. Assim, a rápida evaporação da água intrínseca pode ocasionar rupturas nas paredes da biomassa, favorecendo a extração dos compostos bioativos para a fase solvente. Outra característica de MAE é que, em vasos de extração selados, um aumento na pressão pode ser proporcionado pela rápida dissipação de calor, e a pressão pode reduzir a tensão superficial e a viscosidade do solvente, favorecendo sua penetração na matriz facilitando e a transferência de massa da amostra para si. Além disso, diferentes materiais respondem de maneira diferente às micro-ondas incidentes, e isso pode levar à extração seletiva de certos compostos [51, 53].

Embora o uso de MAE em escala industrial ainda seja incipiente e enfrente alguns obstáculos instrumentais a serem superados, há relatos sobre a ampliação de escala com essa técnica. Petigny et al. [54], por exemplo, relataram que a MAE foi mais eficiente que a hidrodestilação clássica para a recuperação de compostos voláteis e não voláteis das folhas de boldo. Um processo em escala de laboratório gerou um produto com propriedades sensoriais aprimoradas que poderiam facilitar sua integração a uma formulação cosmética perfumada. Esse processo foi ampliado por um fator de 30 vezes para um aparelho piloto de micro-ondas e foi considerado

mais sustentável que a hidrodestilação convencional devido a uma maior eficiência energética e agilidade. Garcia-Garcia et al. [55] fizeram uma avaliação do ciclo de vida para a extração de pectina de casca de laranja por MAE em escala piloto, e o produto obtido atendeu a todos os critérios exigidos de qualidade alimentar para a pectina comercial. MAE apresentou um melhor rendimento e causou menos de 25% do impacto ambiental do processo tradicional. O trabalho de Radoiou et al. [56] apresentou um método industrial para preparo de extrato de cannabis usando micro-ondas de 915 MHz acoplado com operação de fluxo contínuo à pressão atmosférica, permitindo processar maiores volumes de biomassa em menos tempo do que os métodos de extração existentes e com maior eficiência de extração, com facilidade de ampliação para a escala industrial. Além de eliminar a necessidade de etapas adicionais necessárias para este tipo de biomassa como a descarboxilação, o processo permite a recuperação de até 95% dos compostos ativos.

Com base nestes trabalhos, MAE apresentou-se como uma possibilidade alternativa para a produção de extratos de sementes ou torta residual de sementes de maracujá, e seu potencial para esta aplicação foi explorado neste trabalho. Os resultados obtidos encontram-se no **CAPÍTULO 2** desta tese.

Tabela 3: métodos de preparo de extratos de semente de maracujá.

Material/ Preparo	Extração	Pós extração	Compostos	Referência
Semente/ Liofilização e moagem	30% 1,3-*butylene glycol* (BG)	Concentração por evaporação e liofilização.	Piceatanol (37.06 μg mg^{-1}) Scirpusin B (14.98 μg mg^{-1})	[40]
Semente/ Liofilização e moagem	EtOH 80%	Centrifugação e liofilização.	Piceatanol (85.4 μg mg^{-1}) Scirpusin B (54.7 μg mg^{-1})	[57]
Semente/ Liofilização e moagem	**Agitação a temperatura ambiente**. Extração dupla - S/L: 1:10 - 80% EtOH	Centrifugação e filtração do extrato.	-	[39]
Semente/ Liofilização e moagem	**Refluxo a 80°C** S/L: 1:10 - 80 % EtOH - 120 min	Centrifugação, evaporação e liofilização.	Piceatanol (94.9 μg/mg)	[58]
Semente/ Liofilização e moagem	**Refluxo a 90°C** EtOH 90 %- 90 min	Centrifugação Extração L-L com Hexano Concentração do extrato hidralcoólico sob vácuo.	Piceatanol (570 mg/100 g) Scirpusin B (360 mg/100 g)	[59]
Semente/ Lavagem, secagem em estufa 50 °C e moagem.	**Refluxo** MeOH 40% 30 min	Concentração a vácuo Extração L-L com n-hexano e EtOAc Análise das 3 frações: hexano, EtOAc e aquosa	EtOAc: quercetina, ac.rosmarínico, ac.clorogênico AQ: ac. kójico, ac. Gálico	[60]
Semente/ Lavagem, secagem t amb e moagem.	Hexano (2X) S/L: 1:10 - 40 °C - 1000 rpm - 12h **Agitação mecânica** EtOH 66,62% 17,39 % de sólidos - - 24 h	-	Piceatanol	[61]

Semente/ Moagem Torta/ sem pré-tratamento.	**SC-CO_2** Sementes: 150 bar, 40 ◦C 0.5 kg CO_2/h **Maceração** Torta EtOH:H_2O 1:1 (v/v)	**-**	**-**	[62]
Torta e sementes/ sem pré-tratamento	**Maceração:** 7 dias S/L: 1:5 Ordem de polaridade: Hexano, EtOAC, EtOH, EtOH:H_2O 50:50 Agitação manual 1x ao dia. **UAE:** S/L: 3 g:50 mL Ordem de polaridade: idem anterior 45 min, banho 55 kWH. **SC-CO_2**	-	-	[63]
-	**3 etapas de SC-CO_2 e uma de PLE (*pressurized liquid extraction*).**	-	Piceatanol (4ª fração, 5% em massa)	[64]
-	**Banho termostático sob agitação constante**. S/L: 1:10 Planejamento experimental: (2^3, 6 axiais, 6 PC) t (°C): 16,4 -83,6 EtOH (%): 13-97 T (min): 12,8-142,7	Centrifugação e filtração	-	[65]

Em relação à viabilização da aplicação do piceatanol em um produto para skincare, um estudo duplo cego com 32 mulheres entre 35 e 54 anos mostrou que a administração oral do extrato de semente de maracujá (5 mg de piceatanol) promoveu, ao final de 8 semanas, uma melhora na hidratação cutânea das voluntárias [66]. Apesar deste resultado, estudos relacionados à ingesta de piceatanol mostraram que, em ratos, a sua absorção é inferior à do resveratrol, seu análogo [67]. Este composto é biotransformado, como esperado, pela microbiota intestinal humana, com grandes diferenças de velocidade, intensidade e caminhos metabólicos entre indivíduos [68]. Em células hepáticas de camundongos e humanos, o piceatanol é rapidamente convertido nos isômeros rapontigenina e isorapontigenina e, após injeção intravenosa em camundongos, notou-se que que ele sofre reações de glucuronidação, sulfação e o-metilação, levando a uma também rápida excreção do composto e seus metabólitos [69].

Assim, entende-se que, para uma ação eficaz do piceatanol sobre a pele, a aplicação tópica pode ser uma via interessante para a obtenção dos efeitos benéficos observados *in vitro*. Dessa forma, no que compete à via tópica de administração, a literatura aponta que aplicação de um extrato hidroalcólico (EtOH 96 %) de sementes de maracujá preparado por maceração foi capaz de inibir o crescimento da bactéria *Propionibacterium acnes,* causadora da acne, *in vitro* [70]. Quando aplicado sobre uma cultura de queratinócitos humanos linhagem HaCaT, o piceatanol não apresentou toxicidade e a inibiu a produção de citocinas pró-inflamatórias, a proliferação e a migração celulares promovidas por *P. acnes*, eventos característicos dos indivíduos que apresentam o problema de acne vulgar [71]. Neste tipo de afecção da pele, é clara a preferência para o uso local em detrimento do sistêmico. Contudo, como explanado, caso se intencione que este composto seja capaz de balancear os efeitos de um eventual desbalanço do sistema redox cutâneo, é necessário que ele esteja biodisponível em camadas mais profundas da pele.

Sobre a permeação cutânea do piceatanol, Hung et al. [72] afirmaram que esta molécula apresenta uma penetração 11,6 vezes menor que a do resveratrol quando em veículos como tampões aquosos com diferentes pH, óleo de soja e em sistema hidrogel, mostrando uma possível dificuldade de difusão deste composto pela pele. Por outro lado, no modelo de Eskandari et al. [73] para determinação da atividade antioxidante de compostos em pele, o piceatanol foi classificado no grupo dos compostos lipofílicos (log K_{ow} = 2,9), que exercem sua atividade antioxidante entre 2 e 20 min. A rutina, um composto

polifenólico natural e antioxidante, não apresentou resultados por ser considerada muito hidrofílica para permear a barreira cutânea e realizar sua ação (log K_{ow} = -1,3).

Assim sendo, os dados constantes na literatura até o momento do presente trabalho não definem o perfil de permeação cutânea do piceatanol e, sabendo-se que seu comportamento é condicionado a fatores externos às características da própria molécula, ensaios de permeação cutânea em condições estabelecidas tornam-se fundamentais para o desenvolvimento de formulações tópicas efetivas. Entendendo-se, pelos dados disponíveis até este momento, que a difusão do piceatanol pela pele pudesse vir a ser um gargalo no desenvolvimento de um produto tópico, optou-se pela avaliação do efeito concomitante da presença de uma molécula promotora de permeação.

Os promotores de permeação são compostos que interagem com a pele e geram diferentes efeitos, tais como o aumento de fluidez do manto lipídico, a formação de poços de ativo entre os lipídeos, a extração dos lipídeos, a desnaturação ou modificação da conformação das proteínas ou a modificação do domínio aquoso do estrato córneo. Conhecidamente, existem mais de 350 compostos que agem como promotores de permeação, alguns deles sendo o ácido oleico, o diethylene glycol monoethyl ether (Transcutol®), o propilenoglicol, o etanol, dimethyl isosorbide, ureia e derivados, azona e derivados, ácidos graxos, fosfolipídeos, isopropyl myristrate e alguns terpenos [74, 75].

Além dos citados, outro promotor de permeação é o espilantol (Figura 9A), composto já aplicado em cosméticos e presente nas partes aéreas de *Spilanthes acmella* ou *Acmella oleracea* (Figura 9B), conhecida popularmente como jambu no Brasil. O espilantol pode ser extraído do material vegetal por solventes com uma gama de polaridades, desde hexano até misturas de MeOH:H_2O, dado o fato de esta molécula ser anfifílica.

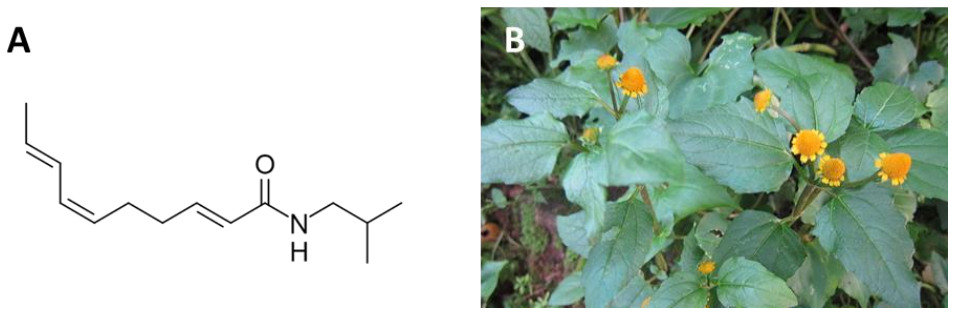

Figura 9: A. estrutura molecular do espilanol. B. flores de *Spilanthes acmella* [76]. ക്രാക്രൗർ, CC BY-SA 3.0 <https://creativecommons.org/licenses/by-sa/3.0>, via Wikimedia Commons.

A revisão de Barbosa et al. [77] sobre o espilantol cita produtos comerciais com atividade antienvelhecimento (Gatuline, SYN-COLL, ChroNOline) e declara a existência de cerca de 30 patentes que descrevem produtos de *skincare* feitos a partir de uma variedade de espécies de *Spilanthes.* Estes produtos têm a característica de inibir contrações em músculos subcutâneos, promovendo um efeito antirrugas, ou *botox-like* [78].

Os efeitos do espilantol sobre rugas vêm sendo corroborados por estudos recentes. Savic et al. [79] realizaram uma otimização de um sérum antirrugas com extrato de jambu, chegando em uma formulação com 15 % de emolientes e 1 % de emulsificantes. Os testes *in vivo* revelaram ausência de potencial irritante, indicando uma tolerância/ segurança preliminar. Além disso, uma melhora nos parâmetros de rugas da pele nas regiões ao redor dos olhos e boca foi observada em apenas 2 semanas de uso do sérum. Ye e colaboradores [80] também realizaram um trabalho *in vivo* com uma formulação contendo retinol e o extrato de jambu. Em chinesas, a formulação foi aplicada ao redor dos olhos e, após 6 semanas de uso, houve uma redução do valor do índice de melanina e um aumento do índice de claridade. Uma redução das rugas e um aumento da firmeza da pele também foram observados.

Os extratos de *S. acmella* e o espilantol apresentam outras atividades também interessantes para aplicações cosméticas. Wu [81], Abeysiri [82], Abeysinghe [83] e Barbosa et al. [77] relatam as atividades antioxidante e anti-inflamatória dos extratos de *Spilanthes*. Paulraj et al. [84] também revisaram o assunto e revelam que, popularmente, plantas do gênero *Spilanthes* são usadas, em casos de inflamação, ferimentos e lesões de mucosas. Neste caso, infusões ou decocções das partes aéreas ou raízes são administradas por via oral ou tópica, por meio de compressas ou banhos. O trabalho de Moro et al. [85] mostra que o extrato de jambu a 20 % é capaz de favorecer a capacidade de produção e organização do colágeno em tendões lesionados em ratos. Trazendo para o universo da aplicação como um ativo para a proteção da pele, este estudo indica um potencial uso do jambu para a reconstrução da derme, embora testes comprobatórios sejam necessários.

Stein et al. [86] mostraram evidências sobre a atividade anti-inflamatória dos extratos de folhas e flores do jambu, associando esta ação à inibição da enzima quimase, à supressão do NO, uma citocina pró inflamatória, e à atividade antioxidante. Considerando

que o envelhecimento cutâneo de causas extrínsecas possui um componente inflamatório, o extrato de jambu poderia, eventualmente, atuar em sinergia ao extrato de sementes de maracujá neste sentido, sendo uma possível associação vantajosa nos cuidados com a pele.

Quanto à ação promotora de permeação, De Spiegeleer et al. [87] avaliaram o efeito de aumento da permeação cutânea da cafeína, da testosterona, do ibuprofeno e de seis micotoxinas na presença de espilantol. Os ensaios de permeação cutânea e cinética de difusão realizados em pele humana mostraram que o espilantol promoveu um aumento de permeação componente e concentração dependente, aumentando a permeação da testosterona, da cafeína e das micotoxinas de baixa massa molar.

Diante das propriedades expostas, o extrato de jambu, rico em espilantol, mostrou-se como um candidato interessante a ser avaliado em conjunto com o piceatanol do extrato de sementes de maracujá, tanto por seu papel de promotor de permeação cutânea, quanto por suas propriedades bioativas. Por este motivo, ele foi associado às formulações que compõem esta tese.

As formulações de protetores solares estão disponíveis na forma de loções, cremes, bastões, géis, óleos, manteigas, pastas e *sprays*. Em geral, emulsões e suspensões são as formas cosméticas mais predominantes deste produto no mercado, destacando-se também os géis e pós, para peles oleosas, e os aerossóis, que proporcionam fácil aplicação. Independentemente da forma eleita, o desenvolvimento de um produto cosmético passa pelas etapas de planejamento, que envolve a geração de ideias e pesquisas de matérias-primas e produtos concorrentes, a geração de conceito, que traduz as necessidades dos consumidores em atributos do produto, o desenvolvimento da formulação per se, que gera um protótipo para avaliação e ajustes e, por fim, o registro em órgão sanitário conforme a legislação local e a comercialização do produto [88, 89].

No estágio de protótipo, o estudo de estabilidade é de fundamental importância para garantir que o cosmético atenda aos padrões de funcionalidade, estética, e qualidade física, química e microbiológica preconizados. Trata-se de um estudo que fornece indicações sobre o comportamento do produto exposto a condições ambientais no intervalo de tempo entre a fabricação e o término de sua validade [90, 91]. Para nortear a respeito da interação entre os extratos de maracujá, de jambu, e os filtros solares, optou-se pela

incorporação inédita destes ativos em um emulgel como formulação protótipo, e as considerações sobre a estabilidade físico-química das combinações propostas estão descritas no **CAPÍTULO 3** desta tese.

Entendendo-se a necessidade de difusão do piceatanol e do espilantol pelas camadas da pele para o potencial exercício de suas atividades observadas em culturas celulares, estudos de permeação cutânea *in vitro* foram realizados com as diferentes combinações entre os ativos como forma de se avaliar a funcionalidade dos protótipos propostos neste trabalho. O **CAPÍTULO 4** trata do perfil de permeação exibido pelo piceatanol, do extrato da torta de semente de maracujá, quando na presença dos filtros solares e do espilantol proveniente do extrato de jambu sobre um modelo sintético, não baseado em animais, para predição da potencial interação entre eles *in vivo*.

Por fim, apresenta-se uma **DISCUSSÃO** acerca das constatações e aprendizados dos capítulos anteriores, buscando nortear quais seriam os passos necessários para a obtenção de um produto cosmético baseado nestes ativos, e a **CONCLUSÃO** destaca os principais ensinamentos deste trabalho.

OBJETIVOS

OBJETIVOS

Dados os entendimentos de que:

(i) para uma proteção holística da pele contra os danos causados por fatores externos, é interessante combinar ações de bloqueio, de reforço e de reparo, e considerando que estas duas últimas requerem a difusão dos ativos por camadas mais profundas da pele;

(ii) o piceatanol é um composto fenólico vegetal com grande potencial para agir no reparo da pele e no reforço ao arsenal antioxidante natural, mas que apresenta dificuldades de administração tanto oral quanto tópica no que compete à entrega aos sítios de ação;

(iii) as sementes do maracujá são uma fonte brasileira importante e pouco explorada de piceatanol;

(iv) as partes aéreas de jambu contêm espilantol, que possui propriedades dermocosméticas e de promoção de permeação de ativos pela pele;

(v) atualmente, o bloqueio da radiação solar em formulações se dá por meio de filtros solares orgânicos e inorgânicos;

o OBJETIVO PRINCIPAL deste trabalho foi o de se estudar a interação entre o extrato de sementes de maracujá e das partes aéreas de jambu em formulações fotoprotetoras tópicas no que se refere à estabilidade e à permeação cutânea.

Para se alcançar o objetivo principal, os seguintes OBJETIVOS ESPECÍFICOS foram vislumbrados:

(i) explorar a viabilidade da extração assistida por micro-ondas (MAE) como uma técnica alternativa às já descritas na literatura e passível de escalonamento para a produção do extrato de sementes de maracujá rico em piceatanol, com vistas a agregar valor à cadeia produtiva deste fruto;

(ii) avaliar a estabilidade físico-química dos extratos de semente de maracujá e das partes aéreas do jambu em uma formulação tópica contendo, ou não, filtros solares orgânicos ou inorgânicos na composição, tendo-se

optado, como base, por uma emulsão formada por tensoativo não iônico e estabilizada por agente de consistência baseado em lecitina e polímeros de acrilato;

(iii) avaliar o perfil de permeação cutânea do piceatanol solo, ou na presença do extrato de jambu e dos filtros solares, tendo-se elegido a membrana Strat-M® (Merck Millipore) como modelo de pele.

Para alcançar estes objetivos, métodos analíticos quantitativos foram desenvolvidos por HPLC-MS/MS e UHPLC-DAD, e outras técnicas analíticas como a espectrofotometria UV-vis, a centrifugação analítica, análises de calorimetria exploratória diferencial (DSC), de termogravimetria (TGA) e a microscopia Raman confocal foram empregadas neste trabalho.

CAPÍTULO 1

In vitro diffusion of plant phenolics through the skin: a review update

IN VITRO DIFFUSION OF PLANT PHENOLICS THROUGH THE SKIN: A REVIEW UPDATE

Gisláine C. Silva[1], Rodney A. F. Rodrigues[2], Carla B. G. Bottoli[1*]

[1]Institute of Chemistry, University of Campinas (Unicamp), POB 6154, 13084-971, Campinas, SP, Brazil.

[2]Chemical, Biological and Agricultural Pluridisciplinary Research Center (CPQBA), University of Campinas (Unicamp), 13148-218, Paulínia, SP, Brazil.

*Corresponding author: carlab@unicamp.br

Abstract

OBJECTIVE: The excessive skin exposure to harmful environmental factors leads to inflammation, molecular and cellular damages which disrupt its function, appearance, and health. Preventing or reversing the damages by the topical administration of antioxidants and other compounds is a reasonable strategy, and many plant-based phenolic compounds exhibit free radical scavenging and tissue repair properties. The challenge, however, is to topically deliver these compounds to the correct skin site, and predicting their skin diffusion aids in guiding for the best strategies. Therefore, this article reviews the latest publications on *in vitro* skin diffusion profiles of plant-derived phenolic compounds to give an insight into their behavior in solutions, suspensions, and formulations.

METHOD: The data on plant extracts and isolated plant phenolic compounds *in vitro* skin diffusion assays published over the last six years was compiled and discussed.

RESULTS: Even though the gold standard Franz diffusion cell is the most commonly used method in the assessment of *in vitro* plant phenolic skin diffusion profile, a plethora of skin models and assay conditions is reported for a variety of compounds and extracts in different vehicles.

CONCLUSION: The multiplicity of models and vehicles place an obstacle to establishing correlations among the available data on plant phenolic compounds, but some general statements based on molecular, vehicle and skin features could be made on the basis of the collected information.

Keywords: delivery, skin barrier, chemical analysis, plant phenolics, *in vitro.*

Introduction

Plant phenolics are one of the most widespread classes of molecules found in nature. Today, there are over 8,000 identified phenolic structures with different complexities, and they are classified into categories such as phenolic acids, flavonoids, tannins, stilbenoids and lignans, according to their molecular structures. Plant phenolics are generally involved in color, growth, defense against ultraviolet radiation or pathogens, and other regulatory processes required for plant survival [1–4].

Since plants are part of the human diet, plant phenolics can benefit human organs and physiology. In particular to the skin structures, these compounds exhibit antioxidant, antimutagenic, chelation, and free radical scavenging properties. There is experimental evidence that polyphenol-rich extracts from plants and algae suppress inflammatory signaling pathways and decrease the levels of reactive oxygen species (ROS) in cells and tissues. They also induce the expression of enzymes related to oxygen metabolism and such features are of major importance as the skin is in direct contact with the air components, pollutants, and mainly with UV light, which promote the generation of ROS and reactive nitrogen species (RNS). The excessive exposure to environmental factors, combined with the natural decrease of the cellular metabolism over the years, may lead to an oxidative imbalance in the skin structure, triggering inflammatory processes, molecular and cellular damages. Skin barrier deficiencies, wrinkles, dryness, laxity, and different types of cancer emerge as a result of these processes, and plant phenolics are interesting candidates for skin protection against these problems due to their bioactive properties [3, 5–9].

The delivery of plant phenolics into deeper skin layers, though, is challenging. The oral consumption of vegetables, fruits and beverages, may not offer 100 % of the plant phenolic compounds to the sites of action inside the human body, as they may undergo degradation or be poorly absorbed from the digestive tract into the bloodstream. Also, they may suffer biotransformation reactions and be excreted before reaching the skin structures. Meanwhile, the skin’s stratum corneum (SC) is a limiting barrier to their diffusion through the viable epidermis and dermis, and the physicochemical instability of some of these molecules raise challenges in formulating topical products [4, 5, 9, 10].

The preferrable features for a molecule to diffuse through the skin are a molecular weight (MW) lower than 500 Da, a melting point lower than 200 °C, a log P between 1 and 3, and a proper solubility in water and oils. But beyond the molecular features themselves, the skin barrier may present a permeation variability depending on age, gender, ethnicity, body area, diseases, impairments, and hydration level. As a matter of fact, depending on how hydrated the SC is, its thickness may vary from 10 to 40 μm and, in general, molecules can passively overcome the SC by three main routes: from the most to the least expressive one, they cross the SC structure via intercellular (or paracellular), trans follicular, and transcellular (or intracellular) pathways. The skin hydration may modulate the extent of diffusion and the preference of a molecule for each route [11–13].

Notwithstanding the knowledge in the molecular properties and skin attributes, the vehicle in which a compound is inserted into may change its predicted performance. Hence, it is hard to state features which ensure how a compound will behave in contact with the skin, and prediction depends on experimental data. *In vitro* models for this evaluation have been developed and adapted throughout the years for data assessment of many compounds, and an array of protocols and assay arrangements have been reported, turning the discussion even less trivial. Therefore, in this review article, the published information on plant phenolics skin in vitro diffusion in a six-year span (2017-2022) is presented and discussed in terms of the nature of the compounds, the vehicles, the skin models employed in the investigations and the resulting behavior in each case.

In vitro skin diffusion assays

The Franz cell permeation assay is the current gold standard *in vitro* evaluation of how a molecule diffuses through the skin. The cell was developed in 1970’ and it consists of a donor and a receptor chamber separated by a diffusion membrane. Some variations of the Franz cells, such as the flow-through Bronaugh and Stewart cells and Skin-PAMPA (Parallel Artificial Membrane Permeability Assay), which is a 96-well plate high-throughput version with a mimetic SC membrane have been developed, but they all share the same concept of a donor and a receptor chamber separated by a membrane that represents the skin [11–15].

The membrane choice is the first variable introduced to the experimental arrangements. The use of *ex-vivo* models form human and animal sources are commonly reported and, with the advances on *in vitro* cellular cultivation, the employment of skin cells monolayers (2D models), 3D epidermis (RHE) or full-thickness laboratory made skins as membranes have also been explored in skin diffusion tests. Synthetic membranes made of silicon, cellulose derivates, and polymers are generally used in *in vitro* release tests, which focus on how much a molecule is liberated from a vehicle. However, some variants containing SC lipids, such as ceramides, cholesterol, free fatty acids, and Strat-M™ (Merck Millipore, Burlington, Massachusetts, USA), a 3D structure made of three layers of polyester sulfone/ polyolefins with different diffusivities to mimic the skin environment, have been designed as alternatives to the animal skin for *in vitro* permeation tests [8, 11, 16–20].

A second variable is the fluid used in the receptor chamber. The fluid represents the bloodstream in the system and a suitable sink condition, in which the maximum concentration of the compound in the receptor fluid is less than 1/3 times its saturation point in it, must be guaranteed to avoid compound backflow to the acceptor chamber. Among the acceptor fluids, water or an aqueous buffer are chosen, and alcohol, surfactants, albumin, or other proteins can be added to enhance the solubility of the poorly water-soluble candidates provided that the membrane stability is preserved. [12, 16, 21].

A final source of options is related to the applied dose onto the membrane at the donor chamber. There are two types of assays: infinite and finite doses. In infinite dose, large quantities of the sample (>10 mg cm^{-2}) are placed over the membrane. A graph on the compound concentration in the acceptor fluid versus time is plotted, the curve is fitted to a linear model and the permeability is calculated according to Fick's law of diffusion by the following equation (eq. 1):

$$\text{Permeability (Papp)} = \text{Flux}/Cd \qquad \text{(eq.1)}$$

where Flux is calculated by the ratio between the slope of the model and the cross-sectional area of the membrane, and Cd is the initial concentration of the compound in the donor chamber. Finite dose experiments, on the other hand, use a limited sample quantity (1–5 mg cm^{-2}) and it is a simulation form of a real application of the product [16].

A summary of all the variables in the construction of an *in vitro* skin diffusion assay is presented in Figure 1. The dosage of the permeated compounds in the acceptor fluid and the remaining quantity at the donor chamber can be measured by chromatographic and spectroscopic methods. But the study can also be completed by a view of the compounds through the membranes, in some cases, by using microscopic techniques such as confocal laser scanning microscopy (CLSM), which requires labeling, or Raman spectroscopy, with no need for fluorescent molecules. In any case, a suitable analytical method must be developed and validated [11, 13].

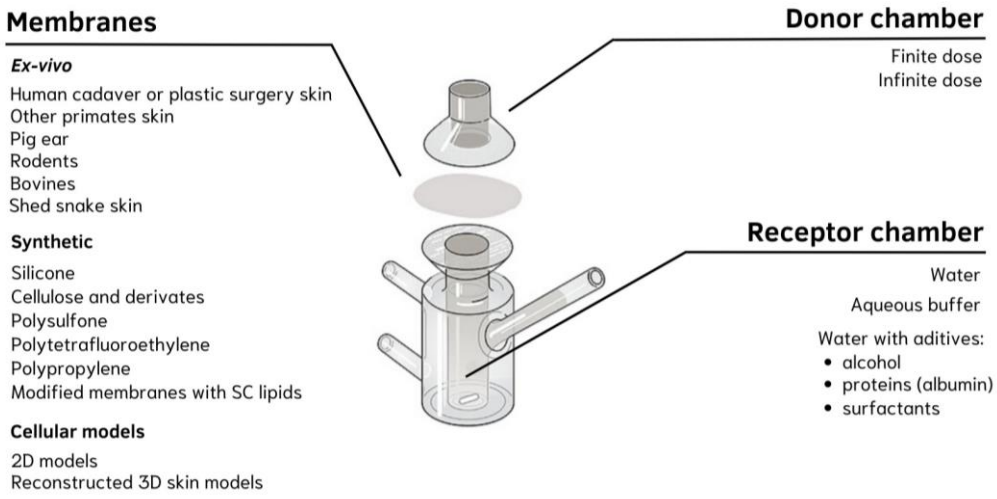

Figure 1: The basic scheme of a Franz cell and the multiple assay possibilities.

Plant phenolics permeation profile

In general, the plant phenolics diffusion profile though the skin has been assessed by loading the donor compartment with a solution, a suspension or a formulation containing them in their free form or loaded into micro-nano capsules, emulsions, or particles. Plant phenolics have been evaluated alone, in their isolated form, in combination with other isolated plant phenolics, and as whole plant extracts or their fractions. Now on, the aspects of the isolated compounds and the extracts will be presented in two separate topics.

Isolated compounds

Plant phenolics exist in a range of structures, and some of them occur as glycosylated species, with a sugar moiety attached at O or C atoms, or as aglycones, with no sugar linked to the molecule. Aside from sugars, other chemical functions such as prenyl and methoxyl units can also be found in their structures [4].

Phenolic acids, for instance, comprise a resonance stabilized structure which allows the donation of an H atom or the quenching of free radicals. They are well documented molecules with health protective properties as antioxidative, antimicrobial, anticancer, anti-inflammatory, anti-mutagenic, and others. In skin care, creams, face masks and serums comprising phenolic acids are recommended in cases of acne, seborrheic and atopic skin. Phenolic acids exist in a plethora of complexities and polarities, as can be inferred from Fig. 2. Most of the given examples fit the log P 1-3 and MW < 500 Da criteria to diffuse through the skin [22, 23].

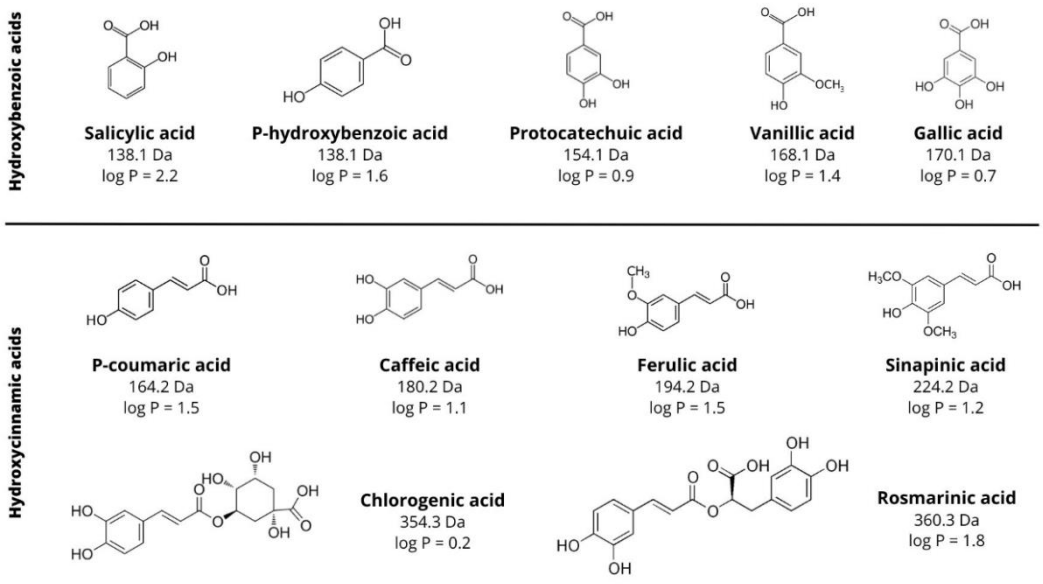

Figure 2: Phenolic acids molecular structures and properties.

Gallic acid (GA) is an example of hydroxybenzoic-derived acid. In Franz cells, GA in Poloxamer hydrogel presented different release and permeation profiles through a cellulose-polytetrafluoroethylene-cellulose membrane (CPC) and stratum corneum-epidermis from human breast (SCE), even though the total permeated GA

amount was nearly the same in both systems after a 9-hour period (23.8 and 17.7 μg cm-1 for CPC and SCE, respectively) [24].

In comparison to GA, caffeic acid (CA), a representative of the hydroxycinnamic-derived acids, lacks one hydroxyl group and presents an extra carbon linking the phenol ring to the carboxylic acid moiety. Emulsions and films have been formulated with CA in the range of 0.2 to 1 %, and their behavior has been assessed onto cellulose membranes and pig ear model. In the release tests, while 0.5 % CA emulsion showed the highest release in cellulose membranes after 30 min, results were statistically the same of 1 % CA emulsion after 1h. The films, on the other hand, did not exhibit a CA concentration interference up to 30 min, but the 1 % film stood out after 1 h of the experiment. The fact that the film formulation does not have micelles might have facilitated the release of CA: while 1 % emulsion released around 45 % of this compound, 1 % film allowed the release of nearly 60 % of it. In pig ear skin assays, the permeation percentage from the film excelled the emulsion after 2 h, and they became similar one another after 4 hours. In both cases, CA SC retention was higher than in the dermis and epidermis, but the amount of CA in SC found in film experiments was twice the quantity provided by the emulsion, probably due to a higher release in the beginning of the experiments and to an occlusion effect provided by this formulation [25].

In another strategy, the complexation of hydrogenated soybean phosphatidylcholine with p-coumaric acid, also classified into the hydroxycinnamic group, increased both the liposolubility and aqueous solubility of this phenolic acid. By including the complex into Carbopol 940 hydrogel, a 6-fold increase in p-coumaric skin permeation potential was obtained, contouring this phenolic acid inability to penetrate to deeper skin layers for an adequate photoprotective action [26].

Flavonoids are another class of plant phenolic compounds with a variety of chemical structures, and they also present anti-oxidative, anti-inflammatory, anti-mutagenic, anti-carcinogenic, and enzymatic modulation properties. They all share the flavan nucleus as a basic skeleton (Fig. 3) and, depending on the C ring position to which the B ring is attached to, and on the C ring level of unsaturation and oxidation, the flavonoids can be classified as isoflavones, flavones, flavonols, flavanones, flavanonols, flavanols or catechins, anthocyanins and chalcones [27].

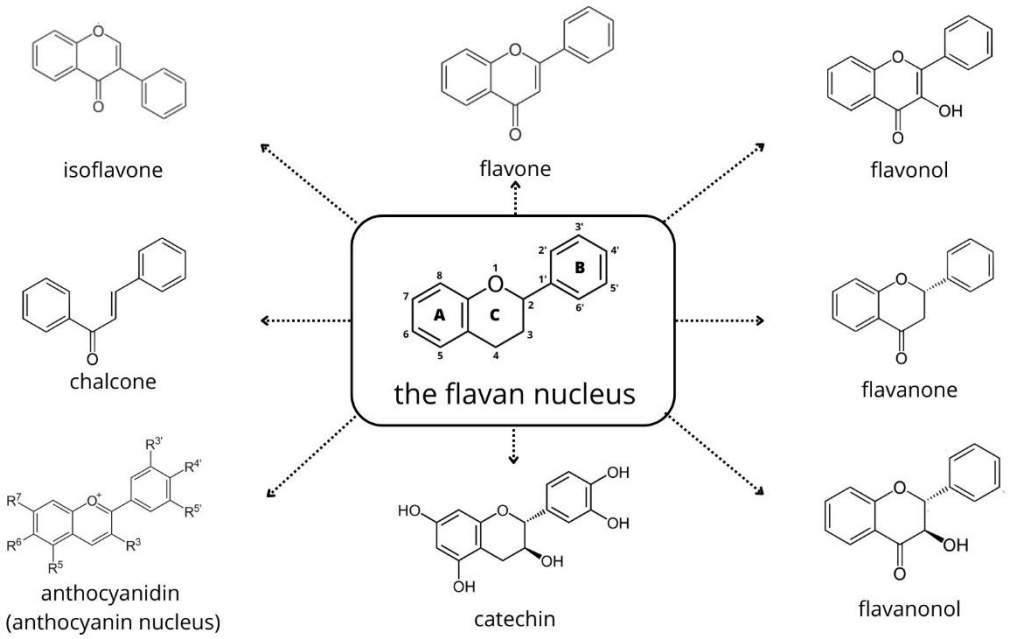

Figure 3: flavonoids base structures

An insight on how flavonoids interact with the skin components was presented by Chuang et al., who evaluated the behavior of eight aglycones or glycosides in Franz cells. Saturated solutions or 6 mmol L^{-1} suspensions of each flavonoid were prepared in 20 % PEG 400 pH 7.4, and they were applied onto full-thickness mouse, baby pig skins, and in disrupted mouse skins after the removal of SC, lipid, sebum, or proteins. Among the aglycones, naringenin (272.3 Da, log P = 2.61), which was extremely soluble in the vehicle, and kaempferol (286.2 Da, log P = 1.96) exhibited the highest skin retentions, while myricetin (318.2 Da, log P = 1.42), the most polar of them, showed the lowest one. The glycosides showed minor skin deposition and the highest fluxes, especially in pig skin. On SC removed mouse skin, the depositions of myricetin and quercetin were 30 % higher, and, in desebumed skin, the overall deposition of flavonoids increased 2 to 6-fold in relation to the full thickness skin. The protein removal had a lower effect when compared to lipid removal in this sense. Hence, SC and sebum, especially the interaction of aglycones with cholesteryl sulfate, seem to have the highest influences on the flavonoids skin diffusion profile. Also, the molecular flexibility of certain flavonoids could lead to a better diffusion than those which present a planar structure [28, 29].

Indeed, naringenin (NG) is a highly water-soluble flavanone with a flexible C-ring. Its permeation was enhanced 13-fold in a barrier defective skin model simulating a psoriatic skin. But computational molecular studies indicated that flavanones with lower hydrogen bond number, total polarity surface, and molecular volume were more prone to diffuse through the skin, as certified by *in vitro* experiments with pig dorsal skin. In a comparison between NG and flavanone, a higher skin absorption was observed for the latter. NG prenylation at the position 6 still allows an *in vitro* 2.15 % degree of permeation into human abdominal skin from a 70 % EtOH solution in 24 h. In the 6-prenylated NG, the substitution of position 7 -OH to a -OCH3 group, or the change positions 5 and 7 -OH for CH3-COO- implies in full skin retention, with no detection at the receptor fluid [30, 31].

Quercetin (QCT, 302.2 Da, log P = 1.5), on the other hand, is a planar molecule of the flavonol subclass. It is known as one of the most potent natural antioxidants, but its low water solubility is deemed as an obstacle for topical bioavailability. Some formulation strategies, however, allow QCT diffusion through the skin. QCT nanocrystals in nanosuspension containing Tween 80 and Poloxamer 188 as dispersants was able to accumulate at the SC and the epidermis of newborn pig skin membranes in Franz cells, being also found at the dermis level. The crystals small size and the dispersants penetration enhancement effect may have been responsible for this performance. In formulations where QCT is soluble, its diffusion was also observed. As a matter of fact, in hydrogels of sodium alginate and polyvinyl alcohol provided an increased penetration and a decreased permeation of QCT in pig ear SC compared to quercetin-mygliol solution. In amphiphilic creams and acidic carbomer gels, QCT presented higher release values when the formulations were added with propylene glycol (PG) or polyethylene glycol 400 (PEG 400). These modifiers, however, promoted different effects on the diffusion of QCT through a pig ear skin membrane in Franz cells, as PEG 400 retarded QCT diffusion in relation to PG, but there has been permeation in both cases to some extent. The addition of olive oil to a hydrogel system was also able to improve in 2-fold QCT release and permeation in mice dorsal skin membranes [32–35].

Interestingly, besides these formulations, QCT itself acted as a skin permeation enhancer for the topical delivery of transferomes containing meloxicam, a lipophilic non-steroidal anti-inflammatory agent. Transferomes, a type of deformable

liposomes, are spherical vesicles delimited by at least one phospholipid bilayer with surfactants embedded in it, and the addition of QCT and dihydroQCT (DHQ) enhanced the meloxicam transferomes diffusion through a full thickness dermatomed human cadaver skin model. Higher amounts of DHQ were found in the epidermis, but both flavonoids reached to the dermal layer under these circumstances [36].

Aside from molecular flexibility and lipophilicity, molecular weight issues can also be contoured according to the formulation composition. Anthocyanins, for example, are anthocyanidin glucosides; hence, they are water soluble compounds. They exist in a range of MW, from lower than 500 Da to higher than 1000 Da, and they are used as food colorants, while numerous *in vitro*, animal, and human studies have demonstrated their free-radical scavenging ability, antimicrobial and anti-inflammatory properties, and the interaction with key enzymes involved in the role of several human diseases, opening an opportunity for the nutraceutical and cosmetic industries. When topically applied In a lipstick base, which is manly a lipophilic environment, a better penetration of lower MW compounds (449–581 Da) was observed *in vitro*, in porcine ear skin, and in human volunteers as expected, but higher MW substances (933-1019 Da) could be found at relevant depths of SC in both assays, even though they do not fit into the <500 Da premise [37–39].

Resveratrol (RVT, Fig. 4), a stilbene, is another notable polyphenolic compound which has attracted the attention of many health professionals due to its beneficial actions to the human body due to its anti-inflammatory and antioxidative properties, being sold as a dietary supplement. RVT is known as a potent lipophilic antioxidant, and it also presents some molecular flexibility as well. Onto pig skin in vertical Franz cell, however, resveratrol remained at the uppermost layers of SC after 24 h when a 5% (v/w) in 70 % ethanol solution was applied onto the skin. The same results were observed *in vivo*, in six healthy women from 25 to 42 years old, phototypes II to IV, treated in the forearm with 10 μL cm^{-2} of the same solution. In the presence of free fatty acids-rich pomegranate seed oil (PSO) or isopropyl palmitate (IP), RVT transdermal transport into pig ear skin *in vitro* was observed, PSO being superior to IP in speeding up this process [40, 41].

Other strategies to enable RVT topical application have been reported, such as its loading into liquid crystalline nanoparticles [18] or niosomes [42]. These particles, included in gel or creams, enhanced RVT transdermal permeation. On the

other hand, microemulsions [43], pickering emulsions [44], gel dispersed solid-lipid nanoparticles [45], and ultra-deformable vesicular cream [46] allowed, in general, RVT sustained release and relatively lower diffusion through the membranes [47]. The addition of permeation enhancers like highly lipophilic terpenes in nanoemulsions, though, can improve RVT translocation through the skin.

The sustained release effects have been reported with other plant phenolics included in particles, vesicles and micro/nanoemulsions as well (Table I), but it is important to highlight that the diffusion, in these cases, are governed by factors as particle size, shape, surface charge density, composition and other parameters not directly related to the molecular structure of the plant phenolic compound per se [48].

Table 1: micro and nano encapsulated plant-derived phenolic compounds diffusion assays and results.

Phenolic compound	Type of entrapment	Vehicle	Diffusion device	Membrane	Receptor fluid	Analytical technique	Results	Reference
Caffeic acid	Chitosan microparticles from hydroalcoholic (MPI) or aqueous (MPII) solutions	Dispersion, film, and emulsion	Franz cell	Cellulose Human abdominal epidermis	pH 5.5 phosphate buffer with ethanol (50:50)	HPLC-UV	MPII was spherical with a smooth surface and exhibited a slower and more controlled release than MPI (porous with non-internalized residual material).	Spagnol et al. [54]
Apigenin	Nanoemulsion	Carbopol-based nanoemulsion gel with tamarind gum emulsifier	Franz cell	Cellophane Full-thickness goatskin	pH 5.5 phosphate buffer	UV-vis spectrophotometer Confocal laser scanning microscopy	52.90 ± 0.95 % of drug release and 0.74 ± 0.05 % of drug retention after 24 h.	Jangdey, Gupta, and Saraf [49]
Curcumin, thymoquinone and resveratrol	Nanoemulsion	Carbopol-based nanoemulsion gel with oleic acid	Franz cell	Rat skin	pH 7.4 phosphate buffer with isopropyl alcohol (8:2)	UHPLC-PDA	Percentage of cumulative amount: Curcumin: 24 ± 1.04% Thymoquinone: 35.01 ± 2.78 % Resveratrol: 31.17 ± 1.56 %	Khatoon et al. [50]
Curcumin	Nanoemulsion	Carbopol-based nano emulsion gel with Labrafac and Transcutol	Dialysis tube Franz cell	Dialysis membrane (12-14 kD) Rat skin	pH 7.4 phosphate buffer with ethyl alcohol (5%)	UV- vis spectrophotometry	66-82 % release after 24 h (12 % when in aqueous suspension) 7-fold skin deposition in comparison to gel formulation.	Algahtani, Ahmad, and Ahmad [17]
Curcumin and resveratrol	Cyclodextrin nanosponges	Hydrogel with carbomer and propylene glycol	Franz cell	Cellulose Pig ear skin	Phosphate buffered saline and methanol (1:1)	HPLC	The nanosponges enhanced the in-vitro release in 10 and 2.5 folds, and the skin permeation in 11.5 and 2.4 folds for curcumin and resveratrol, respectively.	Pushpalatha, Selvamuthu-kumar and Kilimozhi [51]

Curcumin	Microemulsion	Tween 80®, Span 20, lauric acid, isopropyl myristate, water	Franz cell	Human skin (breast or abdomen)	Fetal bovine serum and PBS (pH 7.4) (1:9, v/v)	Fluorescence spectroscopy (microplate reader)	Curcumin-loaded microemulsions and curcumin dissolved in DMSO both penetrated the dermis in a significantly similar manner and elevated quantity.	Greenwald et al. [52]
Curcumin	Supramolecular hydrogels	Micelles of methoxy poly (ethylene glycol)-block-poly (ε-caprolactone) (MPEG-PCL) in α-cyclodextrin solution.	Franz cell	Dorsal mice skin	PBS solution (pH 4.5) containing 5% of tween-80.	Confocal fluorescence microscopy HPLC	The skin deposition weight of curcumin in the curcumin-loaded micelles hydrogel group was 6.23-folds higher than that in the control group (extra micellar curcumin).	Zhou et al. [53]
Epigallocatechin-3-gallate (EGCG) and silibinin	Peptide dendrimers	Phosphate buffer pH 7.4 for silibinin and phosphate buffer pH 6.8 for EGCG.	Franz cell	Abdominal rat skin	Phosphate buffer pH 7.4 for silibinin and phosphate buffer pH 6.8 for EGCG.	HPLC	EGCG 9.82-, 2.04-, and 1.72-fold and silibinin 3.96-, 1.81-, and 1.06-fold increase in skin permeation was observed from peptide dendrimer complex, simultaneous application of compound + peptide dendrimer, and pretreatment of skin with peptide dendrimer, respectively, in comparison with passive diffusion.	Shetty et al. [55]
EGCG	Transferomes (soy phosphatidylcholine and sodium cholate)	Milli-Q water	Franz cell	Abdominal rat skin	Phosphate buffer pH 6.8	HPLC-UV	EGCG alone transfeormes: 2.8-times enhancement in EGCG permeation when compared to plain solution. EGCG with hyaluronic acid: 3.5 times and 1.25 times permeation enhancement in relation to plain solution and EGCG alone transfersomes, respectively.	Avadhani et al. [56]

Genistein	Microemulsion	-	Franz cell	Dermatomed human skin	PBS (pH 7.4): EtOH 8:2	HPLC-UV	Microemulsion with 20% water exhibited 4- and 9-fold higher flux, and 2- and 4-fold higher skin retention as compared to the microemulsion with no water and aqueous suspension, respectively.	Chen et al. [57]
Morin	Phospholipid complex	Carbopol 940 hydrogel	Dialysis Franz cell	Dialysis bags (MWCO 14,000 Da) Dorsal rat skin	PBS, pH 7.4 PBS (pH 7.4): MeOH 70:30 (v/v)	HPLC-UV	Phospholipid complex retarded the release of morin and enhanced the cumulative amount of morin that crossed the skin after 30 h by 2-times in relation to morin gel. The presence of oleic acid and isopropyl myristate in the formulation resulted in higher flux enhancement, but no statistical difference was observed with menthol, azone, oleic acid, or isopropyl myristate after 30 h of treatment.	Yu, Wan, Sun [58]
Naringenin	Nanostructured lipid carriers (NLCs)	Carbopol 940 hydrogel	Franz cell	Cellulose nitrate Collagen	EtOH:water (1:1, v/v)	UV- vis spectrophotometry	NLC system offers a significantly enhanced release of naringenin compared to that of the emulsion. The gel formulation based on the NLC system offered better permeation of naringenin (70 mg cm2) than the emulsion system (58 mg cm^{-2}).	Badea et al. [59]

Orobol	Solid lipid nanoparticles (SLNs) and nanostructured lipid carriers (NLCs)	-	Keshary–Chien diffusion cells	Strat-M Human cadaver skin	PBS containing SDS (0.5%, w/v)	LC-MS/MS	The amount of orobol deposited into the Strat-M membranes from the SLNs and NLCs formulations was significantly enhanced compared to the suspension group at 3 h and 6 h. Similar to the results using artificial membranes, the deposited amount of orobol into human cadaver skin from formulations containing shea butter was significantly higher than that from the suspension group at 6 h.	Kim et al. [87]
Quercetin	Essential oil-based microemulsions (SMEDDS)	Deionized water	Franz cell	Dorsal rat skin	saline:ethanol 8:2	HPLC-UV	The essential oil-based microemulsions could enhance the permeation capacity of quercetin by 2.5–3 times compared to the aqueous solution.	Lv et al. [60]
Quercetin and Resveratrol	Nanostructured lipid carriers (NLCs)	Gel	Franz cell	Strat-M Rat skin	PBS, pH 7.4	UV- vis spectrophotometry Confocal laser scanning microscopy	NLC provided deeper permeation (30 µm) in comparison to gel (10 µm).	Imran et al. [61]
Resveratrol	Microemulsion	-	Franz cell	Polysulfone Strat-M	PBS (pH 7.4):MeOH 70:30 (w/w)	HPLC	Microemulsions allowed sustained and relatively low permeation of resveratrol.	Das et al. [43]
Resveratrol	Pickering emulsions stabilized by chitosan/gum Arabic nanoparticles	-	Franz cell	Cellulose acetate Pig skin	EtOH:H2O (1:1) containing 5 g L-1 of Tween 20®	HPLC Confocal laser scanning microscopy	Pickering emulsions allowed slower release, higher cutaneous retention, and lower permeation of resveratrol, in comparison with a 20% (v/v) ethanol solution (control).	Sharkawy et al. [44]

Resveratrol	Solid lipid nanoparticles (SLN)	Gel	Franz cell	Abdominal human cadaver skin	Phosphate buffer pH 7.4 with 1% Tween 80	HPLC-UV	The amount of drug permeated through the skin at the end of 24 h from the SLN gel was lower than from the plain gel, but SLN gel allowed higher skin retention of resveratrol.	Shrotryia, Ranpise, Vidhate [45]
Resveratrol	Liquid crystalline nanoparticles (LCNPs)	-	Franz cell	Dialysis bags Mouse skin	PBS (pH 7.4): EtOH 99:1	UV- vis spectrophotometry	Up to six-fold enhancement in the transdermal permeation of resveratrol-loaded LCNPs compared to its suspension.	Badie, Abbas [18]
Resveratrol	Ultra-deformable vesicular cream (phospholipid and sodium cholate)	O/W cream	Franz cell	Pig skin	EtOH:H2O (1:1)	HPLC-UV	Higher drug deposition in the skin via vesicular cream formulation in comparison to conventional cream.	Arora, Khurana, Nanda [46]
Resveratrol	Nanoemulsion	Carbopol 940 hydrogel	Franz cell	Rat skin	Phosphate buffer (pH 6.8)	Confocal laser scanning microscopy UV- vis spectrophotometry	Resveratrol deposition in rat skin: nano emulsion = 45.65 ± 4.76%, nano emulsion gel = 62.65 ± 4.98%, conventional gel = 33.42 ± 2.14%, and conventional dispersion = 22.42 ± 1.32%. CLSM studies confirmed the deposition of resveratrol from nanoemulsion gel in rat skin epidermis and dermis.	Sharma et al. [62]
Resveratrol	Niosomes	Carbopol 934 hydrogel	Franz cell	Dialysis bags Rat skin	EtOH:H2O (1:10)	UV- vis spectrophotometry HPLC-UV	Niosomal gel formulation exhibited 4.85 times higher cutaneous delivery than the plain drug suspension.	Negi et al. [42]
Resveratrol	Ethosomes	Carbopol 934P hydrogel	Franz cell	Pig ear skin	Buffer (pH 7.4) and ethanol (70:30)	UV- vis spectrophotometry	Resveratrol permeation rates from the optimized ethosomal formulation and ethosomal hydrogel were 2.18 and 2.04 times higher than the conventional cream	Arora and Nanda [63]

							formulation. These formulations exhibited the highest skin retentions among the ones tested (around 63 %).	
Rosmarinic acid	Nanoemulsion	-	Franz cell	Pig ear skin	Potassium phosphate buffer pH 7.4	UFLC-PDA	Porcine ear skin retention: 1.13 ± 0.19 μg cm^{-2}. No rosmarinic acid was detected in the receptor fluid after 8 h of experiment.	Fachel et al. [64]
Silibinin	Nanocapsules (pomegranate oil)	Gellan gum hydrogel	Franz cell	Mixed cellulose esters	Phosphate buffer (pH 5.5) and ethanol (70:30) or Phosphate buffer (pH 5.5)	HPLC-UV	A higher amount of silibinin was found at the receptor phase when in nanocapsules.	Marchiori et al. [65]

Curcumin (CUR, Fig. 4) is another plant phenolic compound with a great potential to aid in the treatment of skin disorders as psoriasis, ageing and atopic dermatitis. CUR is a lipophilic molecule with some limitations in terms of bioavailability and stability, and its inclusion into liposomes and other nanostructured lipid carriers, nanogels, nanoemulsions, micelles and nanoparticles have been evaluated as possible strategies to overcome these issues. But bare CUR diffusion profile through the skin has also been investigated in oleic acid solution, oleic acid organogels, and hydrogels prepared with the same organogel polymers. A gradual curcumin release was observed to all the formulations in a similar manner, and differences among the permeation profiles appeared after 12 h. The organogels provided the highest curcumin permeation rates and the lowest drug flux and permeability coefficient through the skin in *in vitro* experiments [66, 67].

Mangiferin (MGF, Fig. 4), a glucosyl xanthone found in mango and papaya, is also a poorly water-soluble antioxidant with a great potential to prevent skin disorders. In an infinite dose diffusion experiment taken with alcoholic and aqueous solutions through human cadaver skin in a flow-through cell, MG crossed SC and achieved deeper layers of the epidermis and the dermis, reaching to the acceptor fluid. Ethanol promoted twice the permeation of MGF in relation to the water, probably due to lipidic mantle disruption. The inclusion of MGF into a nanoemulsion with hyaluronic acid (HA) of different MW showed that the formulations low MW HA provided its highest permeation into pig epidermis, especially when combined with Transcutol-P®, and MGF release ability from ethosomes and their derivates, transethosomes and plurethothomes based in Pluronic F127, were also evaluated onto nylon membranes, showing that the last system, which was multilamellar, retained MGF with more efficacy than the other ones [67–70].

Phenolic-rich plant extracts

As with isolated compounds, phenolic-rich plant extracts have been evaluated in solutions, formulations and in micro/nano encapsulated forms. Since extracts comprise a mixture of compounds, a marker substance can be tracked across the skin for the evaluation of its diffusion performance. Alternatively, the behavior of multiple components can be observed at once.

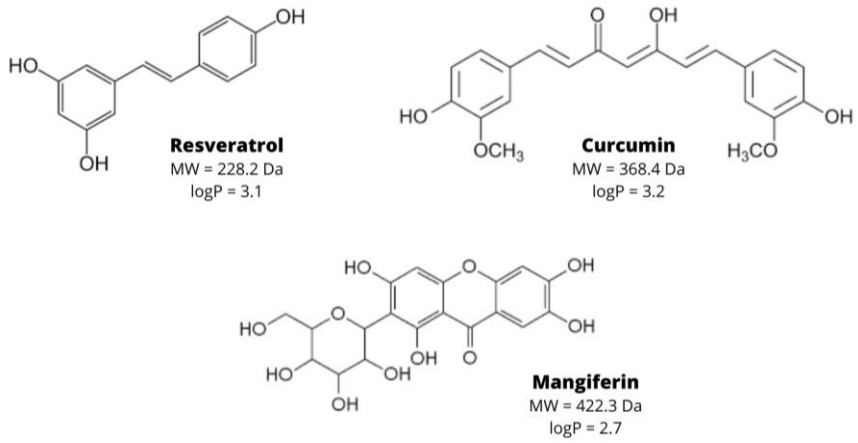

Figure 4: the molecular structures and features of resveratrol, curcumin and mangiferin.

African honeybush (Cyclopia sp.), for example, comprise hesperidin and mangiferin among its main phenolics, and both were used as markers for the permeation of water and 50 % ethanol solutions of green and fermented dried aerial parts on human dorsal skin. An infinite dose protocol in a flow-through cell was applied, and it was observed that hesperidin permeated poorly from the extract, while a moderate to high ability to cross the membrane was seen in solutions of the isolated compound. The capacity of mangiferin in reaching the acceptor fluid from the fermented honeybush extract was higher than from the green aerial parts extract after 24 h, showing that the extract composition modulates the behavior of its various components. [71]

The presence of solvents also influences the results. The recovery of bioactive compounds from plant material with natural deep eutectic solvents (NaDESs), for instance, is an emerging eco-friendly and low-toxicity technology. NaDESs are generally not removed from the extracts and the solvent constitution implies in different effects when applied onto the skin, as in the case of grape pomace anthocyanins recovered in betaine with citric acid (BET-CA), urea (BET-U), or ethylene glycol (BET-EG). On porcine ear skin in flow-through Franz cells, malvidin (331.296 Da, LogP = 2.02), the predominant anthocyanin, was determined in the acceptor fluid at within 24 h. BET-CA was the solvent that provided the best permeation of malvidin among the prepared NaDESs, even though extraction capacity of the evaluated

solvents were similar among them (BET-CA = 56.66; BET-U = 52.41; BET-EG = 51.69 µg of malvidin per liter of extract) [72].

The use of plant extracts in medical, pharmaceutical, and cosmetic formulations, though, has been increasing. Hence, *in vitro* product prototype testing may bring information on an extract performance in a proof-of-concept context. Catechins, for instance, exhibit free radicals scavenging activity, retard UV-induced extracellular matrix degradation, inhibit the production of metalloproteinases and activate collagen synthesis in the skin. Aside *Camellia* (green tea) species, *Byrsonima crassifolia*, a tree from the Amazon biome, contain catechin (CAT, 290.26 g mol^{-1}), epigallocatechin-gallate (EG, 458.37 g mol^{-1}), and quercetin 3-O-β-D-glucopyranoside (QG, 464.38 g mol^{-1}). B. crassifolia hydroethanolic leaf extract enriched fraction incorporated intro Aristoflex® gel and Hostacerin SAF® emulgel have been evaluated onto pig ear skin in Franz cells, and EG was detected at the dermis only in the gel + fraction case. CAT was retained inside the skin structures at 3.2 and 1.5 µg cm^{-2} when in gel and emulgel, respectively, but these values raised to around 5.5 µg cm^{-2} when these vehicles were loaded with the enriched fraction. [29, 73, 74]

Hydrogel was evaluated as a vehicle for 30 % propylene glycol Vitis vinifera and Vitis labrusca wastes extracts. The major compound, quercetin-3-o-glycuronide, was able to be released through a cellulose esters membrane, while anthocyanins and other flavonoids were retained in the hydrogel. In porcine skin, however, no permeation was detected. It is interesting to notice that the presence of propylene glycol, known as a permeation promoter, did not enhance the permeation of the phenolic compounds from *Vittis* under these circumstances. The hydrophilic environment might have prevented the release of the compounds into the skin. [75, 76]

Emulgels are a vehicle type which mix emulsions and gelling agents, and they are adequate for the delivery of hydrophobic molecules. Formulations composed of Carbopol 934P (C934P) and passion fruit (PF), sweet almond (SA), or andiroba (AO) oils were proposed as emulgels for the ethanolic propolis extract (PE) and the byproduct of the propolis extraction (BPE). All the combinations provided proper permeation of PE and BPE phenolic compounds, being the formulation with AO the one which best performed for PE by exhibiting prolonged release, permeation, and skin retention properties. [77, 78]

As in the case of the isolated compounds, the skin diffusion profiles of extracts included into microemulsions have also been assessed by *in vitro* experiments. The cumulative permeated amount of phenylethanoid glycoside (PHG) from a microemulsified *Herba cistanche* extract formulation on excised mouse skin was about 1.68 times higher than from PHG in saline solution. Conversely, the microemulsified methoxyflavones from Kaempferia parviflora extract were able to pass through newborn abdominal pig skin in different extents according to the limonene content, being the highest at 10 % limonene, followed by 5 % limonene, 1 % limonene, no limonene, and extract in water, but the addition of a gelling agent to the 10 % limonene formulation hindered their permeability, reversing the microemulsion permeation enhancer effect. The compositions of the external and internal phases of a microemulsion are also capable of modulating the extent to which a plant phenolic compound diffuse through the skin, as observed with microemulsions of a catechin-rich extract of *Eugenia dysenterica*. The application of an oil-in-water microemulsion onto porcine ear skin promoted double and triple the catechin content in the viable skin after 12 and 24 h, respectively, in comparison to the respective aqueous extract solution, and these values were higher than the ones obtained with the water in oil microemulsion, despite having bigger droplets than it [79–81].

Nanoemulsions of *Punica granatum* peel extract based on pomegranate seed oil (PSO) or medium chain triglyceride oil (MCT) did not allow gallic acid (GA), ellagic acid (EA), or punicalagin (PC) to reach the receptor fluid after 8 h of experiment on a porcine ear *in vitro* assay, even though it is known that nanoemulsions have a high potential to increase the transdermal delivery of molecules through the skin. However, it was shown that the retained amount of GA in the SC increased 2.2-fold in relation to the free extract solution. GA and EA contents found in the epidermis and dermis were 1.78 and 1.36 μg cm^{-2} and 1.10 and 0.97 μg cm^{-2}, respectively, when the PSO nanoemulsion was applied to the skin, and a similar behavior was observed when MCT was used in the formulation instead. Confocal microscopy images supported the findings about the capacity of the proposed nanoemulsion formulations to carry the active compounds through upper skin layers. [82, 83]

Ilex paraguariensis leaf extract polycaprolactone-based nanoparticles presented a similar behavior onto pig ear skin. The extract nanoencapsulation resulted in higher retention of its components into the skin, which could extend their antioxidant topical

effect, as it is composed of phenolic compounds, methylxanthines, flavonoids, and saponins. On the other hand, a nanostructured lipid carrier (NLC) gel of silymarin, a standardized extract of *Silybum marianum* which comprise taxifolin, silychristin, silydianin, silybins, and isosilybins, enhanced its permeation through rat skin and Strat-M^{TM} membranes in 3.7-fold after an 8 h period, possibly as a result of the particle nanosize, which might have led to an increase in silymarin solubility, and of the NLC composition itself, which might have modified the SC structure and facilitated silymarin passage to the deeper strata of the skin [84, 85].

Discussion

The plant phenolic diffusion profiles variety is as wide as their structural diversity. Considering there is a broad array of formulation ingredients which provide almost any physical-chemical desired composition, these profiles variety grows exponentially, and it allows molecules out of the optimal permeation range to translocate through the membrane in *in vitro* tests. The predictions may become even more challenging when dealing with the complex mixtures of an herbal extract. Different methods and solvents may lead to different compositions, and the behavior of a certain compound may change depending on which other compounds it is surrounded with.

But, despite the hurdles in establishing general statements, the collected data shows that SC and sebum are the skin factors which play the major role in preventing plant phenolic compounds to freely diffuse through the skin. Molecules with more flexible backbones, lower hydrogen bond number, total polarity surface, and molecular volume may be more prone to permeate, and the substitution position in the aromatic rings also interferes in the observed results as well as the substitute group itself.

In regard of solubility, a higher flux and lower skin retention of phenolic glycosides in comparison to aglycones can be expected. Also, moderate lipophilicity with an aqueous solubility, as predicted, may lead to a higher diffusion as well. In cases in which a full solubility in the vehicle were not achieved, a deeper penetration was obtained by enhancing the surface area of the particles. In this sense, the pharmaceutical form choice is crucial to the product success. Nanosuspensions, for

instance, would be preferable to dispersions or regular suspensions as it would provide a higher surface area in contact to the skin.

Nevertheless, a higher cumulative release due to a higher vehicle solubility may not always be translated into a better skin retention profile, even in the presence of a permeation promoter. The vehicle viscosity, for example, may be a hindering factor for the release and skin diffusion of plant-derived phenolic compounds. Another element to be considered is occlusion or film formation capacity, which can provide higher release and diffusion due to a skin hydration effect [86]. In addition, entrapping the compounds into micro, nanoemulsions, or polymeric capsules, can provide a sustained release profile and enhance their skin deposition in relation to a solution or formulation of their free counterparts.

The recent literature on the subject also reveals a range of *in vitro* experimental conditions. Several types of synthetic, animal, and human membranes have been mounted in diffusion cells with different kinds of receptor fluids, covering the spectra of available experimental possibilities and posing a defying scenario to data correlation and extrapolation. It also turns a reliable correlation with the in vivo behavior of a certain molecule or extract is also defiant, but this fact does not demerit the importance of the *in vitro* tests as a preliminary tool to guide the choice of the most proper vehicle for a product. However, a certain level of standardization of parameters for the diffusion assays is necessary to turn data comparable and capable to give close-to-real predictions with confidence. The advances in *in vitro* skin bioengineering in the following years could aid in this sense by providing membranes with great similarity with the human skin, as cost, repeatability, and preservation issues are surpassed. Moreover, as the technology evolves, models of different types of skins and parts of the body may be available for diffusion tests in the future. A movement towards miniaturization and high-throughput assays in well-plates, allied to highly sensitive analytical techniques and methods, may also guide the diffusion tests towards a more standardized technique, as several molecules and extracts can be tested simultaneously under the same controlled environment [16].

Concerning plant phenolic compounds, with the constant discovery of new molecules, the number of plant species still to be explored, and the different types of extracts made with them, lowering the test variabilities may provide better diffusion profile prediction and improve the decision-making in the design of novel skincare

products. Also, a more standardized dataset might improve the construction of reliable in silico prediction models by providing more coherent results, and the models may become a second tool to aid the design of new topical formulations.

Conclusion

In terms of *in vitro* cutaneous diffusion of plant-derived phenolic compounds, a variety of assay setups in diffusion cells have been proposed. Different synthetic membranes for release prediction, and artificial membranes, animal and human skins from different parts of the body have served as models to the assessment of the diffusion of isolated compounds and plant extracts in solution, suspension, and formulation, either encapsulated or in their free form. The multiplicity of models and the diversity of vehicles place an obstacle in establishing correlations among the available data, but general statements can be extracted from the disclosed information, namely: (i) SC and sebum are important factors in hindering plant phenolics to penetrate the skin; (ii) flexibility, hydrogen bond number, volume and substitution pattern are features which indicate the easiness with which plant phenolics translocate through the skin; (iii) the solubility of the compound or the extract in the vehicle influences the exhibited diffusion profile; (iv) the presence of a permeation enhancer in the formulation not necessarily provides a higher total amount of diffused compound or a faster penetration or permeation profile; (v) the viscosity of the vehicle and the entrapment of extracts or isolated compounds into micro, nanocapsules or vehicle compounds influence the results; (vi) in general, micro and nanoencapsulation provide advantages in terms of controlled release and skin deposition of plant-derived phenolic compounds; and (vii) in extracts, the presence of the extraction solvent and molecules other than the marker compounds also interfere in the cutaneous diffusion pattern.

The standardization of methods and protocols may provide better diffusion profile prediction and improve the decision-making in the design of novel skincare products with plant-derived phenolic compounds, and the advances in *in vitro* skin bioengineering and high-throughput assays allied to highly sensitive analytical techniques and methods may guide the diffusion tests towards this aim, also helping in the improvement of *in silico* prediction models.

Acknowledgments

This work was financially supported by the National Institutes of Science and Technology (INCTs) [grant numbers: FAPESP/INCT 2014/50867, CNPq 465389/2014-7]. C. B. G. Bottoli acknowledges CNPq for a research fellowship [CNPq 309363/2018-7].

Declaration of interest

The authors have no relevant affiliations or financial involvement with any organization or entity with a financial interest in or financial conflict with the subject matter or materials discussed in the manuscript. This includes employment, consultancies, honoraria, stock ownership or options, expert testimony, grants or patents received or pending, or royalties.

References

1. Mutha RE, Tatiya AU, and Surana SJ. Flavonoids as natural phenolic compounds and their role in therapeutics: an overview. Future Journal of Pharmaceutical Sciences 2021 7:1. 2021;7(1):1–13.

2. Borges A, de Freitas V, Mateus N, Fernandes I, and Oliveira J. Solid Lipid Nanoparticles as Carriers of Natural Phenolic Compounds. Antioxidants 2020, Vol 9, Page 998. 2020;9(10):998.

3. Zhang Y, Cai P, Cheng G, and Zhang Y. A Brief Review of Phenolic Compounds Identified from Plants: Their Extraction, Analysis, and Biological Activity: https://doi.org/101177/1934578X211069721. 2022;17(1).

4. Dai J and Mumper RJ. Plant Phenolics: Extraction, Analysis and Their Antioxidant and Anticancer Properties. Molecules. 2010;15(10):7313.

5. Boo YC. Can Plant Phenolic Compounds Protect the Skin from Airborne Particulate Matter? Antioxidants. 2019;8(9).

6. Tungmunnithum D, Thongboonyou A, Pholboon A, and Yangsabai A. Flavonoids and Other Phenolic Compounds from Medicinal Plants for Pharmaceutical and Medical Aspects: An Overview. Medicines. 2018;5(3):93.

7. Albuquerque BR, Heleno SA 8., Oliveira MBPP, Barros L, and Ferreira ICFR. Phenolic compounds: current industrial applications, limitations and future challenges. Food Funct. 2021;12(1):14–29.

8. Schimek K, Hsu HH, Boehme M, Kornet JJ, Marx U, Lauster R, Pörtner R, and Lindner G. Bioengineering of a Full-Thickness Skin Equivalent in a 96-Well Insert Format for Substance Permeation Studies and Organ-On-A-Chip Applications. Bioengineering (Basel). 2018;5(2).

9. Aljuffali I, Hsu C-Y, Lin Y-K, and Fang J-Y. Cutaneous Delivery of Natural Antioxidants: The Enhancement Approaches. Curr Pharm Des. 2015;21(20):2745–57.

10. Montiel-Sánchez M, García-Cayuela T, Gómez-Maqueo A, García HS, and Cano MP. *In vitro* gastrointestinal stability, bioaccessibility and potential biological activities of betalains and phenolic compounds in cactus berry fruits (Myrtillocactus geometrizans). Food Chem. 2021;342:128087.

11. Chaturvedi S and Garg A. An insight of techniques for the assessment of permeation flux across the skin for optimization of topical and transdermal drug delivery systems. J Drug Deliv Sci Technol. 2021;62:102355.

12. Zsikó S, Csányi E, Kovács A, Budai-Szűcs M, Gácsi A, and Berkó S. Methods to Evaluate Skin Penetration *In Vitro*. Scientia Pharmaceutica 2019, Vol 87, Page 19. 2019;87(3):19.

13. Moniz T, Costa Lima SA, and Reis S. Human skin models: From healthy to disease-mimetic systems; characteristics and applications. Br J Pharmacol. 2020;177(19):4314–29.

14. Rapalli VK, Mahmood A, Waghule T, Gorantla S, Kumar Dubey S, Alexander A, and Singhvi G. Revisiting techniques to evaluate drug permeation through skin. Expert Opin Drug Deliv. 2021;18(12):1829–42.

15. Sinkó B, Garrigues TM, Balogh GT, Nagy ZK, Tsinman O, Avdeef A, and Takács-Novák K. Skin-PAMPA: a new method for fast prediction of skin penetration. Eur J Pharm Sci. 2012;45(5):698–707.

16. Neupane R, Boddu SHS, Renukuntla J, Babu RJ, and Tiwari AK. Alternatives to Biological Skin in Permeation Studies: Current Trends and Possibilities. Pharmaceutics 2020, Vol 12, Page 152. 2020;12(2):152.

17. Algahtani MS, Ahmad MZ, and Ahmad J. Nanoemulsion loaded polymeric hydrogel for topical delivery of curcumin in psoriasis. J Drug Deliv Sci Technol. 2020;59:101847.

18. Badie H and Abbas H. Novel small self-assembled resveratrol-bearing cubosomes and hexosomes: preparation, charachterization, and ex vivo permeation. Drug Dev Ind Pharm. 2018;44(12):2013–25.

19. Yu J, Wan K, and Sun X. Improved transdermal delivery of morin efficiently inhibits allergic contact dermatitis. Int J Pharm. 2017;530(1–2):145–54.

20. Negi P, Aggarwal M, Sharma G, Rathore C, Sharma G, Singh B, and Katare OP. Niosome-based hydrogel of resveratrol for topical applications: An effective therapy for pain related disorder(s). Biomed Pharmacother. 2017;88:480–7.

21. Liu P, de Wulf O, Laru J, Heikkilä T, van Veen B, Kiesvaara J, Hirvonen J, Peltonen L, and Laaksonen T. Dissolution Studies of Poorly Soluble Drug Nanosuspensions in Non-sink Conditions. AAPS PharmSciTech. 2013;14(2):748.

22. Kumar N and Goel N. Phenolic acids: Natural versatile molecules with promising therapeutic applications. Biotechnology Reports. 2019;24.

23. Przybylska-Balcerek A and Stuper-Szablewska K. Phenolic acids used in the cosmetics industry as natural antioxidants. European Journal of Medical Technologies. 2019;4(25).

24. Sguizzato M, Valacchi G, Pecorelli A, Boldrini P, Simelière F, Huang N, Cortesi R, and Esposito E. Gallic acid loaded poloxamer gel as new adjuvant strategy for melanoma: A preliminary study. Colloids Surf B Biointerfaces. 2020;185:110613.

25. Spagnol CM, di Filippo LD, Isaac VLB, Correa MA, and Salgado HRN. Caffeic Acid in Dermatological Formulations: *In Vitro* Release Profile and Skin Absorption. Comb Chem High Throughput Screen. 2017;20(8).

26. Biswas S, Mukherjee PK, Kar A, Bannerjee S, Jana SN, Haldar PK, and Sharma N. Enhanced permeability and photoprotective potential of optimized p-coumaric acid-phospholipid complex loaded gel against UVA mediated oxidative stress. J Photochem Photobiol B. 2021;221:112246.

27. Panche AN, Diwan AD, and Chandra SR. Flavonoids: an overview. J Nutr Sci. 2016;5:1–15.

28. Chuang SY, Lin YK, Lin CF, Wang PW, Chen EL, and Fang JY. Elucidating the Skin Delivery of Aglycone and Glycoside Flavonoids: How the Structures Affect Cutaneous Absorption. Nutrients. 2017;9(12).

29. ChemSpider | Search and share chemistry. Available at http://www.chemspider.com/.

30. Alalaiwe A, Lin CF, Hsiao CY, Chen EL, Lin CY, Lien WC, and Fang JY. Development of flavanone and its derivatives as topical agents against psoriasis: The prediction of therapeutic efficiency through skin permeation evaluation and cell-based assay. Int J Pharm. 2020;581.

31. Bustos-Salgado P, Andrade-Carrera B, Garduño-Ramírez ML, Alvarado H, and Calpena-Campmany A. Quantification of One Prenylated Flavanone from Eysenhardtia platycarpa and Four Derivatives in Ex Vivo Human Skin Permeation Samples Applying a Validated HPLC Method. Biomolecules. 2020;10(6):1–10.

32. Salehi B, Machin L, Monzote L, Sharifi-Rad J, Ezzat SM, Salem MA, Merghany RM, El Mahdy NM, Kllç CS, Sytar O, et al. Therapeutic Potential of Quercetin: New Insights and Perspectives for Human Health. ACS Omega. 2020;5(20):11849–72.

33. PubChem. Available at https://pubchem.ncbi.nlm.nih.gov/.

34. Esposito L, Barbosa AI, Moniz T, Lima SC, Costa P, Celia C, and Reis S. Design and Characterization of Sodium Alginate and Poly(vinyl) Alcohol Hydrogels for Enhanced Skin Delivery of Quercetin. Pharmaceutics. 2020;12(12):1–15.

35. Dyja R and Jankowski A. The effect of additives on release and *in vitro* skin retention of flavonoids from emulsion and gel semisolid formulations. Int J Cosmet Sci. 2017;39(4):442–9.

36. Zhang ZJ and Michniak-Kohn B. Flavosomes, novel deformable liposomes for the co-delivery of anti-inflammatory compounds to skin. Int J Pharm. 2020;585.

37. Westfall A, Sigurdson GT, Rodriguez-Saona LE, and Giusti MM. Ex Vivo and In Vivo Assessment of the Penetration of Topically Applied Anthocyanins Utilizing ATR-FTIR/PLS Regression Models and HPLC-PDA-MS. Antioxidants (Basel). 2020;9(6).

38. Mattioli R, Francioso A, Mosca L, and Silva P. Anthocyanins: A Comprehensive Review of Their Chemical Properties and Health Effects on Cardiovascular and Neurodegenerative Diseases. Molecules 2020, Vol 25, Page 3809. 2020;25(17):3809.

39. Alappat B and Alappat J. Anthocyanin Pigments: Beyond Aesthetics. Molecules 2020, Vol 25, Page 5500. 2020;25(23):5500.

40. Liu W, Zhao Q, Lv L, Yan S, Song Q, Chen T, and Yao Q. Pomegranate Seed Oil Enhances the Percutaneous Absorption of trans-Resveratrol. J Oleo Sci. 2018;67(4):479–87.

41. Alonso C, Martí M, Barba C, Carrer V, Rubio L, and Coderch L. Skin permeation and antioxidant efficacy of topically applied resveratrol. Arch Dermatol Res. 2017;309(6):423–31.

42. Negi P, Aggarwal M, Sharma G, Rathore C, Sharma G, Singh B, and Katare OP. Niosome-based hydrogel of resveratrol for topical applications: An effective therapy for pain related disorder(s). Biomed Pharmacother. 2017;88:480–7.

43. Das S, Lee SH, Chow PS, and Macbeath C. Microemulsion composed of combination of skin beneficial oils as vehicle: Development of resveratrol-loaded microemulsion based formulations for skin care applications. Colloids Surf B Biointerfaces. 2020;194:111161.

44. Sharkawy A, Casimiro FM, Barreiro MF, and Rodrigues AE. Enhancing trans-resveratrol topical delivery and photostability through entrapment in chitosan/gum Arabic Pickering emulsions. Int J Biol Macromol. 2020;147:150–9.

45. Shrotriya SN, Ranpise NS, and Vidhate B v. Skin targeting of resveratrol utilizing solid lipid nanoparticle-engrossed gel for chemically induced irritant contact dermatitis. Drug Deliv Transl Res. 2017;7(1):37–52.

46. Arora D, Khurana B, and Nanda S. DoE directed optimization, development and evaluation of resveratrol loaded ultradeformable vesicular cream for topical antioxidant benefits. https://doi.org/101080/0363904520201716373. 2020;46(2):227–35.

47. Nastiti CMRR, Ponto T, Mohammed Y, Roberts MS, and Benson HAE. Novel Nanocarriers for Targeted Topical Skin Delivery of the Antioxidant Resveratrol. Pharmaceutics. 2020;12(2).

48. Wani TU, Mohi-ud-Din R, Majeed A, Kawoosa S, and Pottoo FH. Skin Permeation of Nanoparticles: Mechanisms Involved and Critical Factors Governing Topical Drug Delivery. Curr Pharm Des. 2020;26(36):4601–14.

49. Jangdey MS, Gupta A, and Saraf S. Fabrication, in-vitro characterization, and enhanced in-vivo evaluation of carbopol-based nanoemulsion gel of apigenin for UV-induced skin carcinoma. Drug Deliv. 2017;24(1):1026–36.

50. Khatoon K, Ali A, Ahmad FJ, Hafeez Z, Rizvi MMA, Akhter S, and Beg S. Novel nanoemulsion gel containing triple natural bio-actives combination of curcumin, thymoquinone, and resveratrol improves psoriasis therapy: *in vitro* and in vivo studies. Drug Deliv Transl Res. 2021;11(3):1245–60.

51. Pushpalatha R, Selvamuthukumar S, and Kilimozhi D. Cyclodextrin nanosponge based hydrogel for the transdermal co-delivery of curcumin and resveratrol:

Development, optimization, *in vitro* and ex vivo evaluation. J Drug Deliv Sci Technol. 2019;52:55–64.

52. ben Yehuda Greenwald M, Frušić-Zlotkin M, Soroka Y, ben Sasson S, Bitton R, Bianco-Peled H, and Kohen R. Curcumin Protects Skin against UVB-Induced Cytotoxicity via the Keap1-Nrf2 Pathway: The Use of a Microemulsion Delivery System. Oxid Med Cell Longev. 2017;2017.

53. Zhou F, Song Z, Wen Y, Xu H, Zhu L, and Feng R. Transdermal delivery of curcumin-loaded supramolecular hydrogels for dermatitis treatment. J Mater Sci Mater Med. 2019;30(1).

54. Spagnol CM, Zaera AM, Isaac VLB, Corrêa MA, and Salgado HRN. Release and permeation profiles of spray-dried chitosan microparticles containing caffeic acid. Saudi Pharmaceutical Journal. 2018;26(3):410–5.

55. Shetty PK, Manikkath J, Tupally K, Kokil G, Hegde AR, Raut SY, Parekh HS, and Mutalik S. Skin Delivery of EGCG and Silibinin: Potential of Peptide Dendrimers for Enhanced Skin Permeation and Deposition. AAPS PharmSciTech. 2017;18(6):2346–57.

56. Avadhani KS, Manikkath J, Tiwari M, Chandrasekhar M, Godavarthi A, Vidya SM, Hariharapura RC, Kalthur G, Udupa N, and Mutalik S. Skin delivery of epigallocatechin-3-gallate (EGCG) and hyaluronic acid loaded nano-transfersomes for antioxidant and anti-aging effects in UV radiation induced skin damage. Drug Deliv. 2017;24(1):61–74.

57. Chen L, Annaji M, Kurapati S, Ravis WR, and Jayachandra Babu R. Microemulsion and Microporation Effects on the Genistein Permeation Across Dermatomed Human Skin. AAPS PharmSciTech. 2018;19(8):3481–9.

58. Yu J, Wan K, and Sun X. Improved transdermal delivery of morin efficiently inhibits allergic contact dermatitis. Int J Pharm. 2017;530(1–2):145–54.

59. Badea G, Badea N, Brasoveanu LI, Mihaila M, Stan R, Istrati D, Balaci T, and Lacatusu I. Naringenin improves the sunscreen performance of vegetable nanocarriers. New Journal of Chemistry. 2017;41(2):480–92.

60. Lv X, Liu T, Ma H, Tian Y, Li L, Li Z, Gao M, Zhang J, and Tang Z. Preparation of Essential Oil-Based Microemulsions for Improving the Solubility, pH Stability, Photostability, and Skin Permeation of Quercetin. AAPS PharmSciTech. 2017;18(8):3097–104.

61. Imran M, Iqubal MK, Imtiyaz K, Saleem S, Mittal S, Rizvi MMA, Ali J, and Baboota S. Topical nanostructured lipid carrier gel of quercetin and resveratrol: Formulation, optimization, *in vitro* and ex vivo study for the treatment of skin cancer. Int J Pharm. 2020;587.

62. Sharma B, Iqbal B, Kumar S, Ali J, and Baboota S. Resveratrol-loaded nanoemulsion gel system to ameliorate UV-induced oxidative skin damage: from *in vitro* to in

vivo investigation of antioxidant activity enhancement. Arch Dermatol Res. 2019;311(10):773–93.

63. Arora D and Nanda S. Quality by design driven development of resveratrol loaded ethosomal hydrogel for improved dermatological benefits via enhanced skin permeation and retention. Int J Pharm. 2019;567.

64. Fachel FNS, Nemitz MC, Medeiros-Neves B, Veras KS, Bassani VL, Koester LS, Henriques AT, and Teixeira HF. A novel, simplified and stability-indicating high-throughput ultra-fast liquid chromatography method for the determination of rosmarinic acid in nanoemulsions, porcine skin and nasal mucosa. J Chromatogr B Analyt Technol Biomed Life Sci. 2018;1083:233–41.

65. Marchiori MCL, Rigon C, Camponogara C, Oliveira SM, and Cruz L. Hydrogel containing silibinin-loaded pomegranate oil based nanocapsules exhibits anti-inflammatory effects on skin damage UVB radiation-induced in mice. J Photochem Photobiol B. 2017;170:25–32.

66. Vigato AA, Querobino SM, de Faria NC, Candido ACBB, Magalhães LG, Cereda CMS, Tófoli GR, Campos EVR, Machado IP, Fraceto LF, et al. Physico-chemical characterization and biopharmaceutical evaluation of lipid-poloxamer-based organogels for curcumin skin delivery. Front Pharmacol. 2019;10:1006.

67. Panahi Y, Fazlolahzadeh O, Atkin SL, Majeed M, Butler AE, Johnston TP, and Sahebkar A. Evidence of curcumin and curcumin analogue effects in skin diseases: A narrative review. J Cell Physiol. 2019;234(2):1165–78.

68. Ochocka R, Hering A, Stefanowicz-Hajduk J, Cal K, and Barańska H. The effect of mangiferin on skin: Penetration, permeation and inhibition of ECM enzymes. PLoS One. 2017;12(7).

69. Pleguezuelos-Villa M, Nácher A, Hernández MJ, Ofelia Vila Buso MA, Ruiz Sauri A, and Díez-Sales O. Mangiferin nanoemulsions in treatment of inflammatory disorders and skin regeneration. Int J Pharm. 2019;564:299–307.

70. Sguizzato M, Ferrara F, Mariani P, Pepe A, Cortesi R, Huang N, Simelière F, Boldrini P, Baldisserotto A, Valacchi G, et al. “Plurethosome” as vesicular system for cutaneous administration of mangiferin: Formulative study and 3D skin tissue evaluation. Pharmaceutics. 2021;13(8):1124.

71. Hering A, Ochocka JR, Baranska H, Cal K, and Stefanowicz-Hajduk J. Mangiferin and Hesperidin Transdermal Distribution and Permeability through the Skin from Solutions and Honeybush Extracts (Cyclopia sp.)-A Comparison Ex Vivo Study. Molecules. 2021;26(21).

72. Punzo A, Porru E, Silla A, Simoni P, Galletti P, Roda A, Tagliavini E, Samorì C, and Caliceti C. Grape Pomace for Topical Application: Green NaDES Sustainable

Extraction, Skin Permeation Studies, Antioxidant and Anti-Inflammatory Activities Characterization in 3D Human Keratinocytes. Biomolecules. 2021;11(8).

73. de Souza RO, Alves G de AD, Forte ALSA, Marquele-Oliveira F, da Silva DF, Rogez H, and Fonseca MJV. Byrsonima crassifolia extract and fraction prevent UVB-induced oxidative stress in keratinocytes culture and increase antioxidant activity on skin. Ind Crops Prod. 2017;108:485–94.

74. Bae J, Kim N, Shin Y, Kim S-Y, and Kim Y-J. Activity of catechins and their applications. Biomedical Dermatology. 2020;4(1).

75. Dresch RR, Dresch MTK, Biegelmeyer R, Argenta DF, da Rocha RF, Teixeira HF, Moreira JCF, and Henriques AT. Potential use of secondary products of the agri-food industry for topical formulations and comparative analysis of antioxidant activity of grape leaf polyphenols. Nat Prod Res. 2018;32(4):486–92.

76. Kis N, Gunnarsson M, Berkó S, and Sparr E. The effects of glycols on molecular mobility, structure, and permeability in stratum corneum. Journal of Controlled Release. 2022;343:755–64.

77. Said dos Santos R, Vecchi CF, Rosseto HC, Bassi da Silva J, Dano MEL, de Castro-Hoshino LV, Baesso ML, and Bruschi ML. Emulgels Containing Carbopol 934P and Different Vegetable Oils for Topical Propolis Delivery: Bioadhesion, Drug Release Profile, and Ex Vivo Skin Permeation Studies. AAPS PharmSciTech. 2020;21(6).

78. Talat M, Zaman M, Khan R, Jamshaid M, Akhtar M, and Mirza AZ. Emulgel: an effective drug delivery system. Drug Dev Ind Pharm. 2021;47(8):1193–9.

79. Ferreira-Nunes R, Silva SMM da, Souza PEN de, Magalhães P de O, Cunha-Filho M, Gratieri T, and Gelfuso GM. Incorporation of Eugenia dysenterica extract in microemulsions preserves stability, antioxidant effect and provides enhanced cutaneous permeation. J Mol Liq. 2018;265:408–15.

80. Yang J, Xu H, Wu S, Ju B, Zhu D, Yan Y, Wang M, and Hu J. Preparation and evaluation of microemulsion-based transdermal delivery of Cistanche tubulosa phenylethanoid glycosides. Mol Med Rep. 2017;15(3):1109–16.

81. Rangsimawong W, Wattanasri P, Tonglairoum P, Akkaramongkolporn P, Rojanarata T, Ngawhirunpat T, and Opanasopit P. Development of Microemulsions and Microemulgels for Enhancing Transdermal Delivery of Kaempferia parviflora Extract. AAPS PharmSciTech. 2018;19(5):2058–67.

82. Baccarin T and Lemos-Senna E. Potential Application of Nanoemulsions for Skin Delivery of Pomegranate Peel Polyphenols. AAPS PharmSciTech. 2017;18(8):3307–14.

83. Souto EB, Cano A, Martins-Gomes C, Coutinho TE, Zielińska A, and Silva AM. Microemulsions and Nanoemulsions in Skin Drug Delivery. Bioengineering. 2022;9(4).

84. Santos LP dos, Caon T, Battisti MA, Silva CHB da, Simões CMO, Reginatto FH, and de Campos AM. Antioxidant polymeric nanoparticles containing standardized extract of Ilex paraguariensis A. St.-Hil. for topical use. Ind Crops Prod. 2017;108:738–47.

85. Shankar VK, Police A, Ajjarapu S, and Murthy SN. Development of silymarin topical formulation: *In vitro* and ex vivo dermal kinetics of silymarin. Int J Pharm. 2023;630:122431.

86. Butkeviciute A, Ramanauskiene K, Kurapkiene V, and Janulis V. Dermal Penetration Studies of Potential Phenolic Compounds Ex Vivo and Their Antioxidant Activity *In Vitro*. Plants. 2022;11(15).

87. Kim MH, Jeon YE, Kang S, Lee JY, Lee KW, Kim KT, and Kim DD. Lipid Nanoparticles for Enhancing the Physicochemical Stability and Topical Skin Delivery of Orobol. Pharmaceutics. 2020;12(9):1–16.

CAPÍTULO 2

Passion fruit seed extract enriched in piceatannol obtained by microwave-assisted extraction

https://doi.org/10.1016/j.scp.2021.100472

Received 24 March 2021;
Received in revised form 30 May 2021;
Accepted 3 June 2021

Sustainable Chemistry and Pharmacy 22 (2021) 100472

Contents lists available at ScienceDirect

Sustainable Chemistry and Pharmacy

journal homepage: www.elsevier.com/locate/scp

Passion fruit seed extract enriched in piceatannol obtained by microwave-assisted extraction

Gisláine C. Silva [a], Rodney A.F. Rodrigues [b], Carla B.G. Bottoli [a,*]

[a] Institute of Chemistry, University of Campinas (Unicamp), POB 6154, 13084-971, Campinas, SP, Brasil
[b] Pluridisciplinary Research Center for Chemistry, Biology, and Agriculture (CPQBA), University of Campinas, 13148-218, Paulínia, SP, Brasil

Abstract

Apart from being food, passion fruit (*Passiflora edulis* Sims) offers seeds to be used as an oil source, and the residual seed cake from oil extraction contains piceatannol, a molecule that can prevent skin damages. In this work, microwave-assisted extraction (MAE) was evaluated as a technique for the preparation of piceatannol-rich seed cake extracts, and its performance was compared to the conventional Soxhlet extraction. MAE and Soxhlet exhibited different selectivities for the seed cake compounds. A sequential MAE at 87 °C, with 70% EtOH, for 30 min each cycle, provided a fine brown powder with 27.17 ± 0.9 μg of piceatannol per mg of the extract, while Soxhlet extraction for 120 min resulted in a dark lumpy extract containing 13.03 ± 0.4 μg mg^{-1}. Thus, MAE was shown to be a promising alternative to produce a passion fruit seed extract for cosmetic purposes, adding value to a residue from the passion fruit chain by providing a faster extraction and a more color friendly and easier-to-handle product with higher levels of piceatannol in comparison to the conventional method.

Keywords: Piceatannol, passion-fruit seed extract, MAE, food chain residue valorization.

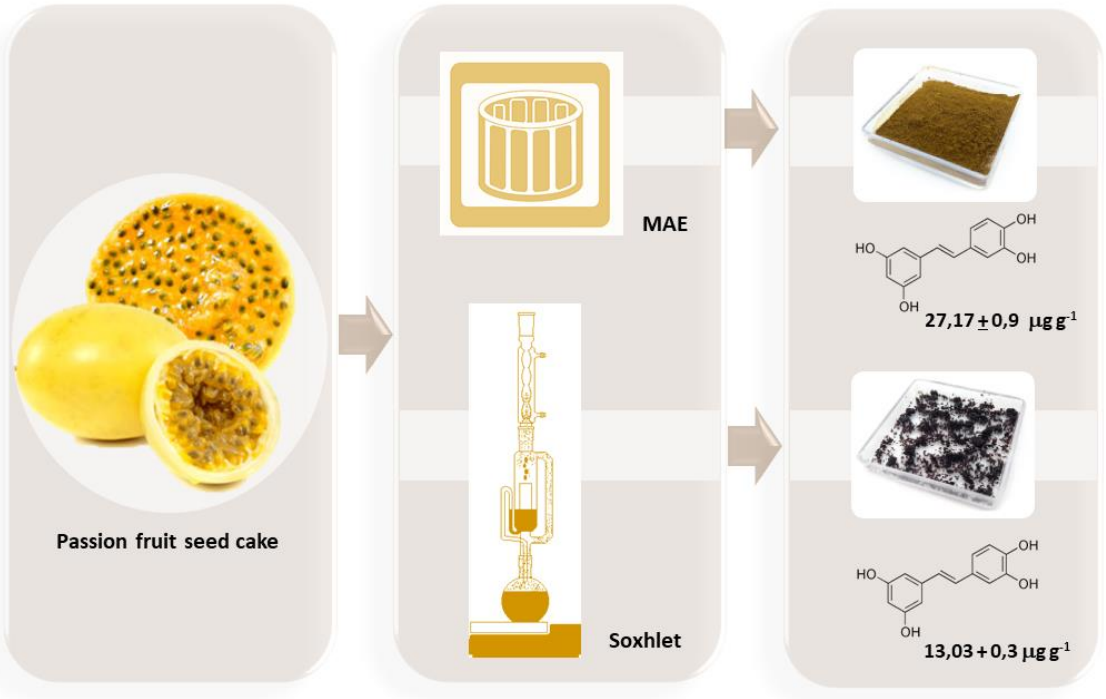

Graphical abstract

Highlights:

- Passion fruit seeds and residual seed cake from oil extraction contain piceatannol.
- Microwave-assisted extraction provides a fine brown powder seed cake extract.
- Soxhlet extraction provides a lumpy dark seed cake extract.
- MAE provides twice the piceatannol in half of the time for Soxhlet extraction.

Introduction

Brazil is the world's largest passion fruit (*Passiflora edulis*) producer, and it is responsible for putting around 602,000 tons of this fruit into the market in 2018. Although the largest part of this production is internally consumed, Brazil also exports to countries, such as Portugal, Spain, Australia, the UK, Uruguay, and the USA. Brazil also processes passion fruit and exports its juice: in 2019, around 444,000 kg of these products were sent to other countries, 75% of this amount being sold to the USA (“Maracujá - Portal Embrapa,” n.d.)

Roughly, the pulp corresponds to 23% of the weight of this fruit, while the peel and the seeds contribute to 50 and 27% of its mass, respectively. Peels and seeds are not used in the passion fruit juice and pulp industry and may become an environmental liability if not reused. The peels can be used as fertilizers and for animal feed. Several reports on the nutritional values of the peel floor have been published and this part of the passion fruit can also be a source of pectins, which can be used as a consistency agent. The seeds are a source of an oil that is used in food and cosmetics and the residual cake from oil extraction processes can be used as a skin exfoliator in soaps and other cosmetic formulae (Ferrari et al., 2004; “Os usos múltiplos do maracujá - Revista Globo Rural | Agricultura,” n.d.).

The seeds and the residual cake from passion fruit seed oil extraction are also an unexplored source of bioactive phenolic compounds. One of them is piceatannol, a stilbene compound capable of inhibiting *in vitro* melanin synthesis in human skin cancer cells, stimulating collagen production by fibroblasts cell cultures, and protecting epidermal skin cells against harm caused by ultraviolet radiation. Therefore, there is still some space for further exploration of passion fruit seeds in cosmetic, pharmaceutical, or food products, enhancing the value of the passion fruit production chain (Maruki-Uchida et al., 2013; Matsui et al., 2013, 2010).

Passion fruit seed extracts containing piceatannol are generally prepared by the contact of the biomass with a mixture of ethanol and water, but butylene glycol, methanol, and supercritical CO_2 are also reported as extraction solvents. In some cases, an *n*-hexane degreasing step is performed before the extract is produced. Among the extraction techniques, the classic ones such as static and mechanical maceration, and reflux are used, as well as advanced techniques like supercritical fluid

and ultrasound-assisted extraction (da Silva et al., 2018; de Santana et al., 2017; Kawakami et al., 2014; Maruki-Uchida et al., 2013; Matsui et al., 2010; Oliveira et al., 2016; Uchida-Maruki et al., 2015; Viganó et al., 2017).

Microwave-assisted extraction (MAE) is another advanced technique that has proven itself successful for the extraction of phytochemicals from plants due to its unique operation. By the induction of molecular dipole rotation, which allows internal, rapid, and selective heating of the samples, higher recoveries of different compounds are expected in shorter times and with lower energy consumption in comparison with conventional extractions. Even though there are hurdles to be overcome in terms of instrument and homogeneous heating, it is possible to find some reports on the scaling up of MAE processes to pilot levels and some companies claim to obtain some bioactive products for their portfolios by this technique. Therefore, considering that MAE could be a potential alternative for obtaining piceatannol rich passion fruit seed extracts, the present study aimed at the evaluation of MAE parameters for the highest piceatannol recovery from the defatted seed residual cake and a comparison of the technique with a classical heating process having the same aim (Garcia-Garcia et al., 2019; Li et al., 2019, 2013; Petigny et al., 2014).

Materials and methods

Residual seed cake and reagents

Residual seed cake resulting from cold press oil extraction (referred to herein as “seed cake”) was obtained from Extrair Óleos Naturais (Rio de Janeiro, Brazil). Analytical grade ethanol (Synth, SP, Brazil) and ultrapure water were used as solvents. Analytical grade *n*-hexane produced at Unicamp Institute of Chemistry Pilot Plant (Campinas, SP, Brazil) was used in the residual cake defatting process. Analytical standards for piceatannol and kaempferol were purchased from TRC (Toronto, Canada) and Sigma Aldrich (Darmstadt, Germany), respectively. HPLC grade methanol and acetonitrile (Tedia, Fairfield, Ohio, USA) and analytical grade formic acid (Synth, São Paulo, Brazil) were used for the mass spectrometry and separation assays.

Defatting

In a glass flask with a screw cap, 250 mL of *n*-hexane were added to 25 g of the seed cake. The suspension was maintained under magnetic stirring for 1 h at room temperature. Cake-solvent separation was performed manually after sedimentation of the defatted cake. The recovered cake was spread onto a surface for *n*-hexane evaporation in a fume hood.

Preliminary evaluation of MAE conditions

MAE extractions were performed in a Start E bench-scale microwave extractor (Milestone, Bergamo, Italy) using different proportions of EtOH:H_2O as extraction solvents. An experimental full 2^3 central composite design with 6 axial points (α = 1,68) and 6 central point replicates was performed to evaluate the effects of the EtOH proportion in the extraction solvent and the extraction time and temperature, according to the ranges in Table 1.

Table 1: Central composite design parameters for preliminary MAE evaluation.

Factor	-α	-1	0	+1	+α
T (ºC)	53	60	70	80	87
t (min)	5	15	30	45	55
EtOH (%)	53	60	70	80	87

For all the experiments, a seed cake:solvent ratio of 1:30, w/v (0.500 g of the defatted seed cake to 15 mL of extraction solvent) was used. All the extractions were performed with a maximum magnetic stirring speed and a heating profile composed of a 5 min temperature raise at the beginning of each assay and a 10 min temperature reduction at the end. All the extracts were collected by filter paper vacuum filtration and the solvents were removed with a direct $N_{2\ (g)}$ flux over solutions protected from direct light. The extract dry mass and the ratio between chromatographic peak areas of piceatannol and kaempferol *(A_{pic}/A_{kaemp})* were the responses evaluated.

The A_{pic}/A_{kaemp} ratio was determined by the injection of a 400 mg mL^{-1} in a MeOH:H_2O solution (50:50, v/v) of each extract, spiked with standard kaempferol (2.5 mg mL^{-1}) into an HPLC-DAD-ESI-QqQ system (Alliance 2695 pump, Alliance 2998

DAD and Micromass Quattro Micro API mass spectrometer from Waters, Milford, Massachusetts, USA). The separations were carried out using a Waters NovaPak C18 column (150 mm x 3.9 mm, 4 µm) eluted with 0,1% H_2O:HCOOH (A) and acetonitrile, ACN (B) in the following gradient: 40% B (0-4 min), 40-100% B (4-7 min), 100% B (7-9 min), 100-40% B (9-12 min). Samples of 5 µL were injected with a 0.3 mL min^{-1} mobile phase flow rate. The peaks of piceatannol (m/z 245>135) and kaempferol (m/z 287>153) were detected in MRM positive mode. The spectrometer was set to 30 V of cone voltage, 3.0 kV of capillary voltage, 3.0 V of extractor cone voltage, 150 °C of source temperature, 350 °C of desolvation temperature, 350 L h^{-1} of desolvation gas flow ($N_{2(g)}$), and 100 L h^{-1} of cone gas flow ($N_{2(g)}$). Peak integration was performed in MassLynx 4.0 after Savitzky–Golay smoothing.

Fingerprint analyses

The fingerprint analyses of all the extracts of the preliminary evaluation were performed by direct infusion in an ESI-QqQ Micromass Quattro Micro API mass spectrometer (Waters, Milford, Massachusetts, USA). A 5 µL sample of 1 mg mL^{-1} in MeOH:H_2O (50:50, v/v) solution of each extract was injected into the spectrometer by a 0.2 mL min^{-1} flow of ACN:H_2O:HCOOH (50:50:0.1, v/v/v) mobile phase. Data were acquired in the positive mode for 1 min, in the range of m/z 100 to 1000, under the same spectrometer settings described in 2.3.

Evaluation of MAE in cycles

The optimized condition for the MAE of seed cake was used for cyclic extraction. Five MAE cycles were performed on 0.500 g of the material and the extract of each cycle was filtered and dried according to 2.3. This assay was done in duplicate. The extract dry mass and the A_{pic}/A_{kaemp} ratio were measured in unicate and triplicate for each extract, respectively, according to 2.3.

Conventional Soxhlet extraction

Soxhlet extraction was conducted according to Uchida-Maruki et al. (2015). Briefly, 100 mL of 80% EtOH was refluxed over 10.0 g of defatted seed cake for 120 min. The extract was collected, and the solvent was removed with a direct $N_{2\ (g)}$ flux over the solution protected from direct light. The process was carried out in triplicate. Fingerprint analysis was carried out according to 2.4.

Piceatannol quantification in the extracts

Piceatannol was quantified by the standard addition method. Solutions of 5.0 mg of the optimized MAE extract or the Soxhlet extract in 50:50 (v/v) MeOH:H_2O were spiked with standard piceatannol from 0 to 15 µg L^{-1}, in triplicate for each concentration, using a final volume of 5.0 mL. The solutions were analyzed by HPLC according to the conditions described in 2.3.

Statistics and data treatment

Data from the central composite design was analyzed using Design Expert 9.0. One-way ANOVA and *T student* test were done in Microsoft Excel 2016. The linearity of the quantification curves was verified by ActionStat 3.7.

Results

Preliminary evaluation of MAE conditions

The results from the central composite design experiments are summarized in Table 2. Dry mass varied between 30.7 to 69.9 mg, which represents an extraction yield (w/w) of 6.1 to 14.0% in relation to the initial seed cake mass. The A_{pic}/A_{kaemp} ratio was between 0.59 and 1.53. Even though a variation was observed in both responses, the lack of adjustment of the proposed models was significant and, thus, it was not possible to model the data. For the dry mass, the best fit model presented an R-squared value of 0.8341, while the A_{pic}/A_{kaemp} ratio model had an R-squared value of only 0.4152. The dry mass and A_{pic}/A_{kaemp} ratio for the center points were 57.9 ± 0.8 mg and 0.80 ± 0.1, respectively. Fingerprint analysis suggested that the chemical

profiles among the extracts were similar under the used conditions, showing varying intensities of the most intense m/z peaks for the 20 assayed conditions (mass spectra in Supplementary material A).

Table 2: Central composite design experiments results.

Parameters				Responses	
Experiment	**T (°C)**	**EtOH (%)**	**t (min)**	**$A_{135/153}$**	**Dry mass (g)**
1	60	60	15	0.59	0.0510
2	80	60	15	1.09	0.0639
3	60	80	15	1.04	0.0480
4	80	80	15	1.32	0.0550
5	60	60	45	1.27	0.0559
6	80	60	45	0.93	0.0538
7	60	80	45	1.29	0.0506
8	80	80	45	1.53	0.0586
9	53	70	30	0.60	0.0343
10	87	70	30	1.05	0.0638
11	70	53	30	0.99	0.0623
12	70	87	30	1.39	0.0307
13	70	70	5	0.66	0.0393
14	70	70	55	1.03	0.0563
15	70	70	30	0.84	0.0621
16	70	70	30	0.72	0.0699
17	70	70	30	0.79	0.0474
18	70	70	30	0.79	0.0597
19	70	70	30	0.99	0.0506
20	70	70	30	0.69	0.0579

In the face of these results, the decision on the optimal conditions for the following tests relied on choosing the ones with values of A_{pic}/A_{kaemp} ratio higher than

1, combined with values of dry mass above the overall mean. Six of the 20 experiments satisfied these criteria (Figure 1) and, among them, experiments 2, 4, and 10 were chosen to be repeated due to their lower extraction times (15 or 30 min). The conditions were executed in triplicate to promote a better comparison of their results by one-way ANOVA.

Figure 1: A_{pic}/A_{kaemp} ratio (bars) and dry mass of the extract (squares) from each round of the central composite design. Experiments marked with an "⋆" presented a A_{pic}/A_{kaemp} ratio above 1 and a dry mass value above the mean.

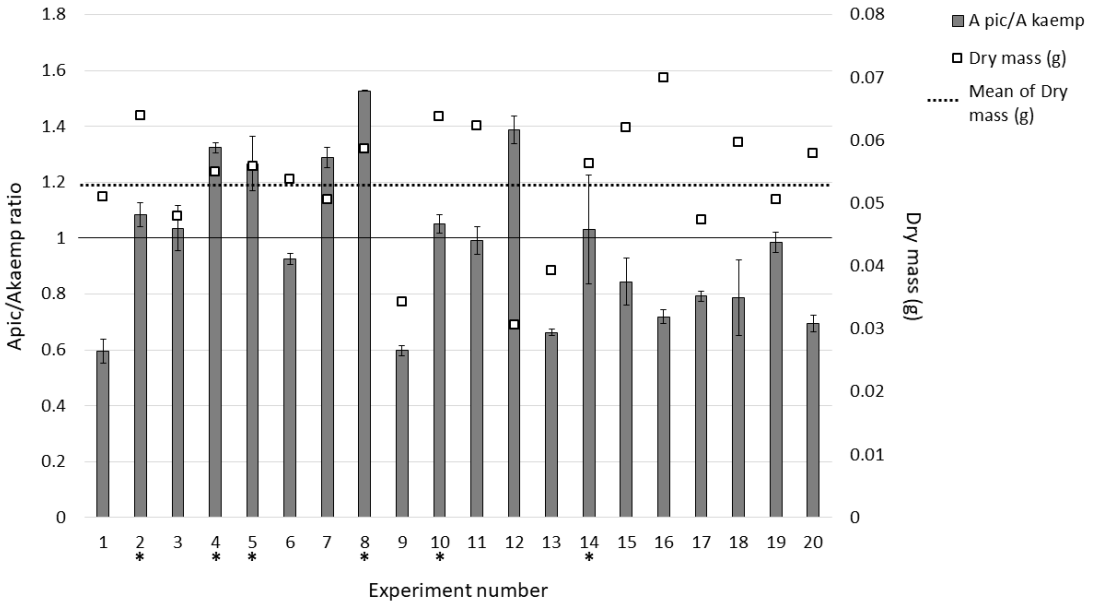

In these assays, extracts with A_{pic}/A_{kaemp} ratios above 1, as expected, and dry mass values within the previously observed range were obtained (Table 3). It can be observed that the values for the A_{pic}/A_{kaemp} ratio and dry mass obtained under the conditions of experiment 10 are higher than what is achieved under conditions 2 and 4. One-way ANOVA (Tables 4 and 5) showed that these results were statistically different (95% confidence), and, even though condition 10 had the highest extraction time within this group, it was chosen as the optimal one due to its relatively higher piceatannol recovery and extraction yield (w/w).

Table 3: Results of experiments 2, 4, and 10 in triplicate.

Parameters				Responses	
Experiment	**T (°C)**	**EtOH (%)**	**t (min)**	**$A_{135/153}$**	**Dry mass (g)**
2	80	60	15	1.23 ± 0.2	0.0404 ± 0.003
4	80	80	15	1.11 ± 0.2	0.0379 ± 0.003
10	87	70	30	1.86 ± 0.1	0.0472 ± 0.002

Table 4: One-way ANOVA for A_{pic}/A_{kaemp} ratio results from conditions 2, 4, and 10.

Source of variation	***SS***	***Df***	***MS***	***F_{calc}***	***P-value***	***F***
Among groups	0.976752	2	0.488376	14.23991	0.005269	5.143253
Within groups	0.205778	6	0.034296			
Total	1.18253	8				

Table 5: One-way ANOVA for dry mass results from conditions 2, 4, and 10.

Source of variation	***SS***	***Df***	***MS***	***F_{calc}***	***P-value***	***F***
Among groups	0.000138	2	6.92E-05	8.360478	0.018415	5.143253
Within groups	4.97E-05	6	8.28E-06			
Total	0.000188	8				

Evaluation of MAE in cycles

Cyclic extraction under the experiment 10 conditions revealed that one single cycle allows the highest mass of dry extract and the highest A_{pic}/A_{kaemp} per gram of extract. However, a one-step extraction was not exhaustive. Some quantity of piceatannol was still found after a fifth cycle of MAE, but the mass recovered after each extraction decreased dramatically. The dry mass for the second cycle is about 30% of

the first cycle, while, from the third cycle onward, the recovery corresponds to 10% of the initial dry mass (Figure 2).

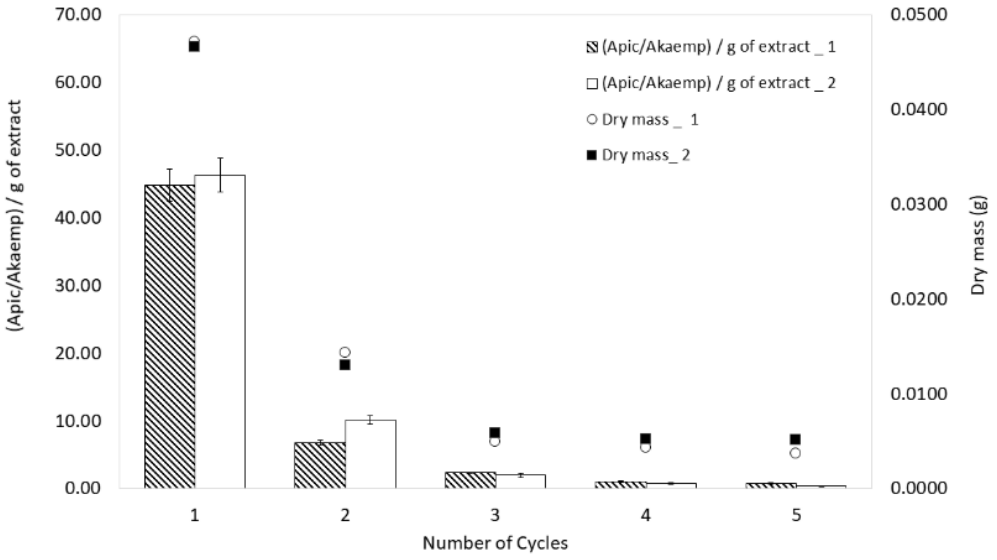

Figure 2: A_{pic}/A_{kaemp} ratio per gram of extract and dry mass recovered in each MAE cycle.

Given that most of the mass was provided by two MAE cycles, a new extraction assay was performed, and the liquid extracts recovered from the two cycles were mixed before solvent removal. For this 60 min process, an amount of 27.17 ± 0.9 µg of piceatannol per mg of the extract was found. The quantification model was proven to be linear within the range evaluated, with a correlation coefficient of 0.9911, a normal distribution of the residues, and with no dependence among the observations (Figure 3). It is interesting to note that, after solvent removal, the dry extract was a fine light brown powder without requiring any additional procedures (Figure 4).

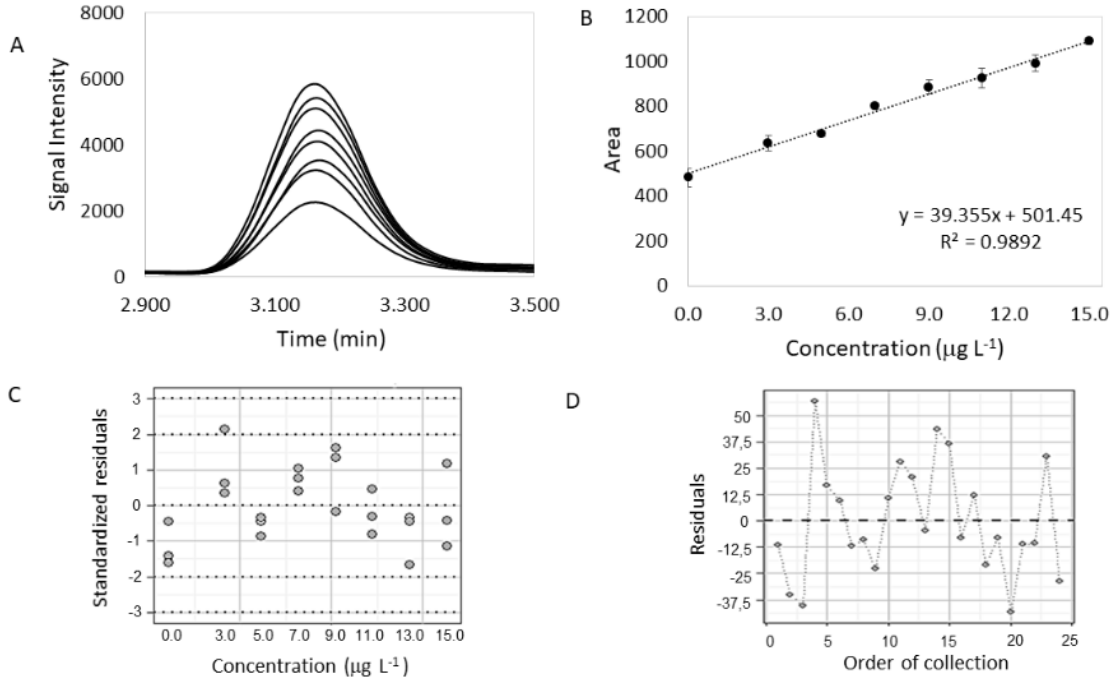

Figure 3: Piceatannol quantification in MAE passion fruit seed cake extract. A. Chromatograms in MRM mode, m/z 245 > 135, of the samples spiked with 0 (lowest) to 15 µg L^{-1} (highest) of standard piceatannol. B. Quantification curve and linear model. C. Standardized distribution of the residues. D. Residues versus collection order. Durbing-Watson test of independence: P-value $_{95\%}$ = 0.315.

Figure 4: Visual aspect of passion fruit seed cake extract obtained by MAE.

Conventional Soxhlet extraction

The replicates showed similar chemical profiles according to the fingerprint analysis, but the spectra were different from what was observed for MAE, indicating that the conditions applied in these techniques promoted different selectivity of passion

fruit seed compounds for the extraction solvent (Figure 5). This is also confirmed by the physical aspect of the dry Soxhlet extract, which appeared as dark lumps (Figure 6).

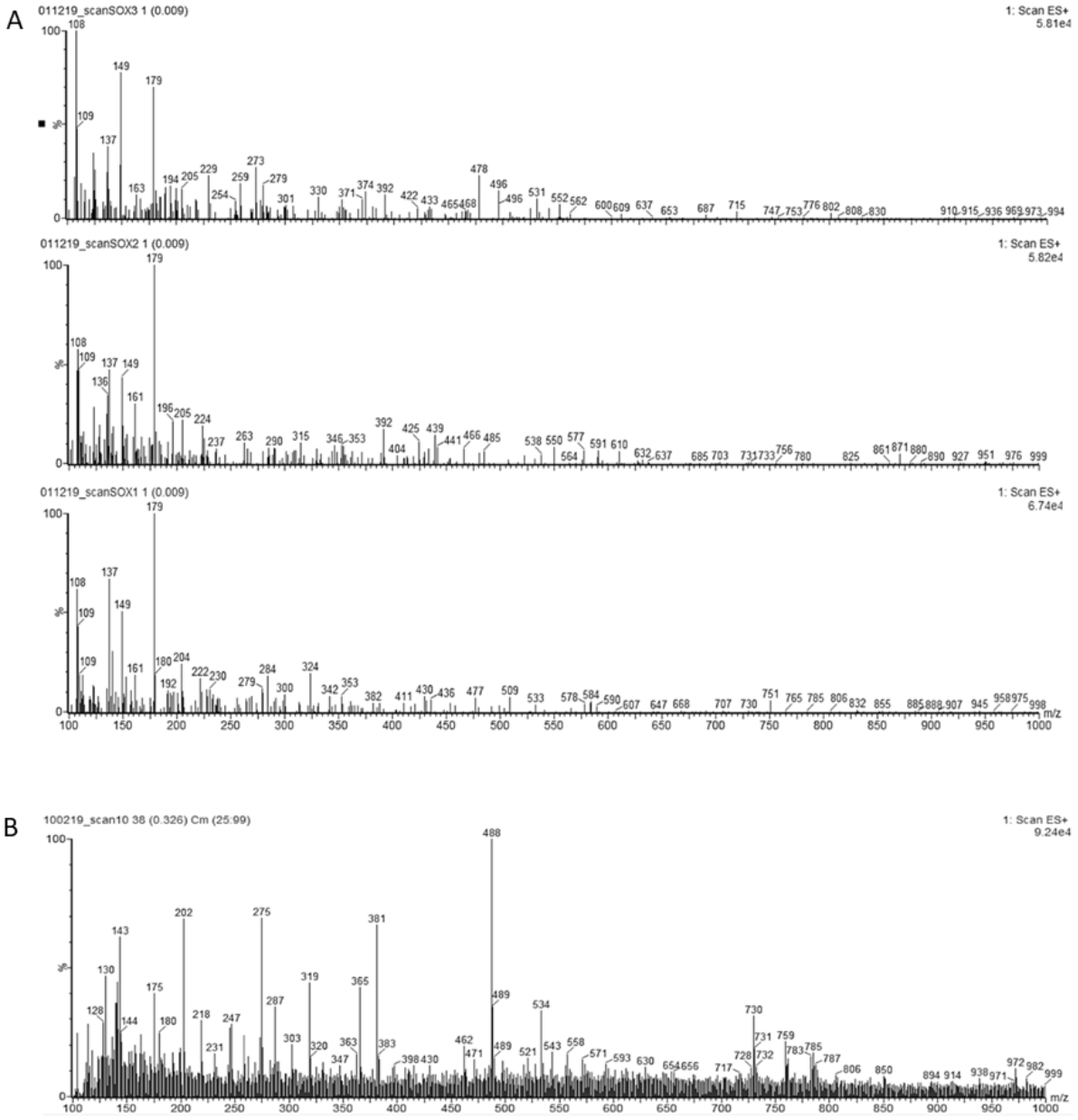

Figure 5: Fingerprint analyses of the triplicate of Soxhlet (A) and experiment 10 MAE (B) passion fruit seed cake extracts.

Figure 6: Visual aspect of passion fruit seed cake extract obtained by Soxhlet extraction.

Soxhlet extraction provided 81.51 ± 5.73 mg of dry extract, which corresponded to an extraction yield of 0.8% (w/w), and its piceatannol concentration was of 13.03 ± 0.4 µg mg^{-1}. The quantification curve for this extract was also proven to be linear within the range evaluated and presented a correlation coefficient of 0.9927. The residues were normally distributed and no dependence among the observations was observed (Figure 7).

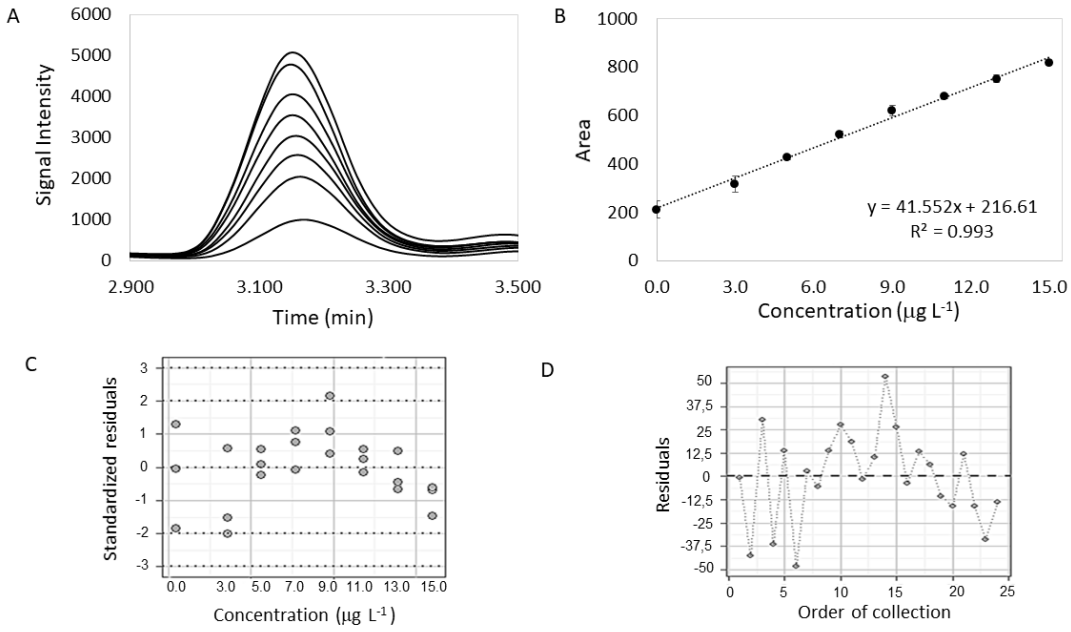

Figure 7: Piceatannol quantification in the Soxhlet passion fruit seed cake extract. A. Chromatograms in MRM mode, m/z 245 > 135, of the samples spiked with 0 (lowest) to 15 µg L^{-1} (highest) of standard piceatannol. B. Quantification curve and linear model. C. Standardized distribution of the residues. D. Residues versus collection order. Durbing-Watson test of independence: P-value $_{95\%}$ = 0.8713.

Discussion

As mentioned, MAE is an advanced technique that provides the induction of molecular dipole rotation, allowing internal, rapid, and selective heating of the samples. It was introduced in the 1970s for acid digestion of samples aiming at metal analysis and its use expanded to the extraction of organic molecules in the 1980s. Since then, an increase in the application of MAE for the extraction of bioactive compounds from plant and waste materials has been observed (Li et al., 2019; Poole, 2020).

The heating phenomenon in MAE occurs by the interaction between an incident microwave radiation and dielectric molecules having a dipole moment. This interaction results in molecular movement and, therefore, in temperature elevation. Despite being a heating-based extraction technique, its inside-out heat dissipation mechanism of action makes it unique and different from the conventional jacket heating or reflux extractions, in which heat is dissipated from the outside to the inside of the sample. This is probably the reason why heating in MAE is faster than in conventional techniques and results in shorter processing times and lower energy consumptions (Chemat et al., 2017; Li et al., 2019; Poole, 2020).

Other important features of MAE are also evident. One of them is that, in sealed extraction vessels, an increase in pressure can be provided by fast heat dissipation: pressure promotes mass transfer from the sample to the solvent by the phenomena of solvent surface tension and viscosity reductions, which favor solvent penetration into the sample matrix, and target compound solubility enhancement in the extractor solvent. Another aspect of MAE is that its inside-out heating mechanism allows water within the matrix to be heated. This ruptures the biomasses walls by the rapid evaporation of intrinsic water molecules and favors the extraction of the biocompounds into the solvent phase. Lastly, different materials respond differently to incident microwaves, and this leads to the selective extraction of certain compounds (Chemat et al., 2017; Li et al., 2019).

Indeed, traditional Soxhlet extraction and MAE resulted in passion fruit seed cake extracts with different aspects. The first difference consists in their chemical profiles, shown in Figure 4: while Soxhlet extracts exhibited higher relative abundances for m/z 179, MAE extracts showed the highest peaks mainly for m/z 488 and 381.

Therefore, the techniques favored different selectivities in the extraction of seed cake compounds, even though the extraction solvents were quite similar. This variation leads to the distinct qualities of the obtained extracts, as seen in Figures 4 and 6. Since piceatannol exerts biological activities on the skin, formulating a topical product with the Soxhlet extract could become a real challenge due to its dark color and lumpy aspect. On the other hand, the light brown powder readily available after solvent removal from the MAE extract might foster an easier incorporation into creams and lotions.

Compared to Soxhlet, MAE was also proven to be more advantageous for piceatannol extraction from the passion fruit seed cake. While the Soxhlet extract corresponded to 0.8% of the initial cake mass, MAE allowed a recovery between 6.1 to 14.0%, which means that, in terms of product quantity, MAE would be more profitable. Even though a one-step MAE was not exhaustive under the evaluated conditions, two MAE cycles could be considered reasonable in terms of extraction time and piceatannol recovery. In a two-step MAE, which results in a 60 min process, a quantity of 27.17 ± 0.9 μg of piceatannol per mg of the extract could be achieved, in contrast to only 13.03 ± 0.4 μg mg^{-1} for a 120 min Soxhlet extraction.

Industrial-scale MAE use is still incipient, and it faces some instrumental hurdles to be overcome, but reports on the scaling-up of this technique are encouraging. Petigny et al. (2014) reported that MAE was more efficient than classical hydrodistillation for the recovery of volatile and non-volatile compounds from boldo leaves. A lab-scale process generated a product with improved sensorial properties that could facilitate its integration into a perfumed cosmetic formulation. This process was scaled-up by a factor of 30 times to a pilot microwave apparatus and it was claimed to be more sustainable than conventional hydrodistillation due to greater energy efficiency and less time. Garcia-Garcia et al. (2019) made a life-cycle assessment for the extraction of pectin from residual orange peels by pilot-scale MAE, and the obtained product met all the criteria required for a food-grade commercial product. MAE had a better yield and caused less than 25% of the environmental impact of the traditional process. Based on the present results, MAE seems to also be a promising technique to produce passion fruit seed or seed cake extracts with high levels of piceatannol and adequate physical properties for the formulation of topical products that enhance the value of a sub utilized residue from the passion fruit industry.

Conclusions

In this study, MAE was evaluated as a technique for the preparation of passion fruit seed extract, and it was proven to be superior to Soxhlet extraction in terms of extraction yield and piceatannol quantity. A double MAE at 87 °C, with 70% EtOH for each 30 min cycle provided a fine brown powder with 27.17 ± 0.9 μg of piceatannol per mg of the extract. In contrast, Soxhlet extraction in twice the time of MAE resulted in a dark lumpy extract containing only half of the piceatannol content. The chemical profiles of all tested MAE conditions were quite similar but were distinct from what was observed for the Soxhlet process. The extract obtained by MAE has a considerable potential to be incorporated into topical formulations such as creams and lotions for skin care and, even though the use of industrial-scale MAE is still discrete, there is a potential for scaling-up the conditions addressed here to give value to a less explored residue.

Appendix

Supplementary material: Fingerprint analyses of the 20 extracts from MAE preliminary evaluation.

Acknowledgments

This work was financially supported by the National Institutes of Science and Technology (INCTs) [grant numbers: FAPESP/INCT 2014/50867, CNPq 465389/2014-7]. C. B. G. Bottoli acknowledges CNPq for a research fellowship [CNPq 309363/2018-7].

References

Chemat, F., Rombaut, N., Meullemiestre, A., Turk, M., Perino, S., Fabiano-Tixier, A.S., Abert-Vian, M., 2017. Review of green food processing techniques. Preservation, transformation, and extraction. Innov. Food Sci. Emerg. Technol. 41, 357-377. https://doi.org/10.1016/j.ifset.2017.04.016

da Silva, M.V., de Oliveira, F. dos S., Demczuk Junior, B., Haminiuk, C.W.I., Visentainer, J.V., 2018. Hygroscopic equilibrium of microencapsulated extract of passion fruit seed and its effect on the antioxidant capacity. J. Food Process Eng. 41, e12597. https://doi.org/10.1111/jfpe.12597

de Santana, F.C., de Oliveira Torres, L.R., Shinagawa, F.B., de Oliveira e Silva,

A.M., Yoshime, L.T., de Melo, I.L.P., Marcellini, P.S., Mancini-Filho, J., 2017. Optimization of the antioxidant polyphenolic compounds extraction of yellow passion fruit seeds (*Passiflora edulis* Sims) by response surface methodology. J. Food Sci. Technol. 54, 3552–3561. https://doi.org/10.1007/s13197-017-2813-3

Ferrari, R.A., Colussi, F., Ayub, R.A., 2004. Caracterização de subprodutos da industrialização do maracujá-aproveitamento das sementes. Rev. Bras. Frutic. 26, 101–102. https://doi.org/10.1590/s0100-29452004000100027

Garcia-Garcia, G., Rahimifard, S., Matharu, A.S., Dugmore, T.I.J., 2019. Life-cycle assessment of microwave-assisted pectin extraction at pilot scale. ACS Sustain. Chem. Eng. 7, 5167–5175. https://doi.org/10.1021/acssuschemeng.8b06052

Kawakami, S., Kinoshita, Y., Maruki-Uchida, H., Yanae, K., Sai, M., Ito, T., 2014. Piceatannol and its metabolite, isorhapontigenin, induce SIRT1 expression in THP-1 human monocytic cell line. Nutrients 6, 4794–4804. https://doi.org/10.3390/nu6114794

Li, H., Zhao, Z., Xiouras, C., Stefanidis, G.D., Li, X., Gao, X., 2019. Fundamentals and applications of microwave heating to chemicals separation processes. Renew. Sustain. Energy Rev. 114, 109316. https://doi.org/10.1016/j.rser.2019.109316

Li, Y., Fabiano-Tixier, A.S., Abert-Vian, M., Chemat, F., 2013. Microwave-assisted extraction of antioxidants and food colors, in: Food Engineering Series. Springer, pp. 103–125. https://doi.org/10.1007/978-1-4614-4830-3_5

Maracujá - Portal Embrapa [WWW Document], n.d. URL https://www.embrapa.br/mandioca-e-fruticultura/cultivos/maracuja (accessed 7.23.20).

Maruki-Uchida, H., Kurita, I., Sugiyama, K., Sai, M., Maeda, K., Ito, T., 2013. The protective effects of piceatannol from passion fruit (*Passiflora edulis*) seeds in UVB-irradiated keratinocytes. Biol. Pharm. Bull. 36, 845–849. https://doi.org/10.1248/bpb.b12-00708

Matsui, Y., Sugiyama, K., Kamei, M., Takahashi, T., Suzuki, T., Katagata, Y., Ito, T., 2013. Seeking a new anti-skin-aging material: piceatannol and its derivatives from passion fruit (*Passiflora edulis*) seed, in: ACS Symposium Series. American Chemical Society, pp. 189–202. https://doi.org/10.1021/bk-2013-1129.ch012

Matsui, Y., Sugiyama, K., Kamei, M., Takahashi, T., Suzuki, T., Katagata, Y., Ito, T., 2010. Extract of passion fruit (*Passiflora edulis*) seed containing high amounts of piceatannol inhibits melanogenesis and promotes collagen synthesis. J. Agric. Food Chem. 58, 11112–11118. https://doi.org/10.1021/jf102650d

Oliveira, D.A., Angonese, M., Gomes, C., Ferreira, S.R.S., 2016. Valorization of

passion fruit (*Passiflora edulis* sp.) by-products: sustainable recovery and biological activities. J. Supercrit. Fluids 111, 55–62. https://doi.org/10.1016/j.supflu.2016.01.010

Os usos múltiplos do maracujá - Revista Globo Rural | Agricultura [WWW Document], n.d. URL https://revistagloborural.globo.com/Noticias/Agricultura/noticia/2014/09/os-usos-multiplos-do-maracuja.html (accessed 1.8.21).

Pan, Z.H., Ning, D.S., Fu, Y.X., Li, D.P., Zou, Z.Q., Xie, Y.C., Yu, L.L., Li, L.C., 2020. Preparative isolation of piceatannol derivatives from passion fruit (*Passiflora edulis*) seeds by high-speed countercurrent chromatography combined with high-performance liquid chromatography and screening for α-glucosidase inhibitory activities. J. Agric. Food Chem. 68, 1555–1562. https://doi.org/10.1021/acs.jafc.9b04871

Petigny, L., Périno, S., Minuti, M., Visinoni, F., Wajsman, J., Chemat, F., 2014. Simultaneous microwave extraction and separation of volatile and non-volatile organic compounds of boldo leaves. From lab to industrial scale. Int. J. Mol. Sci. 15, 7183–7198. https://doi.org/10.3390/ijms15057183

Poole, C.F., 2020. Milestones in the development of liquid-phase extraction techniques, in: Liquid-Phase Extraction. Elsevier, pp. 1–44. https://doi.org/10.1016/B978-0-12-816911-7.00001-3

Uchida-Maruki, H., Inagaki, H., Ito, R., Kurita, I., Sai, M., Ito, T., 2015. Piceatannol lowers the blood glucose level in diabetic mice. Biol. Pharm. Bull. 38, 629–633. https://doi.org/10.1248/bpb.b15-00009

Viganó, J., Zabot, G.L., Martínez, J., 2017. Supercritical fluid and pressurized liquid extractions of phytonutrients from passion fruit by-products: economic evaluation of sequential multi-stage and single-stage processes. J. Supercrit. Fluids 122, 88–98. https://doi.org/10.1016/j.supflu.2016.12.006

PASSION FRUIT SEED EXTRACT OBTAINED BY MICROWAVE-ASSISTED EXTRACTION: A PICEATANNOL RICH PRODUCT WITH ADVANTAGEOUS FEATURES FOR FORMULATIONS

Gisláine C. Silva, Rodney A. F. Rodrigues and Carla B. G. Bottoli*

SUPPLEMENTARY MATERIAL

Fingerprint analyses of the 20 extracts from MAE preliminary evaluation. For spectrometric conditions, see item 2.4. Spectra are disposed in ascending order, from experiment 1 to 20.

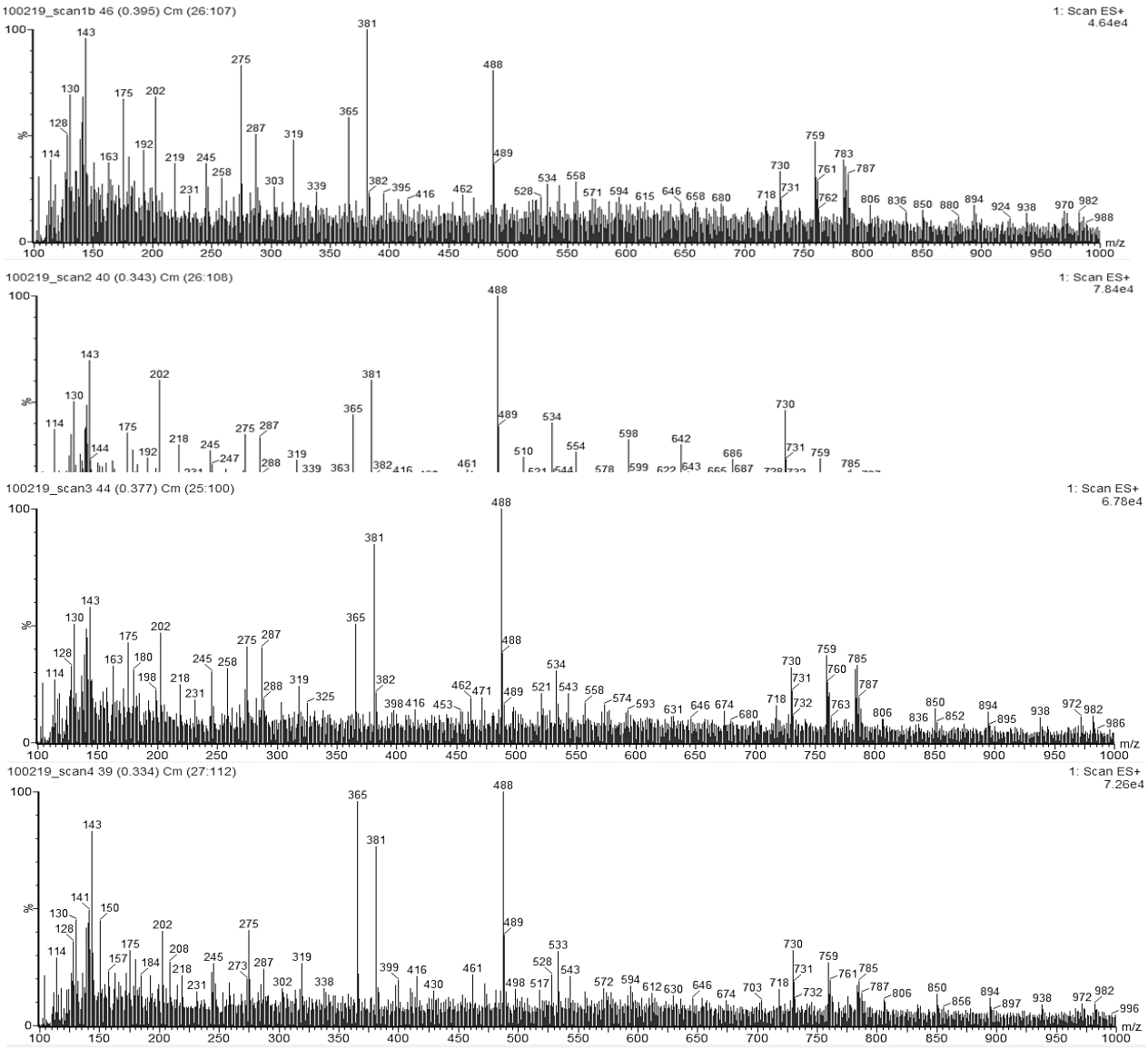

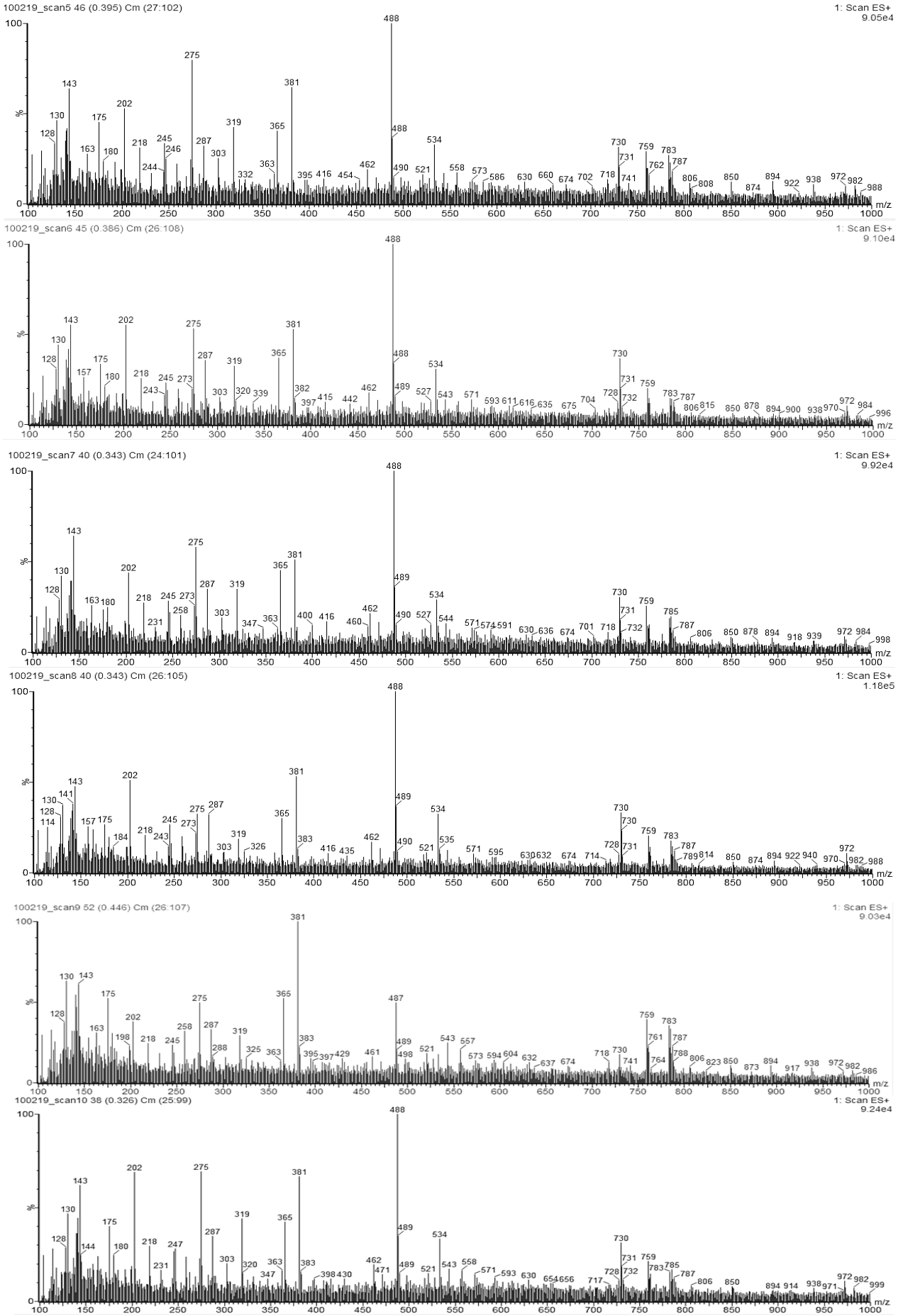
100219_scan5 46 (0.395) Cm (27:102)
1: Scan ES+
9.05e4
100219_scan6 45 (0.386) Cm (26:108)
1: Scan ES+
9.10e4
100219_scan7 40 (0.343) Cm (24:101)
1: Scan ES+
9.92e4
100219_scan8 40 (0.343) Cm (26:105)
1: Scan ES+
1.18e5
100219_scan9 52 (0.446) Cm (26:107)
1: Scan ES+
9.03e4
100219_scan10 38 (0.326) Cm (25:99)
1: Scan ES+
9.24e4
%
m/z

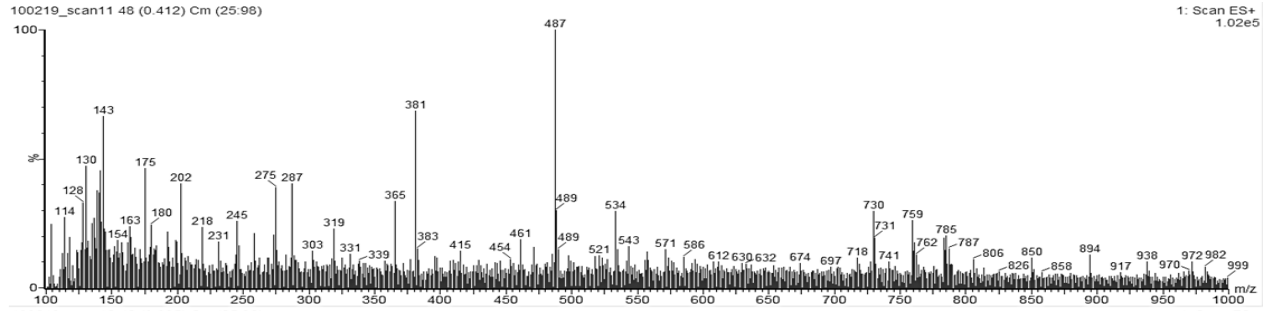
100219_scan11 48 (0.412) Cm (25:98)
1: Scan ES+
1.02e5
%
m/z

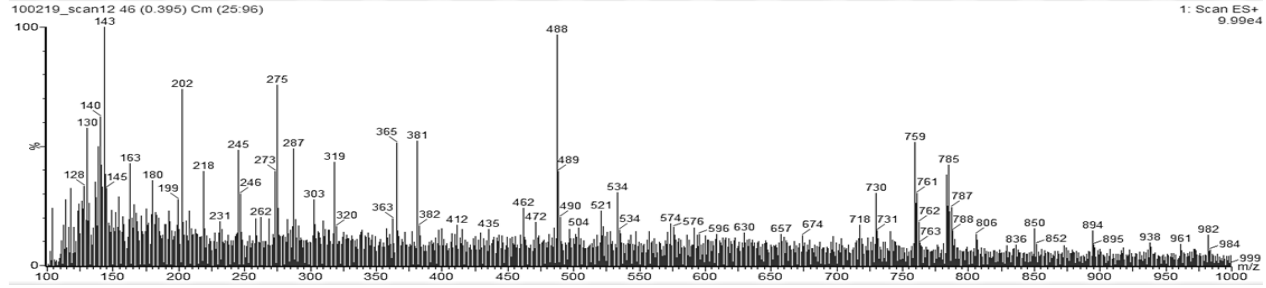
100219_scan12 46 (0.395) Cm (25:96)
1: Scan ES+
9.99e4
%
m/z

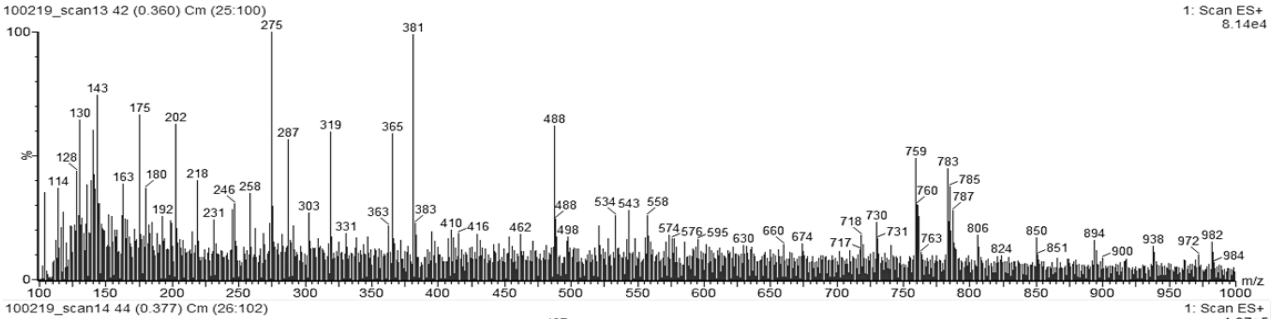
100219_scan13 42 (0.360) Cm (25:100)
1: Scan ES+
8.14e4
%
m/z

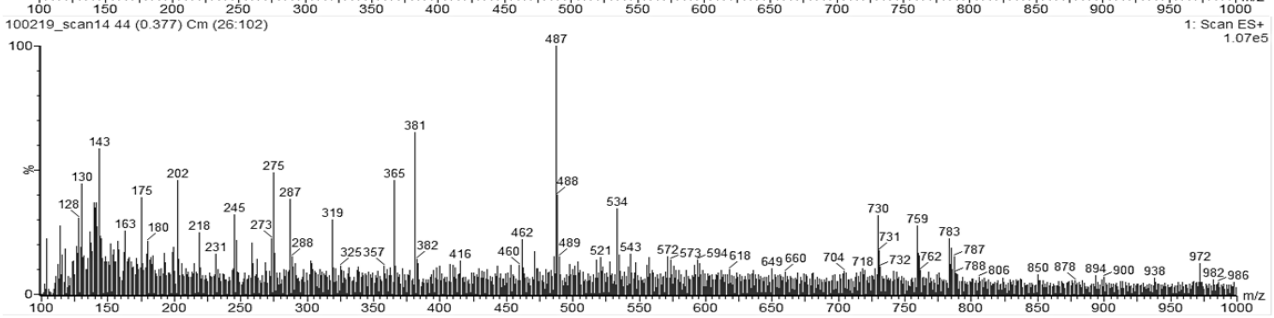
100219_scan14 44 (0.377) Cm (26:102)
1: Scan ES+
1.07e5
%
m/z

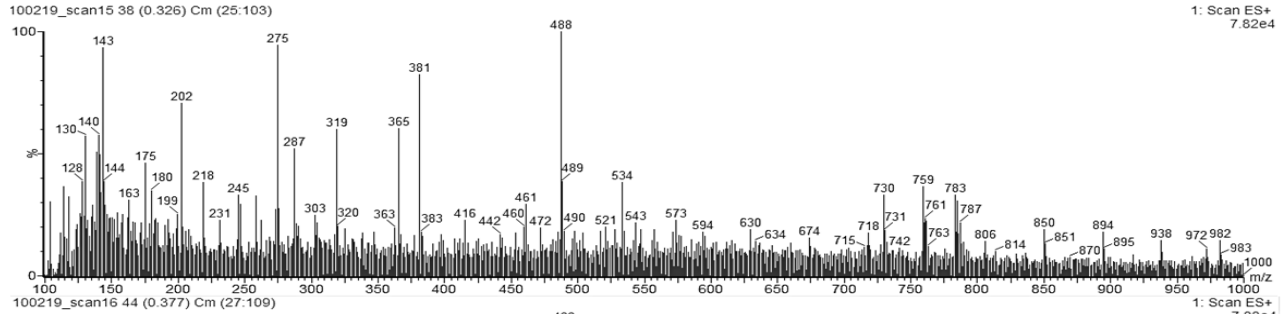
100219_scan15 38 (0.326) Cm (25:103)
1: Scan ES+
7.82e4
%
m/z

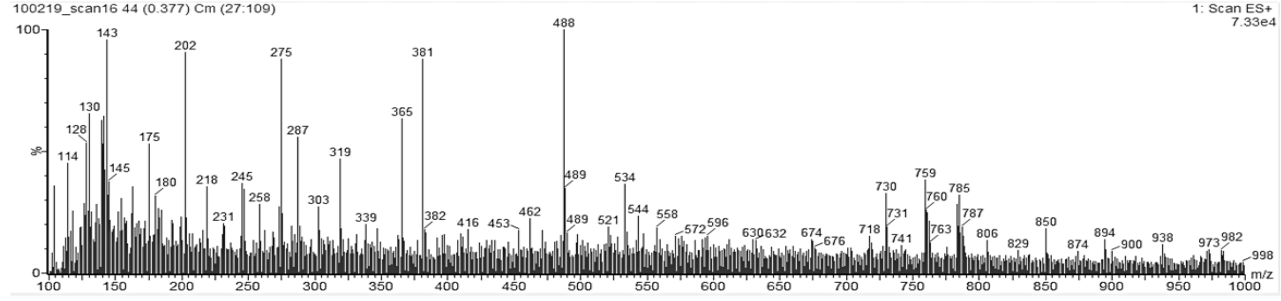
100219_scan16 44 (0.377) Cm (27:109)
1: Scan ES+
7.33e4
%
m/z

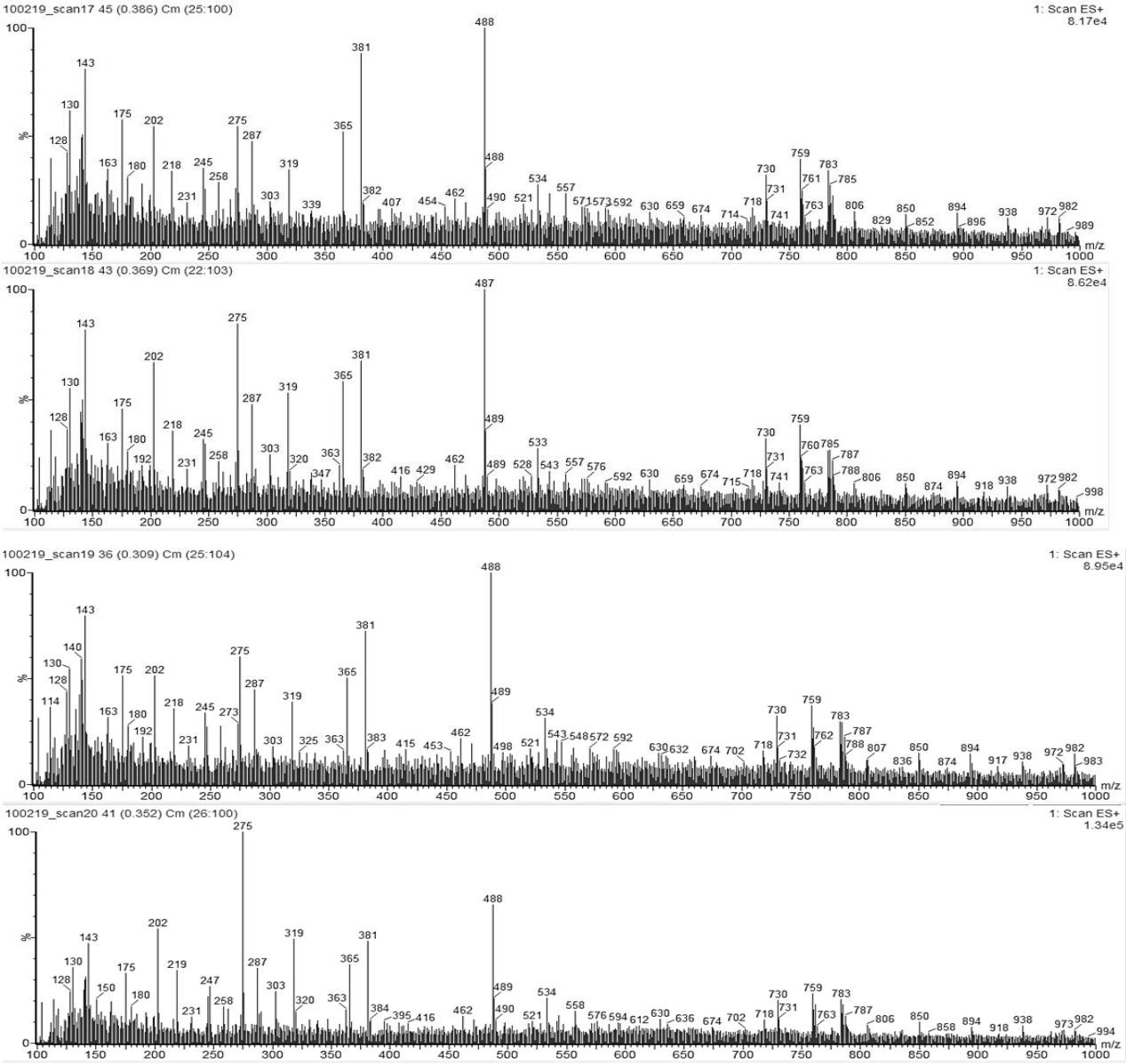
100219_scan17 45 (0.386) Cm (25:100)
1: Scan ES+
8.17e4
100219_scan18 43 (0.369) Cm (22:103)
1: Scan ES+
8.62e4
100219_scan19 36 (0.309) Cm (25:104)
1: Scan ES+
8.95e4
100219_scan20 41 (0.352) Cm (26:100)
1: Scan ES+
1.34e5
%
m/z

CAPÍTULO 3

Piceatannol and spilanthol-rich extracts in emulsions comprising organic and inorganic ultraviolet filters: a compatibility study

PICEATANNOL AND SPILANTHOL-RICH EXTRACTS IN EMULSIONS COMPRISING ORGANIC AND INORGANIC ULTRAVIOLET FILTERS: A COMPATIBILITY STUDY

Gisláine C. Silva[1], Rodney A. F. Rodrigues[2], Carla B. G. Bottoli[1*]

[1]Institute of Chemistry, University of Campinas (Unicamp), POB 6154, 13084-971, Campinas, SP, Brazil.

[2]Chemical, Biological and Agricultural Pluridisciplinary Research Center (CPQBA), University of Campinas (Unicamp), 13148-218, Paulínia, SP, Brazil.

*Corresponding author: carlab@unicamp.br

Abstract

OBJECTIVE: To evaluate the compatibility of a piceatannol-rich passion fruit seed extract (P_{ext}), a spilanthol-rich paracress (jambu) extract (J_{ext}), and their combinations with organic and inorganic UV filters in an emulsion.

METHOD: A base emulsion based on a non-ionic emulsifier and an acrylate-based gelling agent (B_{em}) was added with organic (O_{em}) or inorganic (I_{em}) filters. P_{ext}, J_{ext}, or both were added to the emulsions, and the stability was evaluated by analytical centrifugation, UV spectroscopy, DSC, TG, and by the quantification of piceatannol and spilanthol before and after their exposure to temperature cycles.

RESULTS: The UV spectra of the emulsions were not altered by the extracts. Except for I_{em}, all the formulations were physically stable. TG curves for all the formulations showed a major mass loss from 25 to about 110-130 °C. The extracts elevated the B_{em} fusion point in about 10 °C, while P_{ext} lowered the temperature of the compound volatilization event in the same extent. Both extracts, mainly J_{ext}, lowered O_{em} temperature of the first TG event, and P_{ext} exhibited instantaneous color change when incorporated into I_{em}. Piceatannol was reduced to 40 % of its initial content in B_{em}, and it was not identified in O_{em} and I_{em} after the twelve-days temperature cycle. Spilanthol was observed in all formulations, but in reduced content in I_{em} after the same period.

CONCLUSION: The extracts did not affect the physical stability, but chemical interactions occurred in all the formulations. The extracts were incompatible with TiO_2 and ZnO in the emulsion proposed in this work. The extracts micro or nano encapsulation, or their inclusion into vehicles with less or no water are suggested for future applications.

Keywords: Chemical analysis, Emulsions, Formulation stability, passion fruit, paracress

Abbreviations

B_{em}: Base emulsion

O_{em}: Organic sunscreen emulsion

I_{em}: Inorganic sunscreen emulsion

P_{ext}: Piceatannol-rich passion fruit seed extract

J_{ext}: Spilanthol-rich paracress (jambu) aerial parts extract

Introduction

In skincare, sunscreens aim to prevent sunburn and other deleterious effects of the skin exposition to the sun. Sunscreens either scatter or absorb sunlight at the skin surface to avoid UV penetration into deeper skin layers. Some studies have demonstrated the protection enhancement effects of bioactive ingredients such as caffeine, vitamins C and E, antioxidants, and plant extracts to sunscreen formulations. However, their efficacies are dependent on their stability in the final formulation, as well as on their ability to penetrate the stratum corneum and reach to the deepest layers of the dermis and the epidermis in ideal concentrations to exert their biological effect [1].

Piceatannol (3,3′,4′,5-trans-tetrahydroxystilbene) is a stilbenoid compound with skin whitening, antioxidant, anti-aging, cutaneous wound-healing, and anti-acne properties, and it is a potential molecule to promote skin protection, health, and youth. It is found in grapes and wines (*Vittis* ssp.), in blueberries (*Vaccinium* ssp.) and several species from the genus *Polygonum, Melaleuca, Cassia, Rheum, Euphorbia, Mezoneuron, Caragana, Partneocissus, Aiphanes, Arachis, Ampelopsis, Picea* and *Byrsonima.* [2–4].

Passion fruit seeds (*Passiflora edulis* Sims.) are also a rich source of piceatannol. Regarding passion fruit seed extracts in skincare, a double-blind study with 32 women between 35 and 54 years old showed that the oral administration of a 5 mg piceatannol standardized extract promoted an improvement in skin hydration at the end of 8 weeks. However, other oral intake studies show that piceatannol exhibits lower absorption than its analog, resveratrol, and it can be biotransformed by the human gut microbiota in different speeds, intensities, and metabolic pathways. In liver cells, piceatannol is quickly converted into the isomers rapontigenin and isorapontigenin, and it undergoes rapid glucuronidation, sulfation, and o-methylation when in the blood stream, being rapidly clearanced [5–9].

Given these metabolic aspects, the topical application of piceatannol might be an interesting alternative for taking profit of its skin benefits. On the cutaneous permeation of piceatannol, Hung et al. [10] stated that this molecule presents 11.6 times less penetration into the skin than resveratrol when in vehicles such as aqueous buffers, soy oil and hydrogel system. In the Eskandari et al. [11] *in vitro* model for

molecular antioxidant activity assessment into the skin, piceatannol was classified in the group of the lipophilic compounds which exert antioxidant activity between 2 and 20 min, while rutin, another natural polyphenolic with a well-established antioxidant activity, showed no results as it was considered too hydrophilic to permeate the skin barrier.

Spilanthol is a natural compound that exhibits a permeation-promoting effect, aside from its well stablished anti-wrinkle activity in the cosmetic industry. It is extracted from the aerial parts of paracress (*Acmella oleracea* L., or *Spilanthes acmella* auct. non (L.) Murr.), known as jambu in Brazil, and there are commercial anti-aging ingredients and patented cosmetic products with a plethora of *Spilanthes* species. Due to these properties, the addition of spilanthol to a piceatannol formulation might be a good strategy to overcome its relatively poor diffusion through the skin [12–15].

To be feasible in terms of effects, the system piceatannol-spilanthol-sunscreen must be stable in a topical formulation, though. Therefore, a piceatannol-rich passion fruit seed extract compatibility evaluation with a spilanthol-rich paracress extract, organic and inorganic UV filters was done in an emulsion formulation to assess the feasibility of these combinations in skincare products.

Materials and Methods

Piceatannol-rich extract from passion fruit seeds (Pext)

The piceatannol-rich extract was prepared from passion fruit residual seed cake from cold press oil extraction (Extrair Óleos Naturais, Rio de Janeiro, Brazil) according to Silva, Rodrigues, and Bottoli [16]. Briefly, the residual cake was defatted with n-hexane (Analytical grade, Unicamp Institute of Chemistry Pilot Plant, São Paulo, Brazil) at a 1:10 w/v ratio, by magnetic stirring the suspension for one hour, at room temperature. The defatted cake was dried by n-hexane evaporation in a fume hood, and it was extracted in a Start E bench-scale microwave extractor (Milestone, Bergamo, Italy) with 70 % EtOH, at 87°C, for 30 min, twice. A cake:solvent ratio of 1:30, w/v was used, and the extractions were performed with a maximum magnetic stirring speed. The extracts were collected by vacuum filtration in filter paper, and the solvent was removed under an N2 (g) flow.

Spilanthol-rich extract from paracress (jambu) aerial parts (J_{ext})

Crude 95 % EtOH paracress (*Spilanthes acmella* auct. non (L.) Murr.) stems, flowers and leaves extract was provided by the Chemical, Biological, and Agricultural Pluridisciplinary Research Center (CPQBA – Unicamp, São Paulo, Brazil). In a separatory funnel, 50 mL of the crude extract was added to 300 mL of analytical grade n-hexane (Unicamp Institute of Chemistry Pilot Plant, SP, Brazil) and it was vigorously shaken. The supernatant fraction was collected, the solvent was evaporated under an $N_{2\,(g)}$ flow. The resulting oil was vacuum-filtered over silica in a sintered plate funnel. A translucent olive-green liquid extract was obtained.

Formulations development

Oil-in-water (O/W) emulsions were produced by Magispharma (São Paulo, Brazil) according to the compositions described in Table 1. The aqueous and oily ingredients, except for DC245TM (Dow Corning, USA) and phenoxyethanol, were separately heated to around 75 °C, and vigorously mixed to form each emulsion until room temperature. The remaining ingredients were mixed into the emulsions with a spatula. Three emulsion types were developed: the “base” emulsion (B_{em}), the “organic sunscreen emulsion” (O_{em}), which is the base formulation added with the organic sunscreens Parsol MCXTM (DSM, Holland), Uvinul A PlusTM and Uvinul T150TM (Basf, Germany), and the inorganic sunscreen emulsion (I_{em}), the base formulation added with TiO_2 (Zano 10 plusTM, EverCare, USA), and ZnO (T-Lite SFTM, Basf, Germany). The content and combination of the organic and inorganic UV filters were defined with the aid of Basf Sunscreen SimulatorTM [17] to provide emulsions with a simulated Sun Protection Factor (SPF) of 10.

The extracts P_{ext} and J_{ext} were incorporated into the emulsions at 2 mg g^{-1} and 1 mg g^{-1}, respectively, by dispersing them in propylene glycol (10 mg g^{-1}) and mixing the dispersions to the emulsions with a spatula. In total, 12 formulations were evaluated in this study (Fig. 1).

Table 1: Compositions of the oil-in-water (O/W) emulsions.

Ingredient	INCI name	Description	Ingredient (%)		
			Base (B_{em})	Organic (O_{em})	Inorganic (I_{em})
Water	Aqua	Vehicle	85.85	79.85	78.35
EDTA	EDTA	Chelating agente	0.1	0.1	0.1
Glycerin	Glycerin	Humectant	1.0	1.0	1.0
Uvinul A plus[1]	Diethylamino Hydroxybenzoyl Hexyl Benzoate	Organic UV filter	-	2.0	-
Parsol MCX[2]	Ethylhexyl Methoxycinnamate	Organic UV filter	-	2.0	-
Uvinul T 150[1]	Ethylhexyl Triazone	Organic UV filter	-	2.0	-
Zano 10 plus[3]	Zinc Oxide (and) Triethoxycaprylylsilane	Inorganic UV filter	-	-	3.5
T-Lite SF[1]	Titanium Dioxide (and) Hydrated Silica (and) Aluminum Hydroxide (and) Hydrogen Dimethicone	Inorganic UV filter	-	-	4.0
BHT	BHT	Antioxidant	0.1	0.1	0.1
Emulium 22[4]	Tribehenin PEG-20 Esters	Non-ionic emulsifier	2.0	2.0	2.0
TGACC	Caprylic/Capric Triglyceride	Emollient	4.0	4.0	4.0
Lecigel[5]	Sodium Acrylates Copolymer (and) Lecithin	Gelling agente	1.0	1.0	1.0
Phenoxyetanol	Phenoxyetanol	Preservative	1.0	1.0	1.0
DC245[6]	Cyclopentasiloxane	Sensory modifier	5.0	5.0	5.0

[1] Basf, Germany, [2] DSM, Holland, [3] EverCare, USA, [4] Gattefossé, France, [5] Lucas Meyer Cosmetics, Canada, [6] Dow Corning, USA

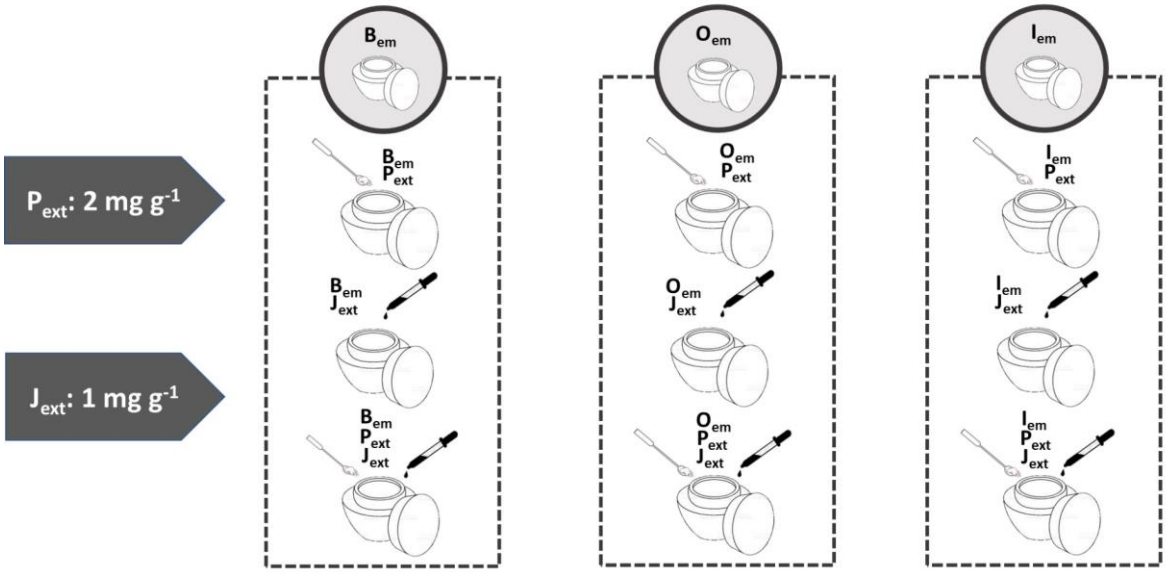

Figure 1: Schematic representation of the 12 formulations. B_{em}: base emulsion. O_{em}: organic sunscreen emulsion. I_{em}: inorganic sunscreen emulsion. P_{ext}: piceatannol-rich passion fruit seed extract. J_{ext}: spilanthol-rich paracress (jambu) aerial parts extract.

Ultraviolet (UV) spectra

One milligram of each formulation was dissolved in 5 ml of analytical grade ethanol (Synth, Diadema, São Paulo), and the UV spectra of the solutions were acquired in an HP 8453 spectrophotometer (Agilent Technologies, California, USA). The samples were loaded into 10 mm optical path quartz cuvettes and the spectral data from 190 to 800 nm were recorded.

Analytical centrifugation

Samples of the 12 formulations were placed in 2 mm optical path polycarbonate cuvettes, and they were centrifuged in a Lumisizer® multisample analytical centrifuge (LUM, GmbH, Berlin, Germany), at 25 °C, for 180 min, at 1500 G (3210 rpm). A total of 120 transmittance profiles were acquired at 865 nm every 5 s at the beginning of the assay, followed by 780 profiles collected every 13 s at the same wavelength until the end of the time. The results were obtained by visual inspection of the cuvettes in comparison with the graphical transmittance profiles. The assay was performed in triplicate for each sample [18].

Thermal analyses

The 12 samples were subjected to differential scanning calorimetry (DSC) and thermogravimetry (TG) analyses adapted from [19]. The assays were done in an oxidative atmosphere. DSC curves were taken in a 2910 DSC equipment (TA Instruments, New Castle, USA), with a heat rate of 15 °C min-1, from 25 to 350 °C. TG analyses were done in a 2950 TGA instrument (TA Instruments, New Castle, USA), from 25 to 400 °C, at a heating rate of 10 °C min^{-1}.

Exposure to temperature cycles

Three 1 ml Eppendorf flasks containing one gram of each formulation were exposed to 5 °C (refrigerator) and 40 °C (stove) on alternate days for 12 days (T_{12}) [20]. The visual aspect of each formulation was inspected at T_0 and T_{12}, and the pH at

the same points was measured by dipping a pH-indicator strip (Merck KGaA, Darmstadt, Germany) into the content of the flasks.

UHPLC-DAD piceatannol and spilanthol quantification

The piceatannol and spilanthol content in the formulations before and after their exposure to the temperature cycles was quantified in a Waters Acquity UPLC system with a binary pump, thermostated column manager, thermostated autosampler, and a photodiode array detector (PAD). For the analyses, 50.0 mg of each formulation and 1.0 ml of 50 % EtOH were mixed in falcon tubes with the aid of a vortex mixer. The suspensions were centrifuged at 3000 rpm for 5 minutes and the supernatants were filtered through 0.22 um regenerated cellulose membranes (GVS, Bologna, Italy) before injection. The samples were kept at 20 °C at the autosampler and 5 µl of each sample was injected per run.

The separations were carried out in an Acquity UPLC column BEH C18 (50 mm × 2.1 mm, 1.7 µm), at 30 °C, eluted with a gradient of 0.1 % formic acid (A) and acetonitrile (B) in the following program: 0 min – 20 % B, 7 min – 80 % B, 8 min – 80 % B, 8.5 min – 20 % B, 10 min – 20 % B. Piceatannol and spilanthol were detected at 323 and 229 nm, respectively.

Quantification curves were constructed over base cream as a matrix. Several tubes comprising 50 mg of base cream and 1.0 ml of 50 % EtOH were mixed in falcon tubes with the aid of a vortex mixer. The suspensions were centrifuged at 3000 rpm for 5 minutes and the supernatants were dried in glass flasks with the aid of an N2 (g) flow. To the dried supernatants, solutions of standard piceatannol (> 98 % purity, ChemScene LLC, New Jersey, USA) and spilanthol (74 % purity, isolated from paracress aerial parts at CPQBA, Paulínia, Brazil) in 50% EtOH were mixed to provide curve points varying from 2 to 10 mg L^{-1} of piceatannol and from 6 to 30 mg L^{-1} of spilanthol. Each curve point was prepared in triplicate.

The chromatographic data were recorded and integrated by Empower 2 software (Waters, Milford, USA) and the curves linearity were certified in Action Stat 3.7 (EstatCamp, São Carlos, Brazil).

Results and Discussion

Concerning general sensorial aspects, B_{em} was a visually fluid, homogeneous and translucid white lotion. O_{em} showed a light-yellow color, and it also presented a homogeneous aspect, as fluid as B_{em}. On the other hand, I_{em} had a white suspension aspect at the eyesight: the inorganic filter particles could be seen homogeneously spread into a fluid translucid white matrix. The incorporation of P_{ext} to the emulsions gave them a yellow-to-orange aspect, while J_{ext} did not change the previously observed aspects of the plain emulsions. The features seen for the formulations comprising P_{ext} were also seen when P_{ext} and J_{ext} were simultaneously combined with the emulsions.

When P_{ext} was incorporated into I_{em}, either alone or together with J_{ext}, an instant change in the orange-yellow color to pink was observed, indicating a possible interaction of this extract with the inorganic filters used in this work. This interaction, however, was not noticed in the UV spectra of the formulations. As seen in Fig. 2, the presence of P_{ext}, J_{ext}, or both caused no major changes in the UV emulsions wavelength absorption profiles.

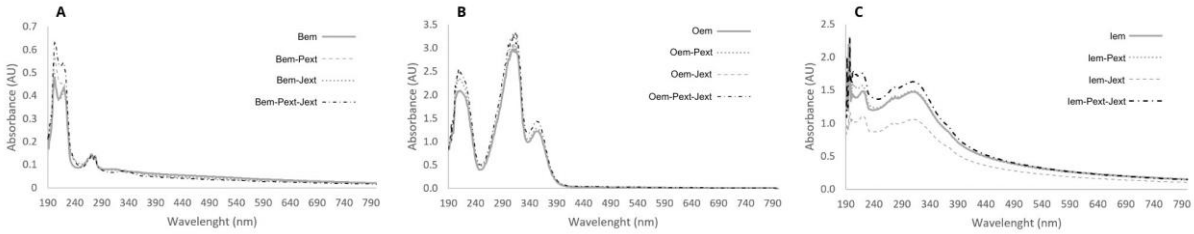

Figure 2: UV spectra of the 12 formulations. B_{em}: base emulsion. O_{em}: organic sunscreen emulsion. I_{em}: inorganic sunscreen emulsion. P_{ext}: piceatannol-rich passion fruit seed extract. J_{ext}: spilanthol-rich paracress (jambu) aerial parts extract.

The formulations' physical stability was evaluated by the analytical centrifugation assay, in a simulation of a 6-month shelf-life. Fig 3. shows the profiles of transmittance over time for B_{em}, O_{em}, and I_{em}, in which B_{em} and O_{em} profiles remained constant over time, and an increasing transmittance at the air-emulsion interface was observed in I_{em} profiles. Hence, while B_{em} and O_{em} remained stable under a simulated six-month simulated period, I_{em} presented phase segregation. By observing the cuvettes of I_{em} and its variants comprising the extracts, a small water layer could be seen at the interface with air, and the inorganic filters precipitated. The extracts

exhibited no ability to stabilize the I_{em} system (Fig 4), and they did not add instability to B_{em} and O_{em} (Supplementary Material, Figs. S1 and S2). I_{em}-P_{ext} and I_{em}-P_{ext}-J_{ext} formulations darkened to a brownish color during the assay.

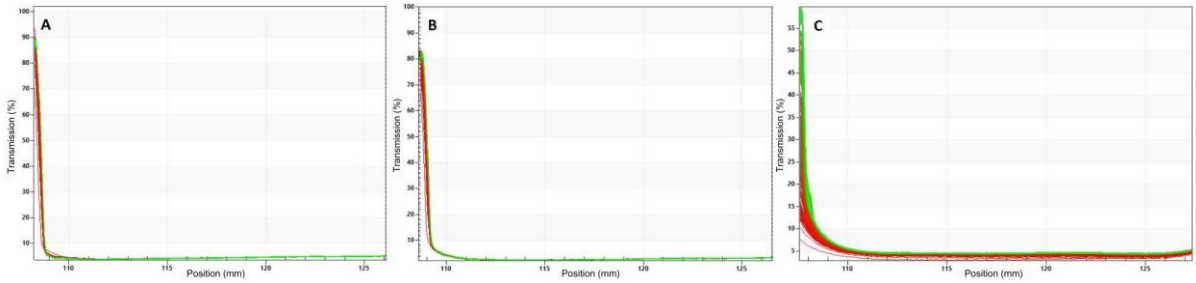

Figure 3: Analytical centrifugation profiles of the emulsions without the extracts (Lumisizer, LUM, GmbH, Berlin, Germany). A: base emulsions, B: organic filter emulsions, C: inorganic filter emulsions.

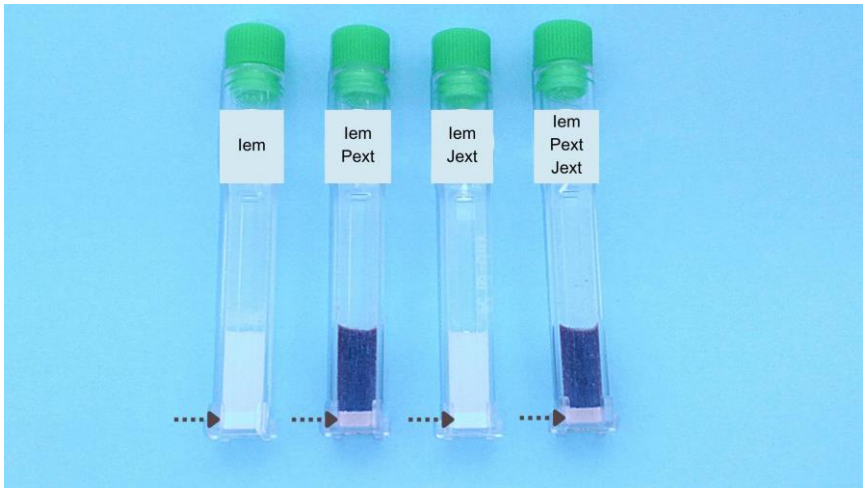

Figure 4: Lumisizer cuvettes (LUM, GmbH, Berlin, Germany) after the analytical centrifugation assay of the inorganic filter cream and its formulations with the extracts. The arrows highlight the inorganic filter precipitate.

Even though the extracts did not interfere at the physical stability of the emulsions, some influence of the extracts on the thermal stability of O_{em} was noticed. Fig 5. shows the TG curves for all the 12 formulations. Eighty to ninety percent of the total mass was lost at 25 to around 110-130°C. A second event accounting for 3-12 % of the overall mass occurred at 240-280 °C. Although the presence of the extracts

induced no major temperature to B_{em} (Fig. 5A), they lowered O_{em} thermal stability in about 10 °C at the first major mass loss (Fig. 5B). P_{ext}, J_{ext} and their mixture provided quite the same effect on it. The TG curves for I_{em} with or without the extracts were quite similar (Fig. 5C) with a slight shift observed for the second mass loss event when both P_{ext} and J_{ext} were present (Fig. 5C). As the incorporation of P_{ext} to I_{em} incurred in an immediate color change from orange-yellow to pink, the assumption that some chemical interactions between them occurred before the TG assay is feasible, hence, they were not recorded. This might explain why no major difference in the TG curves for the I_{em} series were seen.

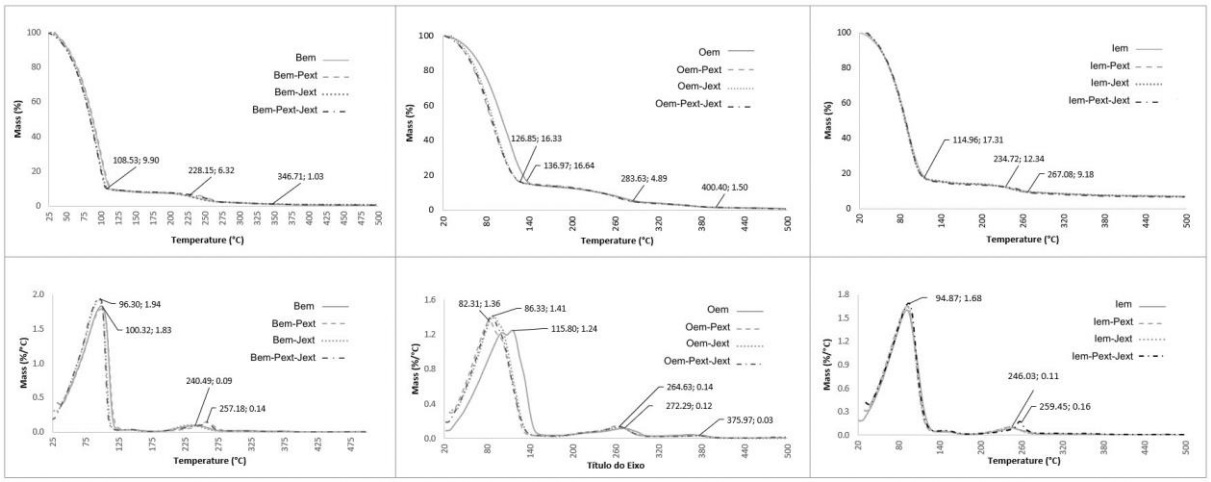

Figure 5: TG curves (upper) and second derivate TG curves (lower) of the formulations. Left: base emulsions, Middle: organic filter emulsions, Right: inorganic filter emulsions.

Complementing TG information, DSC curves showed two main endothermic events with peaks at about 60 and 100 °C, with a third exothermic event at around 260 °C (Table 2, Supplementary material Fig. S3). Combining this information with TG results, the first DSC peak can be attributed to the consumption of energy for the evaporation of water, volatiles, and eventual reactions among the ingredients in an oxygenated atmosphere, corresponding to the major mass loss observed at the TG curves. The second event in the DSC curves correspond to the fusion point of the formulations, as they mark an endothermic process with a peak in a constant mass temperature. Finally, the exothermic peak seen in the DSC curves is within the region of the second mass loss of TG, and it may be attributed to further oxidation or decomposition of compounds.

Table 2: T (°C) and ΔH of the events that occurred at the DSC analyses of the 12 formulations.

	Peak 1			Peak 2			Peak 3		
Sample	T_{onset} (°C)	T_{peak} (°C)	ΔH (J g^{-1})	T_{onset} (°C)	T_{peak} (°C)	ΔH (J g^{-1})	T_{onset} (°C)	T_{peak} (°C)	ΔH (J g^{-1})
B_{em}	**62.92**	**77.62**	**268.10**	**99.37**	**116.17**	**2013.00**	**246.88**	**251.75**	**-23.88**
B_{em}-P_{ext}	▼ 54.94	78.74	▲ 342.40	98.63	▲ 125.48	▼ 1807.00	▲ 254.45	▲ 260.61	▲ -56.39
B_{em}-J_{ext}	66.39	78.36	▼ 197.10	97.02	▲ 123.56	2086.00	244.62	249.91	-30.99
B_{em}-P_{ext}-J_{ext}	64.44	77.08	▼ 153.90	98.34	▲ 125.96	▼ 1910.00	▲ 258.07	▲ 264.69	▲ -44.93
O_{em}	**71.53**	**78.74**	**168.10**	**99.66**	**117.37**	**1694.00**	**238.94**	**247.74**	**-10.43**
O_{em}-P_{ext}	▼ 62.48	75.62	▲ 302.30	▲ 106.47	119.09	▼ 960.40	▲ 255.86	▲ 263.26	▼ -5.32
O_{em}-J_{ext}	▼ 49.98	▼ 68.74	▲ 210.70	97.77	119.72	1917.00	244.55	▲ 266.76	-17.66
O_{em}-P_{ext}-J_{ext}	▼ 54.41	74.19	▲ 313.90	▲ 104.53	118.46	1704.00	▲ 259.86	▲ 268.14	-15.92
I_{em}	**34.36**	**51.57**	**49.41**	*	**123.41**	**2073.00**	**248.89**	**265.43**	**-26.78**
I_{em}-P_{ext}	56.55	70.98	137.70	99.57	121.97	2134.00	258.08	261.63	-1.90
I_{em}-J_{ext}	64.47	76.45	171.90	*	118.86	2021.00	241.77	246.64	-34.27
I_{em}-P_{ext}-J_{ext}	ND	ND	ND	98.58	121.16	2395.00	254.85	262.95	-15.95

ND: not detected

* peak with defects

▲ Enhanced in relation to the corresponding plain emulsion.

▼ Diminished in relation to the corresponding plain emulsion.

From the table above, it became clear that the extracts exerted some influence on the chemical stability of B_{em}. The addition of P_{ext} to it lowered the beginning of the first endothermic event in about 10 °C, and a higher ΔH was also observed in this case. The presence of J_{ext} lowered the energy required for the first event to occur, even when P_{ext} was present. Both the extracts elevated the B_{em} fusion point at around 10 °C, and the ΔH for this transition was lowered when P_{ext} was present in the formulation either alone or combined with J_{ext}. The exothermic event also occurred at a higher temperature and with a higher ΔH when B_{em} was added with P_{ext} or P_{ext}-J_{ext}.

Both extracts caused a first DSC event T_{onset} lowering and ΔH increase for O_{em}, which is consistent with the TG observations. While J_{ext} showed the most pronounced effect over temperature, P_{ext} lowered the energy requirements for the fusion and the decomposition of O_{em}.

The results for the volatilization and decomposition of I_{em} are quite diverse, but the fusion point remained constant with the inclusion of the extracts. Such diversity

may, again, be attributed to events that occurred before the assay, with data not caught by the equipment, and it indicates the incompatibility of the extracts with the inorganic filters in this emulsion.

The chemical interferences of the extracts over the emulsions became more evident after 12 days of temperature cycling. An orange-yellow to a pinkish color change in O_{em} added with P_{ext} and P_{ext}-J_{ext} was seen, while the already pinkish I_{em} comprising P_{ext} or both the extracts turned dark brown at the end of the assay (Fig. 6). The pH values of at the end of the 12 days remained the same for B_{em} (pH 5) and O_{em} (pH 6) with or without the extracts, but I_{em} with either or both extracts had its pHs elevated from 7 to 8, and a rancid odor was noticed.

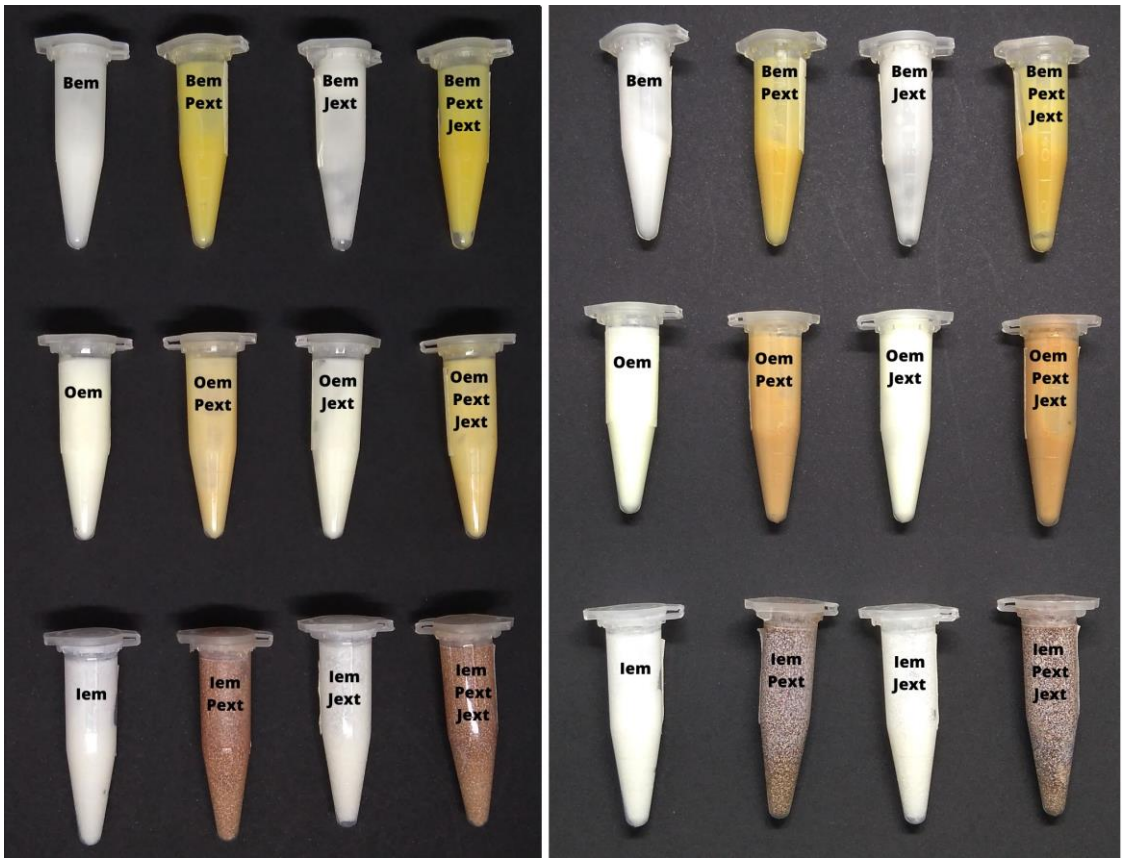

Figure 6: Visual aspect of the 12 formulations at T_0 and T_{12}.

Piceatannol and spilanthol were quantified in the formulations at T_0 and T_{12} (Fig. 7). The quantification curves and the ANOVA of the linear models are presented in the supplementary material (Figs. S4 and S5, respectively). Forty to fifty percent of

the initial piceatannol could be found in B_{em} series after 12 days of temperature cycling, while it was not detected in O_{em} and I_{em} formulations where P_{ext} was present. In I_{em} series, the results at T_0 indicate the instant incompatibility of P_{ext} with the inorganic sunscreens, as the triplicates showed more discrepant and lower mean starting values.

Spilanthol, however, was present in all formulations after 12 days of temperature cycling. There was practically no spilanthol loss in the B_{em} series. Water loss was observed in the O_{em} series at T_{12}, and spilanthol concentration ended up being higher than in T_0. Hence, it can be assumed that nearly no loss of spilanthol occurred in the O_{em} formulations as well. And, as piceatannol, spilanthol content in the I_{em} series at T_0 were lower and more discrepant than in the other emulsions. I_{em}-J_{ext} began the assay with nearly half of the intended spilanthol concentration, probably due to its instantaneous incompatibility with the inorganic sunscreens. After 12 days of temperature cycling, spilanthol concentration fell to 34 % of the initial value.

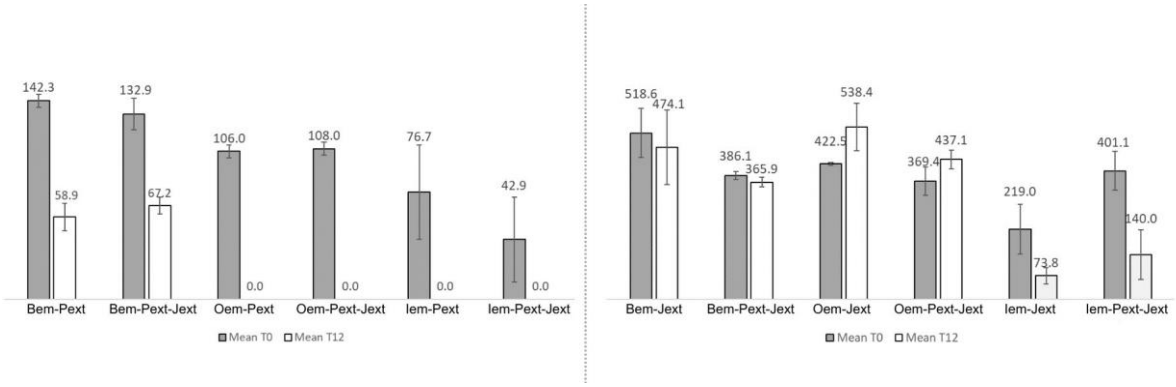

Figure 7: Piceatannol (left) and spilanthol (right) content, in mg per g of cream, of the 12 formulations at T_0 and T_{12}.

It is known that UV light induces stilbenes isomerization. Trans-piceatannol is very sensitive to light and it isomerizes to its cis-form when exposed to light at 366 nm. The cis-form becomes a phenantrenoid ring afterwards by losing two H atoms. Temperatures above 25 °C and pH are also factors that influence piceatannol stability. A recent study on the phenolic compounds of grape pedicel extracts showed that trans-piceatannol was mostly degraded after 2 weeks when the extracts were stored at 40 °C. Resveratrol, a piceatannol analogue, degrade in days in such temperature, while storage at near-zero or negative temperatures preserve it for months in neutral pH. A

pH 6.8 or higher reduces resveratrol half-life dramatically. Since the emulsions were exposed to 5 and 40 °C in alternate days, the observed piceatannol degradation is consistent to what is stated in the literature on it. And since B_{em} presented the lowest pH value among the emulsions, it was reasonable to find piceatannol in it after 12 days of temperature cycling [21–23].

Spilanthol is also a photosensitive molecule, and its stability after UV-B exposure is solvent-dependent, being higher in alcohols and lower in saline solution and water. The molecules 6,9-dihydroxy-deca-2,7-dienoic acid isobutyl-amide and 8,9-dihydroxy-deca-2,6-dienoic acid isobutyl-amide are reported as spilanthol degradation products. Oxidized species appear when a spilanthol solution in dichloromethane or $CDCl_3$ is in contact with air, especially when photosensitizing agents such as chlorophyll is present. Considering that the organic sunscreens absorb UV light, some spilanthol loss would be expected in O_{em} comprising J_{ext} or P_{ext}-J_{ext} mixture. However, the loss was only clearly observed in the I_{em} series [24, 25].

Indeed, I_{em} formulations were challenging in all aspects. The physical stability of the inorganic filters suspension was not achieved, and the extracts made no improvements to the formulations in this sense. The use of thickening agents, for example, could correct this problem. Also, the inorganic filters were more reactive to the extracts than the organic ones. A hypothesis for this effect is that the filters may have catalyzed the extracts oxidation in the presence of light. In environmental sciences, the use of TiO_2 and ZnO as photocatalysts for the degradation of organic and aliphatic contaminants in water has been reported. When irradiated with UV light, these compounds can generate reactive oxygen species from water, and these species start a chain reaction with the compounds present in their surroundings. Since water is the major component of the emulsions, the environmental light may have triggered the extracts oxidation in I_{em}, causing the observed instantaneous color change in formulations where P_{ext} was incorporated. The oxidation could also be attested by the dark color and the rancid odor at the end of the twelve-days temperature cycling, indicating that the formulation lipids were degraded as well [26, 27].

Even though J_{ext} decreased to around 35 % of its initial content after the temperature cycling assay, I_{em} comprising both extracts presented a higher initial spilanthol content than I_{em} containing J_{ext} alone. This is an indication that P_{ext} may have

protected J_{ext} from instant oxidation. Therefore, again, as the formulations are supposed to be used in contact with the skin, air, and light, the compatibilization of the extracts to inorganic filters in formulations containing water must involve their protection to some extent to obtain a safe and effective product.

One feasible alternative to overcome such inconveniences would be micro or nano-encapsulating the extracts to protect them against the surrounding vehicle. The inclusion into systems like cyclodextrins, micro or nano gels or emulsions, liposomes, micro, and nanoparticles, are some of the reported encapsulation strategies [28–31]. Another means of contouring the extracts instability issues would be their evaluation in other compositions to find a more suitable environment. In this sense, the inclusion of the extracts into non-aqueous vehicles, or formulations comprising less water than the one used in the present evaluation might be a possibility to protect them from degradation.

Conclusion

Passion fruit piceatannol-rich seed extract was more stable in the base emulsion than in the presence of organic or inorganic UV filters added to the same system. On the other hand, spilanthol-rich extract from paracress (jambu) was more stable in the proposed emulsions, showing signs of instability only in the presence of the inorganic UV filters. None of the extracts interfered positively or negatively with the physical stability of the formulations, but chemical interactions with their components were observed, mainly in the presence of TiO_2 and ZnO. Therefore, for future application of these extracts or molecules in topical emulsions, their micro, nanoencapsulation, or their inclusion into a non-water or more lipophilic vehicle could be required to provide a safe and effective product.

Acknowledgments

This work was financially supported by the National Institutes of Science and Technology (INCTs) [grant numbers: FAPESP/INCT 2014/50867, CNPq

465389/2014-7]. C. B. G. Bottoli acknowledges CNPq for a research fellowship [CNPq 309363/2018-7].

The authors acknowledge Fundação de Amparo à Pesquisa do Estado de São Paulo (FAPESP) and the Institute of Chemistry from the University of Campinas (IQ - Unicamp) for financing the LUMisizer multiuser equipment with the project 2016/13926-7.

The authors also acknowledge Paulo Ricardo Garcia and Manuela Sabino for the Lumisizer training and support, Lucilia V. Melo for the stability test support, LabFarQui – Unicamp for the UPLC-DAD assays, Fabiana Amorim for DSC and TG assays, and Escola Vinia for the internship and aid in the emulsions design.

Declaration of interest

The authors have no relevant affiliations or financial involvement with any organization or entity with a financial interest in or financial conflict with the subject matter or materials discussed in the manuscript. This includes employment, consultancies, honoraria, stock ownership or options, expert testimony, grants or patents received or pending, or royalties.

References

1. Guan LL, Lim HW, and Mohammad TF. Sunscreens and Photoaging: A Review of Current Literature. Am J Clin Dermatol. 2021;22(6):819.

2. Piotrowska H, Kucinska M, and Murias M. Biological activity of piceatannol: Leaving the shadow of resveratrol. Mutation Research/Reviews in Mutation Research. 2012;750(1):60–82.

3. Arakaki DG, Samúdio dos Santos V, Melo EP de, Pereira H, Silva Figueiredo P, Rodrigues Cortês M, Alexandre Carollo C, Oliveira LCS de, Tschinkel P, Reis F, et al. Canjiqueira Fruit: Are We Losing the Best of It? Foods. 2020;9(4):521.

4. Krambeck K, Santos D, Sousa Lobo JM, and Amaral MH. Benefits of skin application of piceatannol—A minireview. Australasian Journal of Dermatology. 2022.doi:10.1111/AJD.13937

5. Kawakami S, Morinaga M, Tsukamoto-Sen S, Mori S, Matsui Y, and Kawama T. Constituent Characteristics and Functional Properties of Passion Fruit Seed Extract. Life. 2022;12(1).

6. Maruki-Uchida H, Morita M, Yonei Y, and Sai M. Effect of Passion Fruit Seed Extract Rich in Piceatannol on the Skin of Women: A Randomized, Placebo-Controlled, Double-Blind Trial. Vol 64 2018.

7. Setoguchi Y, Oritani Y, Ito R, Inagaki H, Maruki-Uchida H, Ichiyanagi T, and Ito T. Absorption and metabolism of piceatannol in rats. J Agric Food Chem. 2014;62(12):2541–8.

8. Jarosova V, Vesely O, Marsik P, Jaimes JD, Smejkal K, Kloucek P, and Havlik J. Metabolism of stilbenoids by human faecal microbiota. Molecules. 2019;24(6).

9. Dai Y, Lim JX, Yeo SCM, Xiang X, Tan KS, Fu JH, Huang L, and Lin HS. Biotransformation of Piceatannol, a Dietary Resveratrol Derivative: Promises to Human Health. Mol Nutr Food Res. 2020;64(2).

10. Hung C-F, Lin Y-K, Huang Z-R, and Fang J-Y. Delivery of Resveratrol, a Red Wine Polyphenol, from Solutions and Hydrogels in the Skin. Biol Pharm Bull. 2008;31(5):955–62.

11. Eskandari M, Rembiesa J, Startaitė L, Holefors A, Valančiūtė A, Faridbod F, Ganjali MR, Engblom J, and Ruzgas T. Polyphenol-hydrogen peroxide reactions in skin: *In vitro* model relevant to study ROS reactions at inflammation. Anal Chim Acta. 2019;1075:91–7.

12. Barbosa AF, de Carvalho MG, Smith RE, and Sabaa-Srur AUO. Spilanthol: Occurrence, extraction, chemistry and biological activities. Brazilian Journal of Pharmacognosy. 2016;26(1):128–33.

13. Paulraj J, Govindarajan R, and Palpu P. The Genus Spilanthes Ethnopharmacology, Phytochemistry, and Pharmacological Properties: A Review. Adv Pharmacol Sci. 2013;2013:22.

14. Silveira N, Sandjo LP, and Biavatti MW. Spilanthol-containing products: A patent review (1996–2016). Trends Food Sci Technol. 2018;74:107–11.

15. de Spiegeleer B, Boonen J, Malysheva S v., Mavungu JD di, de Saeger S, Roche N, Blondeel P, Taevernier L, and Veryser L. Skin penetration enhancing properties of the plant N-alkylamide spilanthol. J Ethnopharmacol. 2013;148(1):117–25.

16. Silva GC, Rodrigues RAF, and Bottoli CBG. Passion fruit seed extract enriched in piceatannol obtained by microwave-assisted extraction. Sustain Chem Pharm. 2021;22:100472.

17. Sunscreen Simulator. Available at https://sunscreensimulator.basf.com/Sunscreen_Simulator/login.

18. Silva CEP, Tam KC, Bernardes JS, and Loh W. Double stabilization mechanism of O/W Pickering emulsions using cationic nanofibrillated cellulose. J Colloid Interface Sci. 2020;574:207–16.

19. Cefali LC, Ataide JA, Fernandes AR, Sousa IM de O, Gonçalves FC da S, Eberlin S, Dávila JL, Jozala AF, Chaud MV, Sanchez-lopez E, et al. Flavonoid-Enriched Plant-Extract-Loaded Emulsion: A Novel Phytocosmetic Sunscreen Formulation with Antioxidant Properties. Antioxidants. 2019;8(10):443.

20. BRASIL AN de VS (ANVISA). Guia de estabilidade de produtos cosméticos. Available at http://portal.anvisa.gov.br/documents/106351/107910/Guia+de+Estabilidade+de+Produtos+Cosm%C3%A9ticos/49cdf34c-b697-4af3-8647-dcb600f753e2.

21. Latva-Mäenpää H, Wufu R, Mulat D, Sarjala T, Saranpää P, Wähälä K, Donato P di, and Silvestri B. Stability and Photoisomerization of Stilbenes Isolated from the Bark of Norway Spruce Roots. 2021.doi:10.3390/molecules26041036

22. Navarro-Orcajada S, Conesa I, Vidal-Sánchez FJ, Matencio A, Albaladejo-Maricó L, García-Carmona F, and López-Nicolás JM. Stilbenes: Characterization, bioactivity, encapsulation and structural modifications. A review of their current limitations and promising approaches. Crit Rev Food Sci Nutr. 2022.doi:10.1080/10408398.2022.2045558

23. Ferreyra S, Bottini R, and Fontana A. Temperature and light conditions affect stability of phenolic compounds of stored grape cane extracts. Food Chem. 2023;405:134718.

24. Savic S, Petrovic S, Savic S, and Cekic N. Identification and photostability of N-alkylamides from Acmella oleracea extract. J Pharm Biomed Anal. 2021;195:113819.

25. Grymel M, Mazurkiewicz R, Bajkacz S, Bilik J, and Kowalczyk S. Extraction, Purification, Quantification, and Stability of Bioactive Spilanthol from Acmella oleracea. Planta Med. 2023;89(5).

26. Guo Q, Zhou C, Ma Z, Yang X, Guo Q, Zhou C, Ma Z, and Yang X. Fundamentals of TiO 2 Photocatalysis: Concepts, Mechanisms, and Challenges. 2019.doi:10.1002/adma.201901997

27. Sabouni R and Gomaa H. Photocatalytic degradation of pharmaceutical micro-pollutants using ZnO.doi:10.1007/s11356-018-4051-2

28. Rezaei A, Fathi M, and Jafari SM. Nanoencapsulation of hydrophobic and low-soluble food bioactive compounds within different nanocarriers. Food Hydrocoll. 2019;88:146–62.

29. Shishir MRI, Xie L, Sun C, Zheng X, and Chen W. Advances in micro and nano-encapsulation of bioactive compounds using biopolymer and lipid-based transporters. Trends Food Sci Technol. 2018;78:34–60.

30. Sharkawy A, Casimiro FM, Barreiro MF, and Rodrigues AE. Enhancing trans-resveratrol topical delivery and photostability through entrapment in chitosan/gum Arabic Pickering emulsions. Int J Biol Macromol. 2020;147:150–9.

31. Kim MH, Jeon YE, Kang S, Lee JY, Lee KW, Kim KT, and Kim DD. Lipid Nanoparticles for Enhancing the Physicochemical Stability and Topical Skin Delivery of Orobol. Pharmaceutics. 2020;12(9):1–16.

Gisláine C. Silva[1], Rodney A. F. Rodrigues[2], Carla B. G. Bottoli[1]

SUPPLEMENTARY MATERIAL

S1. Analytical centrifugation profiles of the 12 formulations (LUMisizer, LUM, GmbH, Berlin, Germany). For conditions, see the topic “Analytical centrifugation” in Materials and Methods. Bem: base emulsion, Oem: organic filter emulsion, Iem: inorganic filter emulsion, Pext: Piceatannol-rich extract from passion fruit, Jext: Spilanthol-rich extract from paracress (jambu).

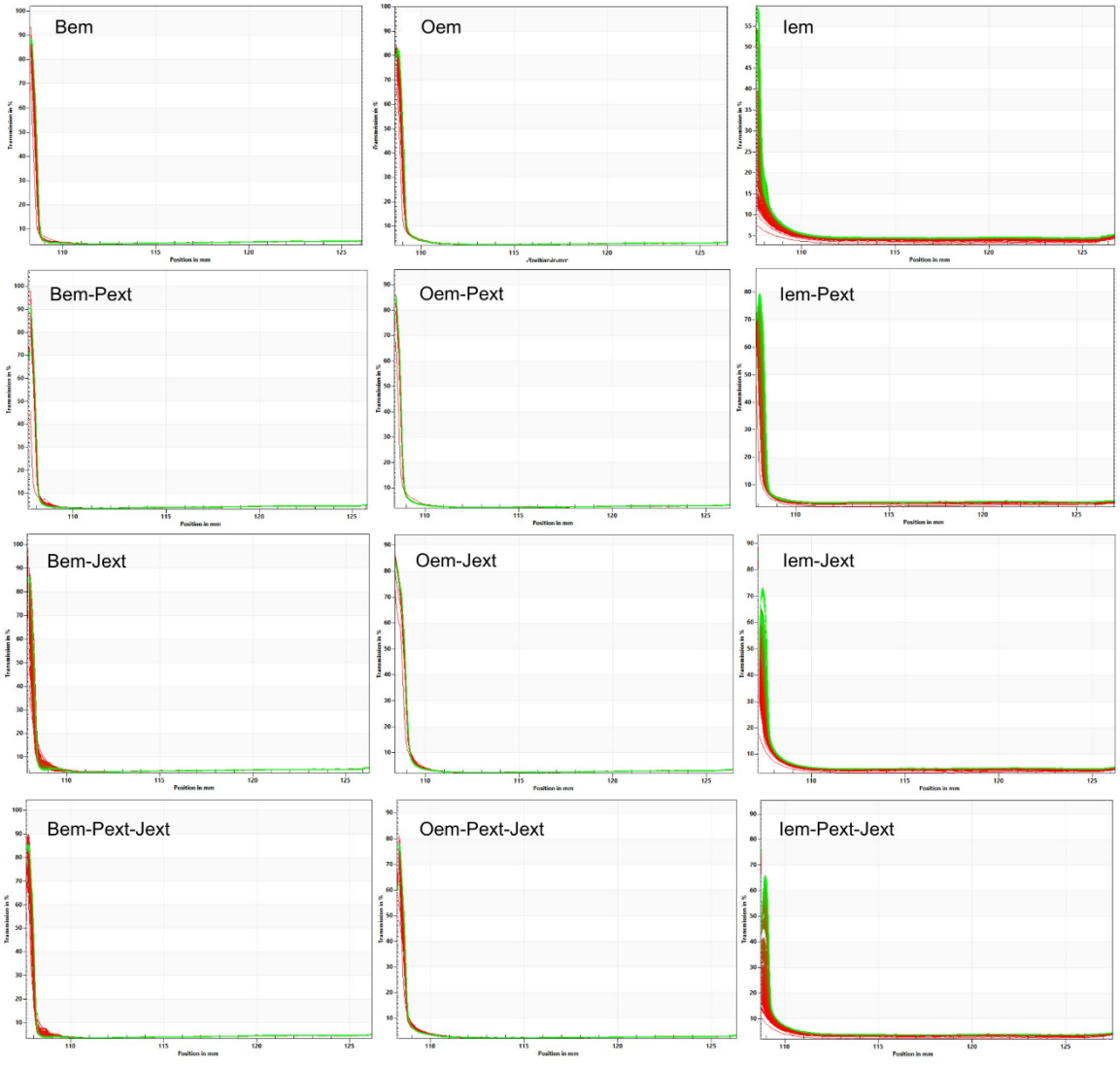

S2. Lumisizer cuvettes (LUM, GmbH, Berlin, Germany) after the analytical centrifugation assay. For conditions, see “Analytical centrifugation” in Materials and Methods Bem: base emulsion, Oem: organic filter emulsion, Pext: Piceatannol-rich extract from passion fruit, Jext: Spilanthol-rich extract from paracress (jambu).

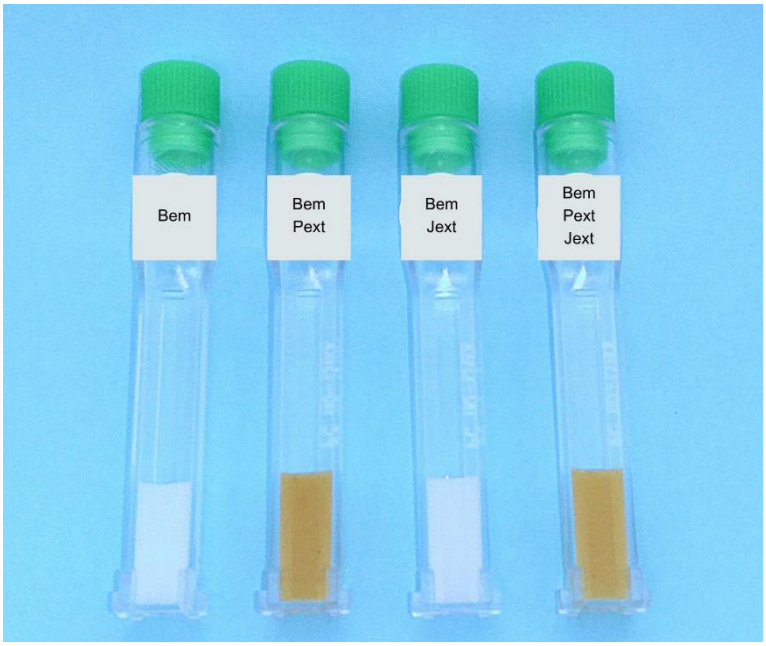

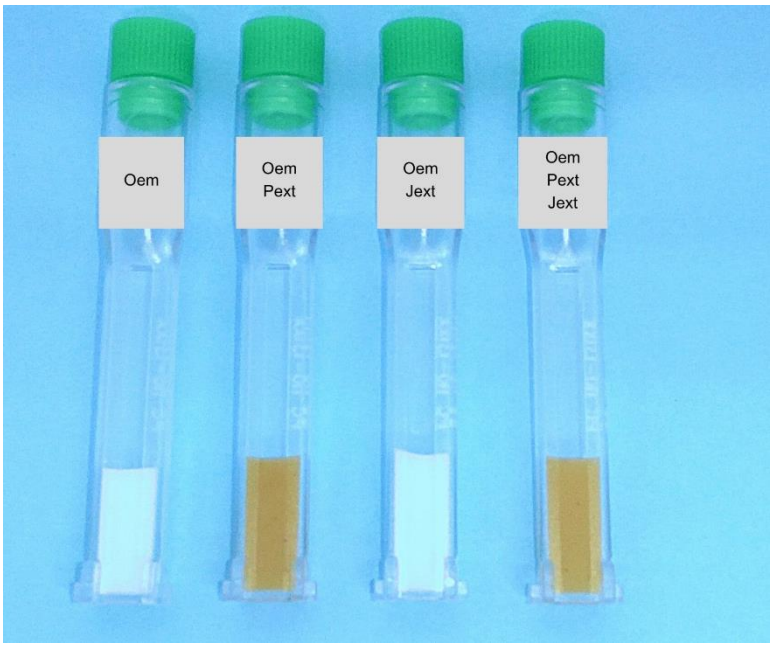

S3. DSC (up) and TG (down) curves of the 12 formulations. For conditions see “Thermal Analyses” in Materials and Methods. Bem: base emulsion, Oem: organic filter emulsion, Iem: inorganic filter emulsion, Pext: Piceatannol-rich extract from passion fruit, Jext: Spilanthol-rich extract from paracress (jambu).

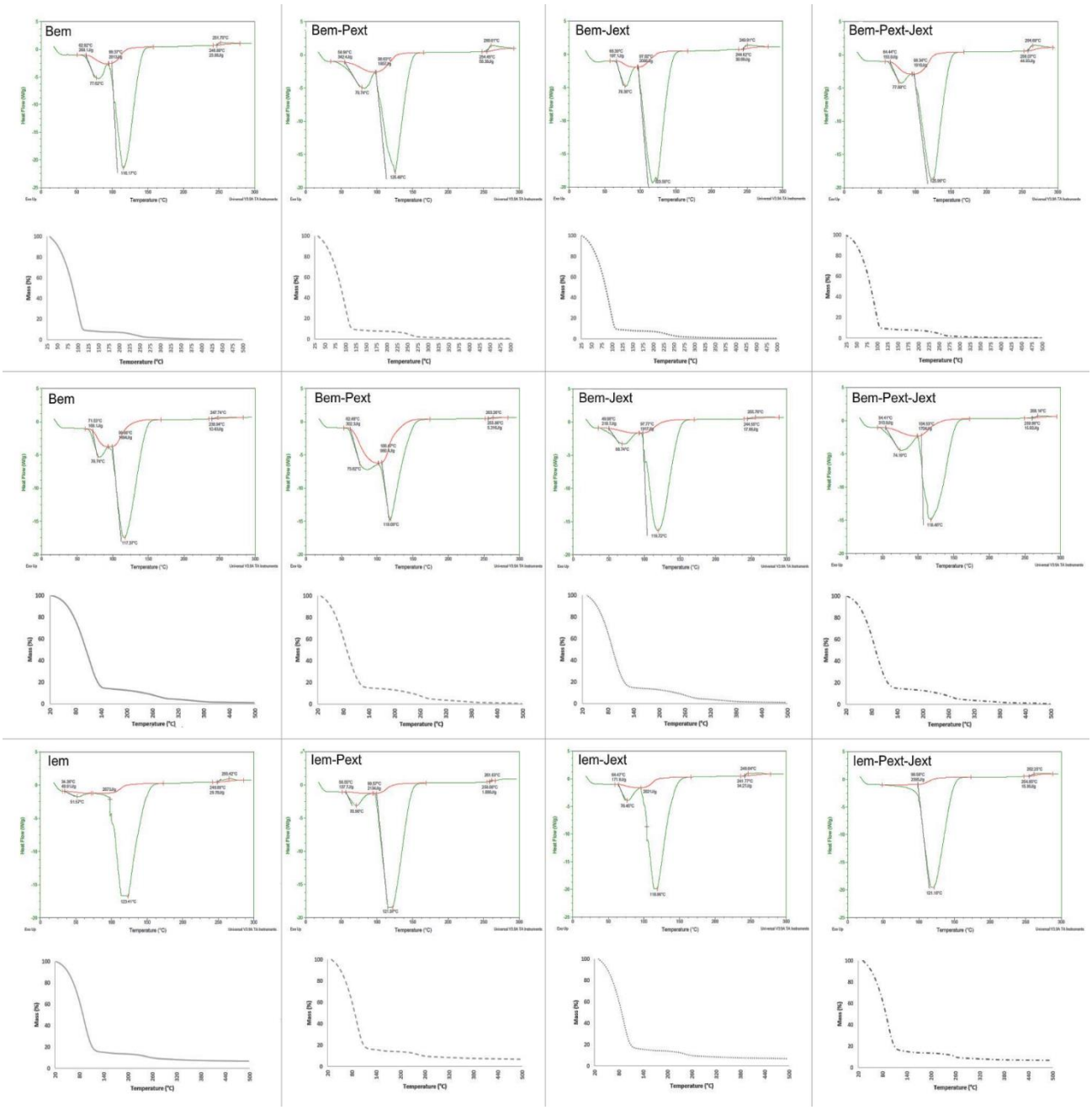

S4. Quantification curves for piceatannol (left) and spilanthol (right) developed in the Waters Acquity UPLC system. Each point is represented by its mean (triplicate) plus the error bar. For conditions, see the topic “Piceatannol and spilanthol quantification” in Materials and Methods.

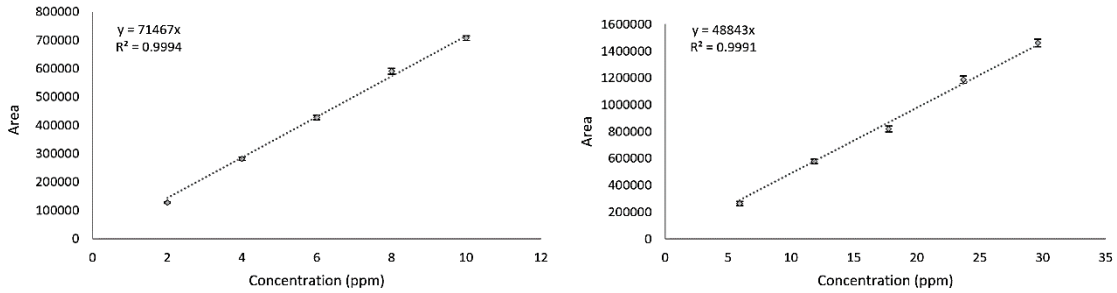

S5. ANOVA analysis for piceatannol (up) and spilanthol (down) curves.

Source of variation	*DF*	*SS*	*MS*	*Fcalc*	*P-value*
Piceatannol Model	1	6.47881E+11	6.47881E+11	12753.4022	7.26792E-17
Residues	13	2022298668	155561436		
Lack of Fit	3	1514291957	504763985.6	9.936167673	0.002407155
Pure Error	10	508006710.7	50800671.07		

Source of variation	*DF*	*SS*	*MS*	*Fcalc*	*P-value*
Spilanthol Model	1	2.70239E+12	2.70239E+12	5428.220626	5.17785E-15
Residues	13	13121289419	1009329955		
Lack of Fit	3	8142886893	2714295631	5.452141761	0.017587877
Pure Error	10	4978402525	497840252.5		

CAPÍTULO 4

The influence of a spilanthol-rich extract and organic sunscreens on the piceatannol delivery across Strat-M™ membranes

THE INFLUENCE OF A SPILANTHOL-RICH EXTRACT AND ORGANIC SUNSCREENS ON THE PICEATANNOL DELIVERY ACROSS STRAT-M™ MEMBRANES

Gisláine C. Silva[1], Rodney A. F. Rodrigues[2], Carla B. G. Bottoli[1*]

[1]Institute of Chemistry, University of Campinas (Unicamp), POB 6154, 13084-971, Campinas, SP, Brazil.

[2]Chemical, Biological and Agricultural Pluridisciplinary Research Center (CPQBA), University of Campinas (Unicamp), 13148-218, Paulínia, SP, Brazil.

*Corresponding author: carlab@unicamp.br

Abstract

Piceatannol is a stilbene compound found in many fruits and plants, and it provides protection against free radicals' damages and stimulates skin repairment mechanisms. Data on the oral and intravenous intake of piceatannol show that it is extensively metabolized and eliminated from the body, and there was a lack of information on the feasibility of its topical application. In this work, a piceatannol-rich passion fruit extract (P_{ext}) was incorporated into an emulsion based on a non-ionic surfactant and thickened by an acrylate-based polymer and lecithin gelling agent. The *in vitro* piceatannol diffusion through a Strat-M™ membrane was evaluated during 3 h in its sole form into the emulsion or in combination with a spilanthol-rich paracrass (jambu) extract (J_{ext}) and a mixture of Parsol MCX™, Uvinul A plus™ and Uvinul T150™ organic sunscreens actives (O_{em}). The piceatannol depth within the membranes was accessed by Confocal Raman Microscopy (CRM). Both P_{ext} and J_{ext} exhibited degradation during the assay, but it was possible to observe that both extracts enhanced the undesired Parsol MCX™ permeation through the membrane, and that piceatannol could penetrate it even though part of it remained at the surface. CRM analyses revealed that J_{ext} and O_{em} promoted piceatannol deposition in a deeper layer of the *stratum corneum*, and they enhanced its permeation depth into the membrane.

Keywords: skin diffusion, passion fruit, paracress, Parsol MCX™, Uvinul A plus™, Uvinul T150™

Abbreviations

B_{em}: Base emulsion

O_{em}: Organic sunscreen emulsion

I_{em}: Inorganic sunscreen emulsion

P_{ext}: Piceatannol-rich passion fruit seed extract

J_{ext}: Spilanthol-rich paracress (jambu) aerial parts extract

Introduction

Piceatannol (trans-3,3,4,5-tetrahydroxystilbene) is a resveratrol-like stilbenoid which has a high peroxide radical-scavenging activity. In *in vitro* assays, this compound was able to protect cells against radical oxygen species (ROS)-induced apoptosis, to inhibit melanogenesis in human melanoma cells, to promote collagen synthesis in cultured fibroblasts, to suppress the formation of UVB-induced ROS, and to reduce the action of the MMP-1 enzyme, which is responsible for collagen degradation (1–3).

This compound can be found in several fruits and plants, such as grapes, white tea, rhubarb, and passion fruit. Brazil is the main passion fruit producer in the world, with an around 600.000-ton production per year. Part of this production is directed to the food and beverage industry, which benefits from the fruit pulp, and passion fruit seeds, a rich source of piceatannol, are, nowadays, an underrated by-product of this industry. The exploitation of this by-product towards the conception of a pharmaceutical or dermocosmetic ingredient for skin care is a great opportunity to enhance the valorization of the passion fruit agro-industrial chain (4,5).

Although piceatannol has whitening, anti-ageing, photoprotective and repair properties, skin hydration improvement was the only result reported in a double-blind study with 32 women between 35 and 54 years old who ingested a 5 mg piceatannol standardized extract for 8 weeks. In experiments on rats, the oral absorption of piceatannol was shown to be lower than resveratrol and an *in vitro* fermentation of piceatannol in fresh feces showed it is intensely biotransformed by the present microbiota. In mice and human liver cell cultures, the compound was rapidly converted into its isomers rapontigin and isorapontigin and, when administered intravenously to mice, a rapid metabolism and clearance of piceatannol was observed (6–9).

Hence, given these reported results, topical application of piceatannol seems to a promising rout in order to achieve its *in vitro* observed properties into the skin. The available information on piceatannol diffusion through the skin up to now are scarce and inconclusive. While the cutaneous permeation of piceatannol was about 11 times lower resveratrol's in different pH aqueous buffers, soybean oil and in hydrogel

system, predictive and *in vitro* models for the prospection of antioxidants for the skin attribute piceatannol a capacity to permeate the skin barrier (10–14).

In cases where the skin diffusion of a compound is not favored, permeation promoters can be used in topical products to promote temporary skin disturbances. Among the promoters, spilanthol ((2E,6Z,8E)-N-(2-Methylpropyl)deca-2,6,8-trienamide), exhibit an excellent migration capacity through the skin layers. This molecule can be extracted from the aerial parts of paracress (*Spilanthes acmella* or *Acmella oleracea*), popularly known as jambu in Brazil, and it is already applied in cosmetics for its anti-wrinkle and anti-aging activities. Aside from it, spilanthol also present antioxidant and anti-inflammatory activities, which might also contribute to the modulation of the skin response against the environmental harmful effects (14–16).

In addition, direct photoprotection can be achieved by blocking sun rays from penetrating deeper layers of the skin, preventing them from triggering radical-based and inflammatory reactions. This is done by sunscreens actives, which are molecules that either scatter the sunlight (inorganic filters) or absorb UV light (organic filters) Hence, combining sunscreens and piceatannol properties in one single formulation could be a good strategy for maintaining the skin's health and youth. (17)

Therefore, this work aimed at evaluating the skin diffusion behavior of a piceatannol-rich passion fruit seed extract in a topical emulsion, alone or in the presence of a spilanthol-rich paracress extract and organic sunscreens, to evaluate the feasibility of the topical application of this compound as an alternative for its oral intake. To that, an emulsion based in a non-ionic surfactant thickened with an acrylate-based polymer and lecithin gelling agent, was developed for the incorporation of the active compounds, and the diffusion profiles of the formulations were evaluated onto Strat-M^{TM} skin model in Franz cells.

Materials and Methods

Piceatannol-rich extract from passion fruit seed material (P_{ext})

The extract was prepared according to Silva, Rodrigues, and Bottoli (18). Briefly, Passion fruit (*Passiflora edulis* Sims.) residual seed cake resulting from cold press oil extraction (Extrair Óleos Naturais, Rio de Janeiro, Brazil) was defatted with

analytical grade n-hexane (UNICAMP, Campinas, SP, Brazil) at a 1:10 w/v ratio by magnetic stirring for 1 h at room temperature (around 25 °C). The defatted cake was extracted with 70 % EtOH in a Start E bench-scale microwave extractor (Milestone, Bergamo, Italy), in a two-cycle process of 30 min each, at 87°C. The extracts from both cycles were collected by vacuum filtration in filter paper, and the solvent was removed under an $N_{2(g)}$ flow.

Spilanthol-rich extract from paracress (Jambu- J_{ext})

Fifty mililiters of 95 % EtOH paracress aerial parts extract (CPQBA, Paulínia, SP, Brazil) were extracted with 300 mL of analytical grade n-hexane (UNICAMP, Campinas, SP, Brazil) in a separatory funnel. The supernatant fraction was collected, the solvent was evaporated under an $N_{2(g)}$ flow, and the resulting oil was vacuum filtered over silica in a sintered plate funnel. A translucent olive-green liquid extract was obtained.

Topical emulsions

Two oil-in-water (O/W) emulsions were prepared according to the compositions described in Table 1. The base emulsion (B_{em}) was formed by a non-ionic surfactant, and it was thickened with an acrylate copolymer and lecithin gelling agent. The organic sunscreen emulsion (O_{em}) was derived from B by adding to it 3 organic ultraviolet (UV) filters, defined with the aid of Basf Sunscreen Simulator™ (19) to provide a simulated Sun Protection Factor (SPF) 10 sunscreen formulation.

Table 1: Compositions of the oil-in-water (O/W) emulsions.

			Ingredient (%)	
Ingredient	**INCI name**	**Description**	**Base (B_{em})**	**Organic (O_{em})**
Water	Aqua	Vehicle	85.85	79.85
EDTA	EDTA	Chelating agente	0.1	0.1
Glycerin	Glycerin	Humectant	1.0	1.0
Uvinul A plus[1]	Diethylamino Hydroxybenzoyl Hexyl Benzoate	Organic UV filter	-	2.0
Parsol MCX[2]	Ethylhexyl Methoxycinnamate	Organic UV filter	-	2.0

Uvinul T 150[1]	Ethylhexyl Triazone	Organic UV filter	-	2.0
Zano 10 plus[3]	Zinc Oxide (and) Triethoxycaprylylsilane	Inorganic UV filter	-	-
T-Lite SF[1]	Titanium Dioxide (and) Hydrated Silica (and) Aluminum Hydroxide (and) Hydrogen Dimethicone	Inorganic UV filter	-	-
BHT	BHT	Antioxidant	0.1	0.1
Emulium 22[4]	Tribehenin PEG-20 Esters	Non-ionic emulsifier	2.0	2.0
TGACC	Caprylic/Capric Triglyceride	Emollient	4.0	4.0
Lecigel[5]	Sodium Acrylates Copolymer (and) Lecithin	Gelling agente	1.0	1.0
Phenoxyetanol	Phenoxyetanol	Preservative	1.0	1.0
DC245[6]	Cyclopentasiloxane	Sensory modifier	5.0	5.0

[1] Basf, Germany, [2] DSM, Holland, [3] EverCare, USA, [4] Gattefossé, France, [5] Lucas Meyer Cosmetics, Canada, [6] Dow Corning, USA

P_{ext} and J_{ext} were incorporated into the emulsions at 2 and 1 mg g^{-1}, respectively. The extracts were dispersed in propylene glycol (10 mg g^{-1}) and mixed to the emulsions with a spatula. From B_{em} and O_{em}, a panel of 6 formulations comprising P_{ext}, J_{ext} or both extracts was constructed as schematized in Fig 1.

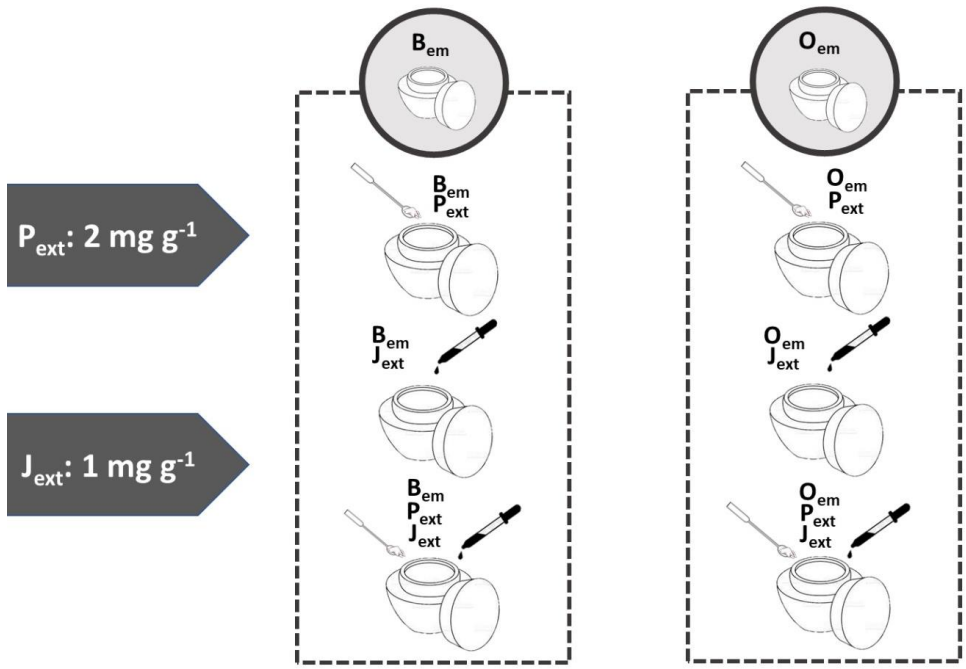

Figure 1: Schematic representation of the formulation pannel. P_{ext}: passion fruit seed extract. J_{ext}: Paracrass extract. B_{em}: base cream. O_{em}: base cream added with the organic filters Parsol MCX™, Uvinul A Plus™ and Uvinul T150™.

Piceatannol and spilanthol quantification

Piceatannol and spilanthol were quantified in the emulsions with a Waters Acquity UPLC system with a photodiode array detector (PAD) (Waters, Milford, Massachusetts, USA). Quantification curves were constructed over B_{em} as a matrix. 50.0 mg of B and 1.0 ml of 50 % EtOH were vortex mixed in falcon tubes. The suspensions were centrifuged at 3000 rpm for 5 minutes and the supernatants were dried in glass flasks with the aid of an $N_{2(g)}$ flow. To the dried supernatants, 50% EtOH solutions of standard piceatannol (> 98 % purity, ChemScene LLC, New Jersey, USA) and spilanthol (74 % purity, isolated from paracrass aerial parts at CPQBA, Paulínia, Brazil) were added to provide curve points varying from 2 to 10 mg L^{-1} of piceatannol and from 6 to 30 mg L^{-1} of spilanthol. Each curve point was prepared in triplicate. Samples were filtered through 0.22 um regenerated cellulose membranes (GVS, Bologna, Italy) prior to the injection.

For the analyses, 50.0 mg of each formulation and 1.0 ml of 50% EtOH were vortex mixed in falcon tubes, and the centrifugation and filtration protocols proceeded as described.

The separations were carried out in an Acquity UPLC column BEH C18 (50 mm × 2.1 mm, 1.7 µm), at 30 °C, eluted with a gradient of formic acid 0.1 % (A) and acetonitrile (B) in the following program: 0 min – 20 % B, 7 min – 80 % B, 8 min – 80 % B, 8.5 min – 20 % B, 10 min – 20 % B. Piceatannol and spilanthol were detected at 323 and 229 nm, respectively. The samples were kept at 20 °C at the autosampler and 5 µl of each sample was injected per run. Chromatographic data were collected by the Empower 2 software (Waters, Milford, USA) and the linearity of the curves was certified with the aid of Action Stat 3.7 (EstatCamp, São Carlos, Brazil).

Receptor fluid selection for Franz cell permeation assays

The stability of P_{ext} and J_{ext} in a hydroalcoholic solution was evaluated. Two milligrams of P_{ext} and J_{ext} were solubilized in 5 ml of methanol and diluted in 95 ml of a 30% or a 50% EtOH hydroalcoholic solution. The solutions were partitioned into 5 ml aliquots in screw-cap glass vials with a magnetic stirrer. The flasks were immersed in a 36 ± 2 ºC water bath with a magnetic stirring mechanism. Four flasks of each solution type were removed from the bath at 0, 1, 2 and 3 h and a 1 ml sample of each flask

was dried under $N_{2(g)}$. Each dry material was resuspended in 300 µL of MeOH:0.1 % formic acid 90:10 for HPLC-MS/MS analyses (Waters, Milford, Massachusetts, USA). Five microliters of each sample were injected into a Waters NovaPak C18 column (150 mm x 3.9 mm, 4 µm) eluted with 0.1% formic acid (A) and ACN (B), at a flow rate of 0.3 mL min^{-1}. with the following gradient: 40% B (0-4 min), 40-100% B (4-7 min), 100% B (7-9 min), 100-40% B (9-12 min).

Piceatannol (m/z 245>135) and spilanthol (m/z 222>123) were detected by the ESI-QqQ Micromass Quattro Micro API mass spectrometer (Waters, Milford, Massachusetts, USA), in positive MRM mode, under the following conditions: cone voltage: 30 V, capillary voltage: 3.0 kV, extractor cone voltage: 3.0 V, source temperature: 150 °C, desolvation temperature: 350 °C, desolvation gas flow ($N_{2(g)}$): 350 L h^{-1}, cone gas flow rate ($N_{2(g)}$): 100 L h^{-1}. Chromatographic peak integration was performed in MassLynx 4.0 after Savitzky-Golay smoothing.

Franz cell permeation assays with Strat-M™ membranes

Five milliliters of the receptor fluid were allocated at the receptor chambers of the Franz cells. Magnetic stirring was set to 350 rpm and the temperature was maintained at 33 ± 2 °C. Two milligrams of each formulation was spread over Strat-M™ membranes (Merck Millipore, Burlington, Massachusetts, EUA), which were allocated between the donor and receptor compartments. 500 µl of the recipient fluid were collected at 30, 60, 90, 120, 150 and 180 min, with equal volume of fresh fluid replacement at each time. The samples had their solvents removed by $N_{2(g)}$ and they were resuspended with 100 µl of 50% EtOH prior to HPLC injection. After 180 mins, the upper surfaces of the membranes were cleaned with cotton, which was extracted with 2 mL of 50% EtOH, for 5 min, under sonication. The membranes were extracted with 5 mL of 50% EtOH, for 5 min under sonication as well. The cotton and membrane extracts were dried under $N_{2(g)}$ and resuspended in 100 and 300 µl of 50% EtOH, respectively, for UHPLC-PAD analysis as described above.

Confocal Raman microscopy analyzes

An extra permeation test was performed with each formulation to collect the membranes after 3 h. The piceatannol depth within each membrane was read with a

confocal Raman microscope (XploRA plus, Horiba scientific), from 500 to 2500 cm^{-1}, under the following conditions: objective lens: 50 X, diffraction grating: 1200 lines mm^{-1} (750 µm), filter: 1 %, laser: 532 nm, slit: 50 µm, hole: 100 µm, accumulation time: 5 s, total accumulations: 15. The standards were read individually under the same conditions. The results were analyzed in Microcal Origin 2018 (OriginLab), by applying the peak analyzer tool after subtracting the baseline via asymmetric multiple least squares smoothing.

Results and Discussion

Public health agencies recommend sunscreen reapplication every 2-3 h or after sweating or swimming to maintain the skin protection against sunburn (20,21). On the basis of this statement, a 3 h period (180 min) was chosen for the evaluation of piceatannol behavior in a gel-cream formulation, with or without J extract and organic sunscreens, on the Strat-M™ skin model to simulate the presumed effective sunscreen duration.

The Strat-M™ membrane is a non-animal skin model which comprises two polyether sulfone layers coated with skin lipids such as ceramides, cholesterol, and free fatty acids. These layers cover a polyolefins base, which would be equivalent to the subcutaneous tissue. In total, the membrane has a 300 µm thickness (22). For the assessment of piceatannol behavior in this skin mimetic system, P_{ext}, a source of piceatannol in this work, was incorporated to B_{em} and O_{em} in the presence or absence of J_{ext}, a spilanthol based ingredient with presumed permeation enhancer property.

The amount of piceatannol and spilanthol in the formulations is presented in Table 2. Since a 2 mg cm^{-1} sunscreen thickness application is an internationally agreed parameter, this rule was applied to the Franz cell permeation assays, and the quantities of piceatannol and spilanthol applied onto the membranes were calculated from this data. Roughly, these amounts were of 0.1 and 0.2 µg, respectively (21).

Table 2: Piceatannol and spilanthol content in the formulations and the corresponding amount applied onto the Strat-M™ membranes.

	Into the emulsions (μg g^{-1})		Per membrane (μg)	
	PICEATANNOL	**SPILANTHOL**	**PICEATANNOL**	**SPILANTHOL**
B_{em}-P_{ext}	42.09 ±1.34	-	0.08 ± 0.01	-
B_{em}-J_{ext}	-	248.31 ± 9.70	-	0.25 ± 0.01
B_{em}-P_{ext}-J_{ext}	48.50 ± 4.43	237.82 ± 9.57	0.10 ±0.01	0.24 ± 0.01
O_{em}-P_{ext}	33.66 ± 0.34	-	0.07 ± 0.01	-
O_{em}-J_{ext}	-	230.36 ± 15.08	-	0.23 ± 0.02
O_{em}-P_{ext}-J_{ext}	36.44 ± 2.86	280.51 ± 11.53	0.07 ± 0.01	0.28 ± 0.01

B_{em}-P_{ext} – Base cream with passion fruit seed extract; **B_{em}-J_{ext}** – Base cream with paracrass extract; **B_{em}-P_{ext}-J_{ext}** – Base cream with passion fruit seed and paracrass extracts; **O_{em}-P_{ext}** – Base cream with the organic filters and passion fruit seed extract; **O_{em}-J_{ext}** – Base cream with the organic filters and paracrass extract; **O_{em}-P_{ext}-J_{ext}** – Base cream with the organic filters, passion fruit seed and paracrass extracts.

For the Franz cell permeation assays, the sink condition, that is, the condition in which the maximum concentration of the target compound is less than 1/3 of its saturation point in the receptor fluid, is a crucial parameter to avoid the compounds reflux from the receptor to the donor chamber. The stability of the target compounds in the receptor fluid during the test is also fundamental for a proper analysis (23,24).

Since P_{ext} and J_{ext} are soluble in 30% or 50% EtOH hydroalcoholic solutions, and these solutions do not affect Strat-M™ integrity, they were chosen as receptor fluid candidates. The 2.0 mg of P_{ext} and J_{ext} extracts were 500 times the maximum theoretical permeation of piceatannol and spilanthol from the emulsions, and they were fully solubilized in the evaluated systems. Hence, sink conditions in both receptor fluid candidates was guaranteed, but piceatannol and spilanthol stability in a 180 min span was higher in 30 % than in 50 % EtOH solution. As seen in Fig. 2, a more intense signal with a lower standard deviation among the replicates was achieved with the extracts in 30 % EtOH, and this led to the choice of this solvent as the most proper receptor fluid for the permeation assays in this work.

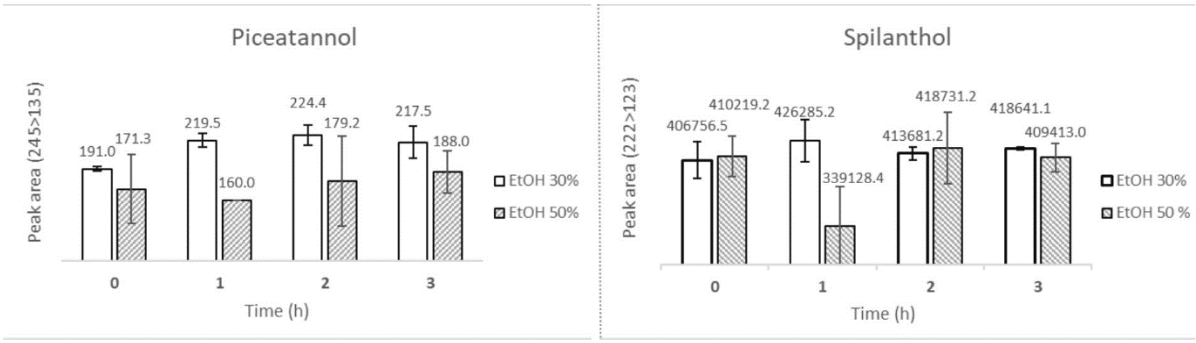

Figure 2: Peak areas of piceatannol (245>135) and spilanthol (222>123) in 30% (white bars) and 50% EtOH (hatched bars), at 0, 1, 2 and 3 h, measured by HPLC-MS/MS. The assay conditions are described at 'Receptor fluid selection for Franz cell permeation assays' section.

In the permeation assays, piceatannol was not found in the receptor fluid up to 180 min. In the O_{em} series of the formulation panel, the presence of the sunscreens, mainly Parsol MCX™, was observed even in the absence of the extracts (Fig. 3a). P_{ext} (Fig. 3b) and P_{ext} plus J_{ext} (Fig. 3c) in O_{em} series promoted a relative increase in Parsol MCX™ permeation through the Strat-M™ membrane, and Uvinul A Plus™ and T150™ were also found in the receptor chamber. J_{ext}, however, was not reproducible and a peak of sunscreens was found at 90 min only to one of the replicates (Fig. 3d).

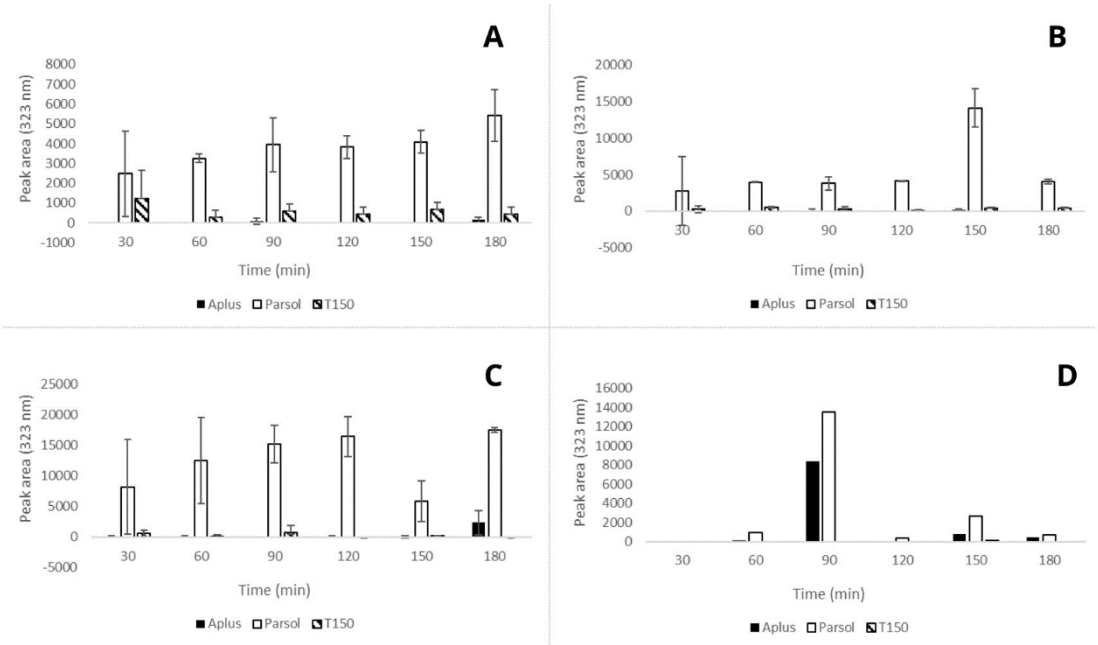

Figure 3: Peak areas of the sunscreens found at the receptor fluids. A: O_{em}. B: O_{em}-P_{ext}. C: O_{em}-P_{ext}-J_{ext}. D: O_{em}-J_{ext}.

A possible explanation for the predominance of Parsol MCX™ in the collector liquids may be related to log P, molecular weight (MW) and molecular flexibility parameters. Parsol MCX™ (MW = 290.4 Da; Log P = 5.3) is the smallest and the least lipophilic molecule among the three sunscreens evaluated in this work. In general, it is stated that molecules with a Log P value between 1-3 and molecular mass up to 600 Da permeate the skin more easily, and Uvinul A Plus™ and T150™ possess MW of 397.5 and 823.1 Da, and Log P of 6.93 and 15.5, respectively, being farther from the ideal permeation parameters. The molecular structures of these sunscreens (Fig. 4) also comprise larger resonance areas than Parsol MCX™, conferring to them larger planar areas and less flexibility to rearrange their conformations and pass through the lipidic mantle of Strat-M™ membrane (23,25).

In a safe and effective formulation, sunscreens should remain at the skin surface, not going deeper than the stratum corneum layer. However, there are records on the presence of sunscreens and their metabolites in plasma and urine of tested animals and human volunteers. The extent to which these molecules achieve the blood stream is dependent on the vehicle composition. Montenegro et al. demonstrated, for example, that octylmethoxycinnamate and butylmethoxydibenzoylmethane filters are influenced by different silicones and emulsifying systems, exhibiting skin permeation in some cases. Concerning Parsol MCX, a preliminary volunteer study from the early 2000' showed that, along with other sunscreen agents present in Coppertone™ lotion, it could be found in higher amounts at the upper stratum corneum layer after 30 min of application. However, no signs of systemic absorption for this sunscreen were observed (26–29).

Hence, the present *in vitro* tests indicates that O_{em} emulsion should be reformulated to avoid Parsol MCX permeation through the skin, especially if combining P_{ext} and J_{ext} to it.

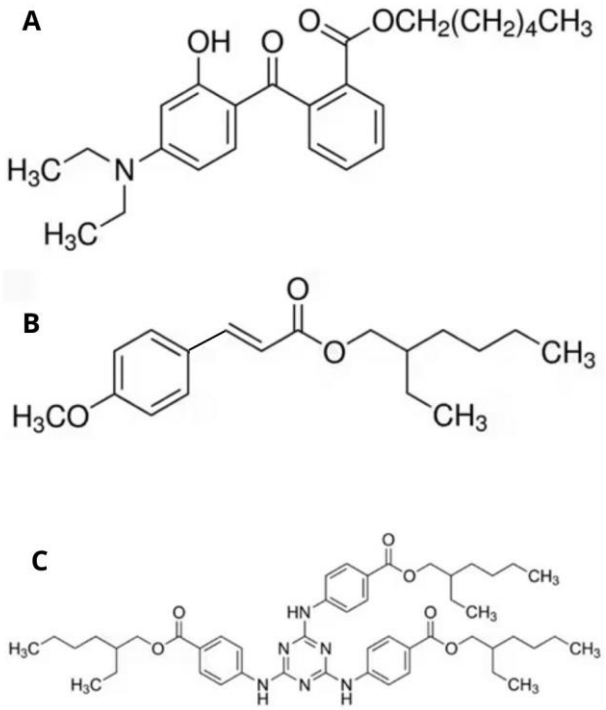

Figure 4: The molecular structure of the organic filters. A: Uvinul A Plus™. B: Parsol MCX™. C: Uvinul T150™.

Although spilanthol was stable in the receptor fluid assay, it was not detected at the receptor fluids of B_{em} and O_{em} formulations, and possible J_{ext} degradation at the membrane may have caused the non-reproducibility of O_{em}-J_{ext} results. In fact, the standard splilanthol chromatogram presented four peaks (Suppl. Mat.1), the major one attributed to spilanthol due to its UV spectra with a λ_{max} = 229 nm. The small peak with a retention time of 1.8 min (λ_{max} = 222.5 and 276.1 nm) was found in the receptor fluids of the emulsions comprising J_{ext}, indicating that it was able to permeate the Strat M™ membrane. A spilanthol or J_{ext} signal was not observed in the cotton extracts, but spilanthol was identified in one membrane of BPJ emulsion as a broad and dividing peak at T_R = 1.852 min, showing that it could penetrate the membrane but also exhibiting instability in this environment (Suppl. Mat. 2). In fact, Grymel et al. observed that, in solutions of spilanthol in dichloromethane or $CDCl_3$ in contact with air, it gradually disappeared, and an oxidized product was formed, especially in the presence of photosensitizing agents. That is the case of chlorophyl in the extract and the organic sunscreens themselves, which may have led to spilanthol depletion in this assay (30).

The presence of piceatannol, though, was seen at the cotton extracts of the assays where P_{ext} was present, aside from the degradation signs (Suppl. Mat. 3). A non-permeated piceatannol residual could be expected, given that the literature indicates a possible diffusion issue in *in vitro* tests (59). The susncreens Uvinul A Plus™ and Parsol MCX™ were also present in the cottons of the O_{em} series, and Uvinul T150™ appeared sporadically. The remaining sunscreens also presented signs of degradation after 3h of permeation assay.

Piceatannol, Uvinul A Plus™ and Parsol MCX™ were also observed at the membranes extracts of the O_{em} series with degradation signs. Piceatannol was present in the membranes extracts of the B_{em} series as well (Suppl. Mat. 2). Aside from the degradation signs, the analysis of the membranes by confocal Raman microscopy made it possible to visualize the extent to which piceatannol was capable of diffusing in each situation.

The Raman spectra of the standards are shown in Fig. 5. B_{em} and spilanthol did not exhibit intense signs, while the region between 1580 and 1700 cm^{-1} presented Raman shifts signals corresponding to piceatannol, O_{em} and the membrane itself.

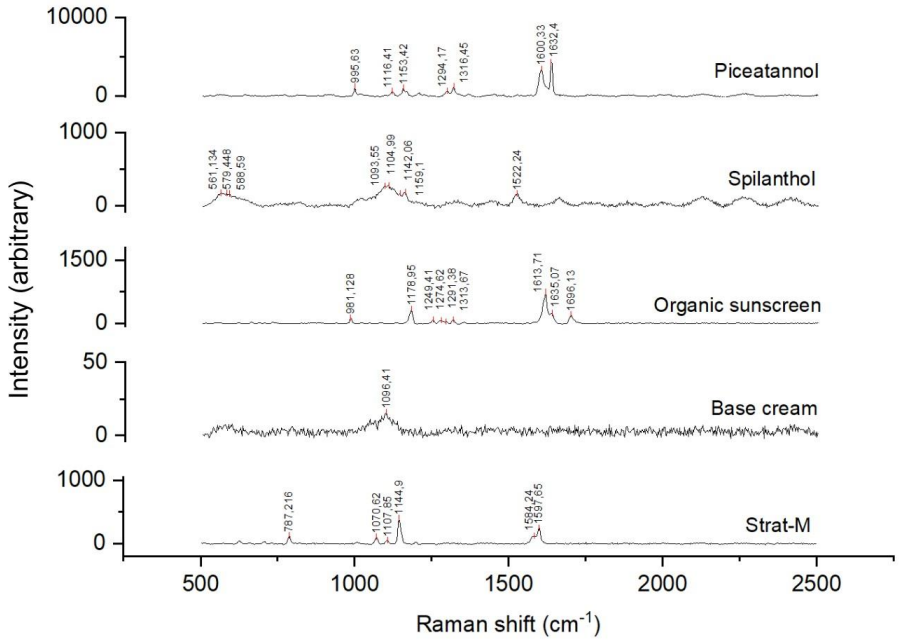

Figure 5: Raman spectra of the standards, emulsions and Strat-M™ surface.

The scanning of the membranes surfaces after a three-hour permeation assay with the emulsions comprising P_{ext} showed peaks attributed to Strat-M™ and a signal at 1600.33 cm^{-1} ($\lambda_{emission}$ = 581.51 nm) attributed to piceatannol. The signal at 1632.4 cm^{-1} ($\lambda_{emission}$ = 582.52 nm) was probably not seen as a result of the presence of degradation products and the low concentration of piceatannol in the samples.

In the depth reading of the membrane permeated with the B_{em} containing P_{ext}, the 1600.33 cm^{-1} signal was observed up to 140 µm from the surface (Fig. 6A and 6B). In the Strat-M™ membrane, this region corresponds to the dermis equivalent, showing that, aside from degradation, piceatannol could reach the depth required for acting on fibroblast and collagen regulation. The J_{ext} addition to the formulation enhanced piceatannol penetration to 220 µm from the surface, indicating that spilanthol was able to act as a permeation promoter for piceatannol (Fig. 6C and 6D). Another remarkable fact in the spectral map of Figure 6C is the inversion of the spectral intensities at 0 (surface) and 20 µm, which indicates that piceatannol was able to accumulate in deeper stratum corneum equivalent layers rather than being retained at the membrane surface.

The same intensity inversion between 0 and 20 µm depth was observed for O_{em}, indicating that formulations with higher oil loads may promote the entry of piceatannol into the stratum corneum (Fig. 6E and 6G). The 1600.33 cm^{-1} signal, in these cases, was observed up to 180 and 220 cm^{-1} for the formulations with and without the addition of J extract, respectively. These results are close to the one obtained with P_{ext} plus J_{ext} in the B_{em}, and J_{ext}, aside from being a permeation promoter due to the amphoteric properties of spilanthol and other N-alkylamides, it is an oil as well.

In all situations, though, the compounds diffusibility through the Strat-M™ membrane in this work were consonant with the *in-silico* predictions made by Frasch (31), Pots and Guy (32), and modified Robinson (33) models, as calculated by The United States Centers for Disease Control and Prevention (CDC) skin permeation calculator (34). Table 3 shows the permeation coefficient (kp) and log kp for piceatannol, spilanthol and Parsol MCX, the only sunscreen with a log P value within the acceptable range of the calculator. Independently of chosen model, piceatannol is the least diffusible of the three compounds, followed by spilanthol, which has kp values about 10 times higher, and Parsol MCX™, with a kp value about 100 times higher than

the kp of piceatannol. Hence, the absence of piceatannol and the signs of spilanthol and Parsol MCX™ in the receptor fluid is coherent, although these last two compounds behavior is not desirable in a safe and effective product.

Table 3: Skin permeation parameters of piceatannol, spilanthol and Parsol MCX™. (Source: CDC skin permeation calculator (34))

	Piceatannol	**Spilanthol**	**Parsol MCX™**
MW (Da)	244.243	221.339	290.397
LogP	2.60	3.99	5.80
Frask method			
kp (cm h^{-1})	5,05E-03	5,39E-02	1,11E-01
log kp	-2,3	-1,27	-0,95
Potts and Guy method			
kp (cm h^{-1})	4,13E-03	5,53E-02	4,04E-01
log kp	-2,38	-1,26	-0,39
Modified Robinson method			
kp (cm h^{-1})	2,89E-03	2,41E-02	7,34E-02
log kp	-2,54	-1,62	-1,13

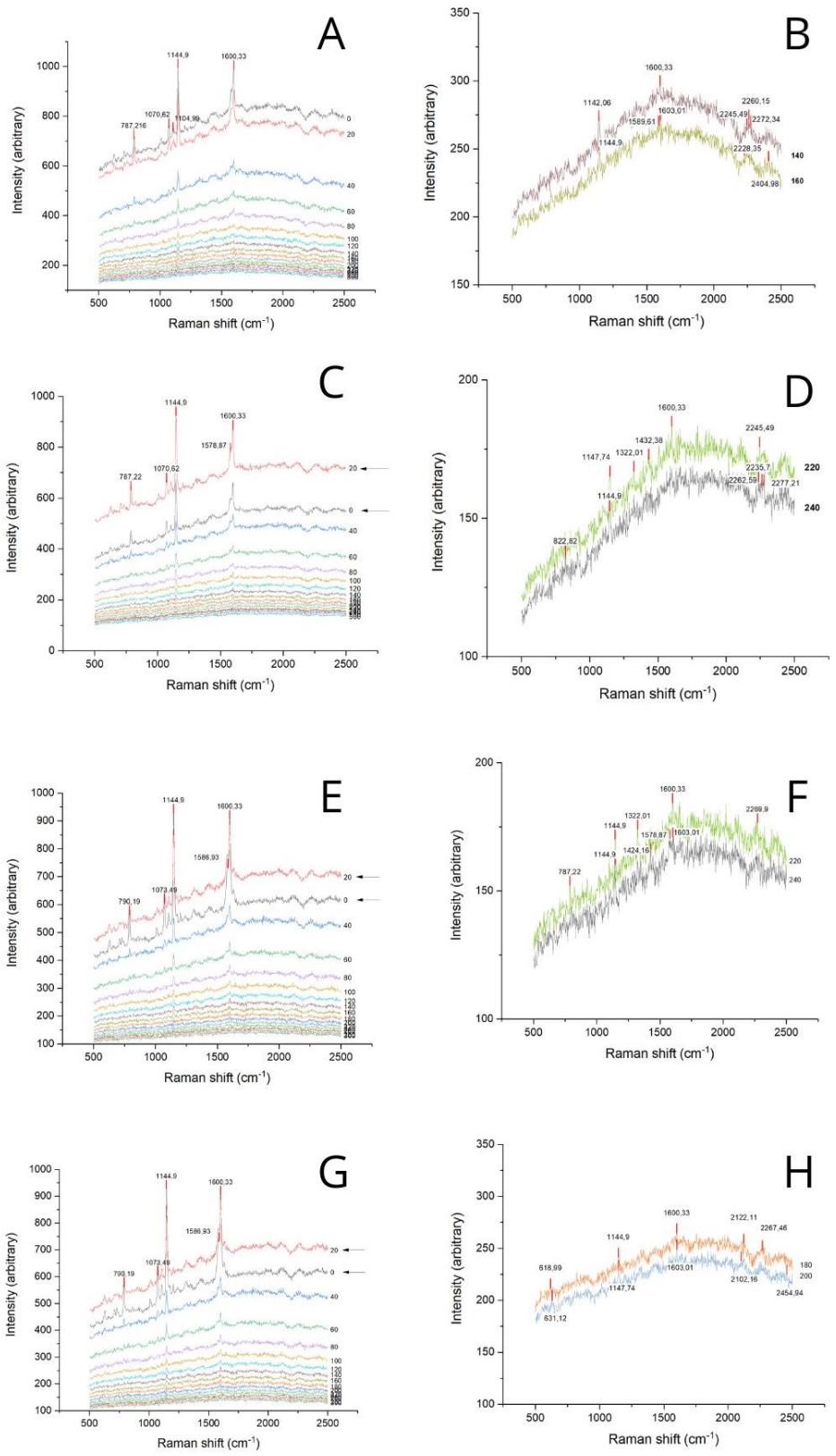

Figure 6: Transversal Raman spectra of the membranes. A: In-depth spectra of B_{em}-P_{ext}. B: B_{em}-P_{ext} spectra at 140 and 160 µm from the surface. C: In-depth spectra of B_{em}-P_{ext}-J_{ext}. D. B_{em}-P_{ext}-J_{ext} spectra at 220 and 240 µm from the surface. E. In-depth spectra of O_{em}-P_{ext}. F. O_{em}-P_{ext} spectra at 220 and 240 µm from the surface. G. In-depth spectra of O_{em}-P_{ext}-J_{ext}. H. O_{em}-P_{ext}-J_{ext} spectra at 180 and 200 µm from the surface.

Conclusion

Despite the degradation of the compounds during the tests, piceatannol was able to reach the Strat-M membrane dermis-equivalent region when incorporated to the emulsion proposed in this work. In the base emulsion, the presence of paracress extract boosted the depth where piceatannol penetrated the membrane in relation to passion fruit seed extract alone in the formulation. The organic sunscreens made a similar effect, with or without the addition of paracress extract, indicating that a more lipophilic environment may favor piceatannol skin permeation. Both the organic sunscreens and paracress extract allowed a greater concentration of actives inside the *stratum corneum* equivalent layer of the membrane in comparison to its surface. Furthermore, the sunscreens permeated the Strat-M membrane to some extent, specially Parsol MCX™, which is the smallest and the most flexible among the ones evaluated in this study. The presence of the extracts into the formulations enhanced the quantity of Parsol MCX™ found in the receptor fluids of the Franz cells and this information should be taken into consideration when developing a topical product combining these ingredients.

Acknowledgments

This work was financially supported by the National Institutes of Science and Technology (INCTs) [grant numbers: FAPESP/INCT 2014/50867, CNPq 465389/2014-7]. C. B. G. Bottoli acknowledges CNPq for a research fellowship [CNPq 309363/2018-7].

The authors acknowledge LabFarQui, of the State University of Campinas Institute of Chemistry (IQ-Unicamp), for Waters Acquity UPLC system experiments, and the National Nanotechnology Laboratory - LNNANO, of the National Center for Research in Energy and Materials – CNPEM, for the confocal Raman microscopy assays.

References

1. Matsui Y, Sugiyama K, Kamei M, Takahashi T, Suzuki T, Katagata Y, et al. Extract of passion fruit (Passiflora edulis) seed containing high amounts of piceatannol inhibits melanogenesis and promotes collagen synthesis. J Agric Food Chem [Internet]. 2010 Oct 27 [cited 2020 Jul 30];58(20):11112–8. Available from: https://pubs.acs.org/doi/full/10.1021/jf102650d

2. Maruki-Uchida H, Kurita I, Sugiyama K, Sai M, Maeda K, Ito T. The protective effects of piceatannol from passion fruit (Passiflora edulis) seeds in UVB-irradiated keratinocytes. Biol Pharm Bull [Internet]. 2013 May [cited 2020 Jul 30];36(5):845–9. Available from: https://pubmed.ncbi.nlm.nih.gov/23649341/

3. Cordova-Gomez M, Galano A, Alvarez-Idaboy JR. Piceatannol, a better peroxyl radical scavenger than resveratrol. RSC Adv [Internet]. 2013 Nov 21 [cited 2020 Jul 22];3(43):20209–18. Available from: https://pubs.rsc.org/en/content/articlehtml/2013/ra/c3ra42923g

4. Dos Santos FAR, Xavier JA, da Silva FC, Jose Merlin JP, Goulart MOF, Vasantha Rupasinghe HP. Antidiabetic, Antiglycation, and Antioxidant Activities of Ethanolic Seed Extract of Passiflora edulis and Piceatannol *In Vitro*. Molecules [Internet]. 2022 Jul 1 [cited 2023 Jun 3];27(13). Available from: https://pubmed.ncbi.nlm.nih.gov/35807309/

5. Krambeck K, Santos D, Sousa Lobo JM, Amaral MH. Benefits of skin application of piceatannol—A minireview. Australasian Journal of Dermatology [Internet]. 2023 Feb 1 [cited 2023 Jun 3];64(1):e21–5. Available from: https://onlinelibrary.wiley.com/doi/full/10.1111/ajd.13937

6. Maruki-Uchida H, Morita M, Yonei Y, Sai M. Effect of Passion Fruit Seed Extract Rich in Piceatannol on the Skin of Women: A Randomized, Placebo-Controlled, Double-Blind Trial [Internet]. Vol. 64, J Nutr Sci Vitaminol. 2018 [cited 2020 Jul 30]. Available from: https://upload.umin.ac.jp/cgi-

7. Dai Y, Lim JX, Yeo SCM, Xiang X, Tan KS, Fu JH, et al. Biotransformation of Piceatannol, a Dietary Resveratrol Derivative: Promises to Human Health. Mol Nutr Food Res [Internet]. 2020 Jan 1 [cited 2022 Dec 24];64(2). Available from: https://pubmed.ncbi.nlm.nih.gov/31837280/

8. Setoguchi Y, Oritani Y, Ito R, Inagaki H, Maruki-Uchida H, Ichiyanagi T, et al. Absorption and metabolism of piceatannol in rats. J Agric Food Chem [Internet]. 2014 Mar 26 [cited 2020 Jul 30];62(12):2541–8. Available from: https://pubmed.ncbi.nlm.nih.gov/24625210/

9. Jarosova V, Vesely O, Marsik P, Jaimes JD, Smejkal K, Kloucek P, et al. Metabolism of stilbenoids by human faecal microbiota. Molecules [Internet]. 2019 [cited 2020 Jul 30];24(6). Available from: /pmc/articles/PMC6471231/?report=abstract

10. Hung CF, Lin YK, Huang ZR, Fang JY. Delivery of Resveratrol, a Red Wine Polyphenol, from Solutions and Hydrogels in the Skin. Biol Pharm Bull [Internet]. 2008 May 1 [cited 2020 Jul 22];31(5):955–62. Available from: https://www.jstage.jst.go.jp/article/bpb/31/5/31_5_955/_article

11. Eskandari M, Rembiesa J, Startaitė L, Holefors A, Valančiūtė A, Faridbod F, et al. Polyphenol-hydrogen peroxide reactions in skin: *In vitro* model relevant to study ROS reactions at inflammation. Anal Chim Acta. 2019 Oct 10;1075:91–7.

12. Anna Malinowska M, Billet K, Drouet S, Munsch T, Unlubayir M, Tungmunnithum D, et al. Grape Cane Extracts as Multifunctional Rejuvenating Cosmetic Ingredient: Evaluation of Sirtuin Activity, Tyrosinase Inhibition and Bioavailability Potential. Molecules [Internet]. 2020 May 8 [cited 2020 Jul 30];25(9):2203. Available from: https://www.mdpi.com/1420-3049/25/9/2203

13. Vitorino C, Sousa J, Pais A. Overcoming the Skin Permeation Barrier: Challenges and Opportunities. Curr Pharm Des [Internet]. 2015 May 27 [cited 2020 Jul 30];21(20):2698–712. Available from: http://www.eurekaselect.com/openurl/content.php?genre=article&issn=1381-6128&volume=21&issue=20&spage=2698

14. Rodrigues Leite-Silva V, Mandelli De Almeida M, Fradin A, Grice JE, Roberts MS. Expert Review of Dermatology Delivery of drugs applied topically to the skin. 2014 [cited 2020 Jul 22]; Available from: https://www.tandfonline.com/action/journalInformation?journalCode=ierg20

15. Wu LC, Fan NC, Lin MH, Chu IR, Huang SJ, Hu CY, et al. Anti-inflammatory effect of spilanthol from Spilanthes acmella on murine macrophage by down-regulating LPS-induced inflammatory mediators. J Agric Food Chem [Internet]. 2008 Apr 9 [cited 2020 Jul 30];56(7):2341–9. Available from: https://pubs.acs.org/doi/abs/10.1021/jf073057e

16. Barbosa AF, de Carvalho MG, Smith RE, Sabaa-Srur AUO. Spilanthol: Occurrence, extraction, chemistry and biological activities [Internet]. Vol. 26, Brazilian Journal of Pharmacognosy. Sociedade Brasileira de Farmacognosia; 2016 [cited 2020 Jul 22]. p. 128–33. Available from: http://dx.doi.org/10.1016/j.bjp.2015.07.024

17. Yamada M, Mohammed Y, Prow TW. Advances and controversies in studying sunscreen delivery and toxicity. Adv Drug Deliv Rev. 2020 Jan 1;153:72–86.

18. Silva GC, Rodrigues RAF, Bottoli CBG. Passion fruit seed extract enriched in piceatannol obtained by microwave-assisted extraction. Sustain Chem Pharm. 2021 Sep 1;22:100472.

19. Sunscreen Simulator [Internet]. [cited 2022 Dec 24]. Available from: https://sunscreensimulator.basf.com/Sunscreen_Simulator/login

20. How to apply sunscreen [Internet]. [cited 2023 Jun 3]. Available from: https://www.aad.org/public/everyday-care/sun-protection/shade-clothing-sunscreen/how-to-apply-sunscreen

21. Diffey BL. When should sunscreen be reapplied? J Am Acad Dermatol. 2001 Dec 1;45(6):882–5.

22. Pulsoni I, Lubda M, Aiello M, Fedi A, Marzagalli M, von Hagen J, et al. Comparison Between Franz Diffusion Cell and a novel Micro-physiological System for *In Vitro* Penetration Assay Using Different Skin Models. SLAS Technol. 2022 Jun 1;27(3):161–71.

23. Zsikó S, Csányi E, Kovács A, Budai-Szűcs M, Gácsi A, Berkó S. Methods to Evaluate Skin Penetration *In Vitro*. Scientia Pharmaceutica 2019, Vol 87, Page 19 [Internet]. 2019 Aug 8 [cited 2022 Feb 26];87(3):19. Available from: https://www.mdpi.com/2218-0532/87/3/19/htm

24. Neupane R, Boddu SHS, Renukuntla J, Babu RJ, Tiwari AK. Alternatives to Biological Skin in Permeation Studies: Current Trends and Possibilities. Pharmaceutics 2020, Vol 12, Page 152 [Internet]. 2020 Feb 13 [cited 2022 Feb 26];12(2):152. Available from: https://www.mdpi.com/1999-4923/12/2/152/htm

25. Chuang SY, Lin YK, Lin CF, Wang PW, Chen EL, Fang JY. Elucidating the Skin Delivery of Aglycone and Glycoside Flavonoids: How the Structures Affect Cutaneous Absorption. Nutrients [Internet]. 2017 Dec 1 [cited 2022 Feb 26];9(12). Available from: /pmc/articles/PMC5748754/

26. Montenegro L, Turnaturi R, Parenti C, Pasquinucci L. *In Vitro* Evaluation of Sunscreen Safety: Effects of the Vehicle and Repeated Applications on Skin Permeation from Topical Formulations. Pharmaceutics [Internet]. 2018 [cited 2023 Jun 3];10(1). Available from: https://pubmed.ncbi.nlm.nih.gov/29495452/

27. Sarveiya V, Risk S, Benson HAE. Liquid chromatographic assay for common sunscreen agents: application to in vivo assessment of skin penetration and systemic absorption in human volunteers. Journal of Chromatography B. 2004 Apr 25;803(2):225–31.

28. Montenegro L, Carbone C, Puglisi G. Vehicle effects on *in vitro* release and skin permeation of octylmethoxycinnamate from microemulsions. Int J Pharm. 2011 Feb 28;405(1–2):162–8.

29. Montenegro L, Carbone C, Paolino D, Drago R, Stancampiano AH, Puglisi G. *In vitro* skin permeation of sunscreen agents from O/W emulsions. Int J Cosmet Sci [Internet]. 2008 Feb [cited 2020 Jul 30];30(1):57–65. Available from: http://www.ncbi.nlm.nih.gov/pubmed/18377631

30. Grymel M, Mazurkiewicz R, Bajkacz S, Bilik J, Kowalczyk S. Extraction, Purification, Quantification, and Stability of Bioactive Spilanthol from Acmella oleracea. Planta Med [Internet]. 2023 Jan 16 [cited 2023 Jun 3];89(5). Available from: https://pubmed.ncbi.nlm.nih.gov/36044910/

31. Frasch HF. A random walk model of skin permeation. Risk Anal [Internet]. 2002 [cited 2023 Jul 1];22(2):265–76. Available from: https://pubmed.ncbi.nlm.nih.gov/12022675/

32. Potts RO, Guy RH. Predicting skin permeability. Pharm Res [Internet]. 1992 [cited 2023 Jul 1];9(5):663–9. Available from: https://pubmed.ncbi.nlm.nih.gov/1608900/

33. Wilschut A, ten Berge WF, Robinson PJ, McKone TE. Estimating skin permeation. The validation of five mathematical skin permeation models. Chemosphere [Internet]. 1995 [cited 2023 Jul 1];30(7):1275–96. Available from: https://pubmed.ncbi.nlm.nih.gov/7749723/

34. Skin Permeation Calculator | NIOSH | CDC [Internet]. [cited 2023 Jul 1]. Available from: https://www.cdc.gov/niosh/topics/skin/skinpermcalc.html

DISCUSSÃO

DISCUSSÃO

O desenvolvimento de novos produtos dermocosméticos é um desafio tanto em relação à farmacotécnica quanto ao atendimento dos anseios do público consumidor. Tanto o maracujá quanto o jambu se enquadram dentro das perspectivas por produtos do segmento de higiene pessoal, perfumaria e cosméticos (HPPC) com ingredientes de origem natural e com produção local, que reflitam e beneficiem suas origens. Com a crescente conscientização da população com relação às mudanças climáticas, a preocupação com a sustentabilidade também tem passado a nortear as inovações em processos e produtos no setor, demandando cada vez mais novos insumos ambientalmente amigáveis e corretos [92–94].

O desafio reside, neste caso, na performance dos ingredientes chamados sustentáveis. Embora não haja um conceito-padrão de sustentabilidade, entende-se que, para ser sustentável, o processo, produto ou ambos devem ser capazes de atender às necessidades da população sem comprometer as futuras gerações. No caso de produtos, em especial somam-se a porcentagem de carbono de origem renovável e a biodegradabilidade a esta definição, além das questões sociais e éticas. As matérias-primas cosméticas que cabem dentro destes quesitos atualmente têm, em geral, originado formulações com desempenho, sensorial e estética inferiores à das produzidas com os insumos convencionais. Assim, para se atingir um patamar de sustentabilidade, é preciso investir no desenvolvimento e aprimoramento dos insumos de origem natural, vegetal ou orgânica - em que a matéria prima é obtida em um sistema orgânico de produção ou é extraída por meio de um processo sustentável não prejudicial ao ecossistema local - para garantir a funcionalidade dos produtos cosméticos concatenada ao comportamento do consumidor frente a estes produtos [93, 95].

No que compete à utilização das sementes do maracujá para obtenção de extratos ricos em piceatanol, observa-se aderência às questões de regionalidade e sustentabilidade, e o uso da técnica de MAE para sua obtenção, em princípio, também vem de encontro com a necessidade de processos ambientalmente amigáveis. As características do extrato obtido neste trabalho mostram-se interessantes ao desenvolvimento de um dermocosmético no sentido do teor de princípio ativo e dos aspectos sensoriais, e abre-se uma oportunidade para uma análise de viabilidade técnico-econômica do processo desenvolvido para sua implantação industrial.

Enquanto processo, espera-se que MAE permita uma redução de gasto energético para a obtenção do extrato, e os resultados apresentados no CAPÍTULO 2 já mostram um ganho em tempo e em rendimento em relação a um método convencional de extração, o que o torna promissor no que compete a questões ambientais.

Desde 1967, a técnica de micro-ondas em escala industrial com aplicações de secagem está comercialmente disponível no mercado e vem sendo aprimorada ao longo do tempo. Contudo, em termos de extração de compostos bioativos a partir de matrizes vegetais, a maior parte dos dados disponíveis provêm da escala laboratorial. A lacuna de estudos sobre a factibilidade da MAE em maiores escalas pode estar relacionada a pontos críticos relativos ao equipamento em si, como os requerimentos para a sua instalação, as condições de processamento dos materiais, e os riscos de operação e segurança [96].

Li et al. [97] descrevem que a complexidade no escalonamento do processo de MAE para compostos bioativos reside em fatores como:

(i) A modelagem teórica de uma cavidade de micro-ondas vazia tem pouca capacidade preditiva para uma cavidade parcialmente carregada, pois a carga causa perturbação do campo elétrico.

(ii) A constante dielétrica de um determinado composto varia espacialmente conforme composição química do meio, densidade aparente da carga e variação de temperatura durante o processo.

(iii) A baixa profundidade de penetração de micro-ondas, dando origem a mecanismos concorrentes de transferência de calor. Por este motivo, o aquecimento uniforme raramente é alcançado em sistemas convencionais de micro-ondas.

Os fabricantes de instrumentos de MAE em escala industrial buscaram otimizar a geometria da câmara, os componentes elétricos e as conexões para resolver os obstáculos impostos pelo escalonamento, de maneira a promover uma distribuição homogênea das micro-ondas pela matriz vegetal com a finalidade de se alcançar uma extração reprodutível e consistente. O uso de fato da técnica no mercado dependerá não só da potencial sustentabilidade de processos que façam uso de seus princípios, mas também de fatores econômicos como a produção de

insumos de alto valor agregado ou exclusivamente preparáveis por micro-ondas [98, 99].

Este trabalho mostrou que a seletividade da MAE em escala de bancada para a extração de compostos da torta desengordurada de semente de maracujá foi distinta da exibida pela técnica de refluxo convencional. Contudo, o coeficiente de variação das respostas obtidas para a sextuplicata do ponto central do planejamento 2^3 variou entre 13 e 14%, indicando uma necessidade de melhoria da reprodutibilidade do processo. Esta dispersão pode ter contribuído para a não obtenção de modelos adequados, embora uma variabilidade de respostas tenha sido observada no conjunto de ensaios.

Quanto às respostas analíticas em si, a ausência de uma matriz branco para cada um dos extratos preparados fez com que se optasse por uma avaliação semiquantitativa do piceatanol, utilizando-se a relação entre a área do pico correspondente a esta molécula e a área do padrão interno kaempferol, não identificado no extrato, como forma de equalizar as respostas de área e de se obter uma variável resposta para triagem de condições com maior agilidade que a quantificação do teor de piceatanol em cada extrato. A resposta A_{pic}/A_{kaemp} foi consistente com o rendimento em massa seca de cada um dos experimentos e, em geral, aqueles que possuíram menores rendimentos apresentaram menor A_{pic}/A_{kaemp}. De toda forma, apesar de algumas limitações dos testes em bancada *versus* escala piloto/industrial, a técnica mostra-se com potencial viabilidade, e, caso implantada, um próximo passo seria a obtenção de um extrato padronizado que, conforme definição da Farmacopeia Brasileira 6ª ed. [100], trata-se de *"um extrato ajustado a um conteúdo definido de um ou mais constituintes responsáveis pela atividade terapêutica"*, ou de um extrato quantificado, o qual é *"ajustado para uma faixa de conteúdo de um ou mais marcadores ativos" .*

Já em termos de produto, formulações multifuncionais têm ganhado espaço na vida das pessoas que buscam praticidade e economia. Protetores solares com efeito matte, pigmentos ou ação antirradicais livres já se encontram disponíveis no mercado, e as inovações tendem em direção à proteção solar baseada em formulações mais naturais, dando preferência aos filtros solares inorgânicos e ao óxido de ferro para formulações coloridas, à inclusão de ativos antioxidantes e que promovam proteção contra danos causados pela radiação infravermelha, visível e pela

luz azul, formando um escudo multiprotetor sobre a pele [92]. No CAPÍTULO 3, demonstrou-se que, na emulsão proposta, o extrato de semente de maracujá produzido neste trabalho não foi capaz de permanecer estável, e a adição de filtros solares à formulação tornaram ainda maior esta instabilidade. O extrato de jambu, no entanto, mostrou-se compatível com os filtros orgânicos, mas instável na presença de filtros inorgânicos.

De fato, o trabalho de Navarro-Orcajada et al. [101] sobre os estilbenos, aponta que o trans-piceatanol é muito sensível à luz, convertendo-se a cis-piceatanol via ciclização intramolecular, e os estilbenos, em geral, possuem como limitações a baixa solubilidade em água e a baixa estabilidade físico-química, sendo facilmente degradados por fatores como o pH, a luz e a temperatura. Latva-Maenpaa et al. [102] investigaram a estabilidade e a foto isomerização de estilbenos isolados das raízes do abeto norueguês, uma conífera do gênero *Picea*, tendo observado que a conversão dos isômeros de trans a cis ocorre logo nas primeiras horas de exposição de soluções metanólicas destes compostos à luz, o que não ocorre quando estas são armazenadas no escuro, a – 20 °C. A exposição do extrato bruto sólido à luz, no entanto, não causa isomerização dos estilbenos. Já em relação ao espilantol, Savic et al. [103] mostraram que o ele e o homoespilantol foram os compostos mais estáveis, dentre nove N-alquilamidas, à radiação UVB após 120 min de exposição, mas os álcoois, em detrimento da água e de solução salina, foram os solventes onde os compostos, em geral, apresentaram a maior estabilidade [104].

É fato que existe uma gama de emulsões base possíveis de serem formuladas com diferentes propriedades e uma diversidade de formas cosméticas onde estes extratos podem ser incorporados com maior estabilidade do que a apresentada no protótipo do presente trabalho, mas, pelos dados apresentados, a proteção deles do contato com o veículo, com a luz e com os filtros solares poderá ser estratégica, principalmente em se tratando de protetores baseados em filtros inorgânicos. A título de exemplo, Taofiq et al. [105] mostraram que a microencapsulação dos ácidos para-hidroxibenzoico, para-cumárico, protocatecoico e cinâmico em alginato de sódio permitiu não só a liberação controlada destas moléculas, como também aumentou a estabilidade destes compostos em creme em comparação com a inclusão direta destas moléculas na formulação. A nanoencapsulação de compostos bioativos também contribui nesse sentido, já que os

sistemas nanoestruturados também promovem melhora na proteção contra degradação, solubilidade, estabilidade e biodisponibilidade dos compostos envoltos por este sistema [106]. E em entendendo que a maior parte da formulação protótipo eleita para este estudo possui a água como seu ingrediente majoritário, abre-se também uma vertente para testes de estabilidade dos extratos em ambientes menos aquosos, como bastões, manteigas e outras que formas que forem desenvolvidas seguindo a tendência do uso racional da água dentro do contexto da sustentabilidade [92].

À parte da estabilidade dos compostos de interesse, um desafio particular foi o desenvolvimento do preparo de amostra dos cremes contendo os extratos para as análises cromatográficas. Em um levantamento bibliográfico com as palavras-chave “topical formulation”, “cream” e “HPLC”, observou-se que a maioria dos retornos estavam ligados à dosagem de princípios ativos em formulações de medicamentos de uso tópico, e os métodos de preparo de amostra reportados consistiam da simples diluição de uma quantidade precisa da formulação em um solvente adequado.

Katakam, Dongala e Ettaboina [107], por exemplo, desenvolveram um método para indicar a estabilidade de um creme de uso tópico contendo acetato de hidrocortisona, cloridrato de pramoxina, sorbato de potássio e ácido sórbico. Em balões de 50 ml a quantidade exata de 31,25 mg das amostras de creme foram pesadas e diluídas com EtOH 80%. As soluções foram sonicadas por 20 min, com eventuais intervenções de agitação manual. Após o processo, os volumes foram acertados, as soluções foram homogeneizadas e filtradas em filtros de nylon (45 mm), descartando-se os 3 mL iniciais. 5 ml dos filtrados foram adicionados a balões de 25 ml e os volumes foram acertados com ACN 60% para injeção em um UHPLC.

De maneira muito semelhante, Papageorgiou et al. [108] trabalharam em um desenvolvimento de método para a quantificação e verificação da estabilidade de cremes cosméticos contendo ácido alfa-lipoico, em concordância com os guias da International Conference on Harmonization (ICH). As amostras foram preparadas por meio de diluição em série e filtração segundo o seguinte protocolo: 10 mg de amostra foram precisamente pesadas e transferidas para um balão volumétrico de 50 ml, onde se adicionaram 40 mL de uma mistura de ácido clorídrico 2 mol L^{-1} e ACN (50:50, v / v). A mistura foi então colocada em um banho ultrassônico por 25 min e, ao final do

processo, o volume foi acertado com o mesmo solvente. 2 g da suspensão foram transferidos para um tubo Eppendorf de 2 mL e foram centrifugados a 16.000 rpm, por 15 min, em temperatura ambiente. O sobrenadante foi filtrado através de filtro PET, e uma alíquota de 0,5 mL do filtrado foi diluída com acetonitrila para um volume de 10 ml antes da análise por HPLC-UV.

Diante destas informações, definiu-se que o ponto de partida para as formulações desenhadas neste trabalho seria uma simples rotina de diluição e centrifugação, utilizando-se o sobrenadante da operação para a quantificação do piceatanol e do espilantol. Deste modo, para um teste inicial com O_{em}, 50 mg foram diluídos em 1 mL de EtOH 50% (v/v) com auxílio de vórtex e a solução foi centrifugada por 10 min a 3000 rpm. Entretanto, a filtração do sobrenadante tornou-se um gargalo, exigindo testes em diferentes modelos de filtros. Tentativas preliminares de preparo envolvendo a extração líquido-líquido do sobrenadante com hexano e a extração em fase sólida (SPE - *solid phase extraction*) com cartuchos ENVI 8 e C18 (Supelco®, Sigma Aldrich, EUA) foram testadas como formas de contorno a esta questão. A Tabela 1 compila as formas de filtros testadas, mostrando que nylon e PVDF não foram compatíveis com o sobrenadante. Vials de celulose regenerada, no entanto, com a pressão imposta com as mãos sobre o filtro acoplado à tampa, permitiram sua filtração a 0,45 e a 0,22 µm, o que não foi conseguido com facilidade ao se acoplar filtros de celulose regenerada a seringas.

Tabela 1: testes de filtração dos sobrenadantes das suspensões de formulação.

Filtro*	Resultado
Vial PVDF 0,45 µm	Não filtrou
Vial RC 0,45 µm	Filtrou com esforço
Vial RC 0,20 µm	Filtrou com esforço
Filtro NY 0,45 µm + seringa	Não filtrou
Filtro PVDF 0,45 µm com grade prévia + seringa	Não filtrou
Filtro PVDF 0,45 µm	Não filtrou
Filtro PVDF 0,22 µm	Não filtrou
Filtro RC 0,45 µm + seringa	Não filtrou

*GVS, Brasil
PVDF - fluoreto de polivinilideno
RC – celulose regenerada
NY - Nylon

Eleito o filtro, 1,0 mg de piceatanol padrão e 1,0 mg de extrato clarificado de jambu foram adicionados a O_{em} para a avaliação da factibilidade de uma etapa de limpeza do sobrenadante com SPE ou extração líquido-líquido. Os sobrenadantes bruto, eluído pelo cartucho Envi-8 e eluído pelo cartucho LC-18 foram avaliados por HPLC-MS, nas condições descritas no CAPÍTULO 1. A fase aquosa resultante da extração líquido-líquido não pôde ser filtrada pelo vial de celulose regenerada e, por este motivo, aboliu-se esta metodologia da avaliação.

A Figura 1 mostra as áreas dos picos de piceatanol e espilantol no sobrenadante bruto, e nos eluatos dos cartuchos Envi-8 e LC-18, todos filtrados em vial com filtro de celulose regenerada. A passagem do sobrenadante pelos cartuchos diminuiu o sinal obtido para estes compostos, indicando que, para o emprego destas alternativas, seria necessário um trabalho de otimização para verificar a possibilidade de se aumentar a recuperação dos analitos de interesse. Como a SPE mostrou perda considerável de analitos em relação ao sobrenadante bruto e este último não apresentou impacto negativo sobre o equipamento, optou-se por seguirem-se os trabalhos sobre o sobrenadante bruto e pelo uso de vials RC 0,20 µm (GVS).

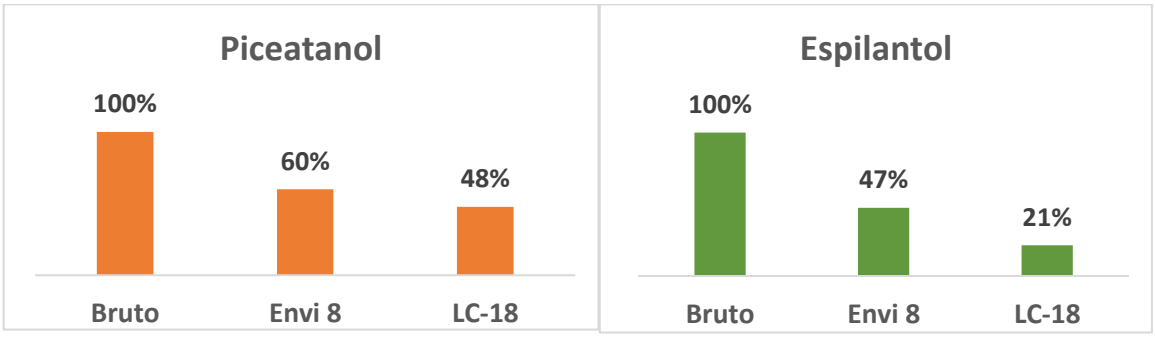

Figura 1: áreas dos picos de piceatanol e espilantol obtidas por HPLC-MS/MS para cada preparo de amostra testado.

Já sobre os testes de difusão cutânea propostos neste trabalho, sabe-se que também é uma tendência que o consumidor opte por produtos não testados em animais. O desenvolvimento e a validação de modelos alternativos para os ensaios de permeação cutânea vêm evoluindo, conforme explicitado no CAPÍTULO 1, para o uso de pele sintética 2D, 3D e de membranas químicas com camadas de lipídeos que mimetizem o estrato córneo da pele. No CAPÍTULO 4, onde se explora o perfil de difusão cutânea *in vitro* das formulações protótipo, optou-se pela membrana Strat-M®

(Merck Millipore) como modelo de pele para os ensaios. Esta membrana, apesar de mimetizar a epiderme, a derme e o tecido subcutâneo em termos de resistência à difusão de compostos, não necessariamente gera resultados correspondentes aos valores absolutos de permeabilidade para a pele humana, A correlação com a pele de orelha de porco, um dos modelos *ex-vivo* mais utilizados nos testes de permeação *in vitro,* mostrou-se elevada, por exemplo, para o rododendrol (lipofílico) em dose finita e infinita. Esta correlação não se repetiu, contudo, com a cafeína (hidrofílica), cuja correlação se deu apenas em protocolo de dose finita. Trabalhos comparando o perfil de permeação de moléculas pela Strat-M® e pela pele de cadáveres humanos também sinalizaram para a ausência de correlação. Entretanto, a membrana não deixa de permitir a extração de informações sobre tendências, sendo útil para guiar o desenvolvimento de uma formulação otimizada [109, 110].

Assim sendo, embora não se possa precisar se o comportamento observado no CAPÍTULO 4 se replicaria *in vivo*, o fato de que um ambiente mais lipofílico permite não só encontrar o piceatanol a profundidades superiores, mas também acumulá-lo em camadas mais profundas do estrato córneo dão um primeiro direcionamento para próximas formulações que possam ser desenhadas com o extrato de semente de maracujá produzido neste projeto. Além disso, na formulação protótipo, o extrato de jambu exerceu função promotora de permeação e pode ser considerado como um adjuvante potencial a ser testado em conjunto nas próximas rodadas do desenvolvimento cosmético. A microscopia Raman confocal foi fundamental neste entendimento, pois permitiu dar uma dimensão da difusão do piceatanol incapaz de ser dada por técnicas cromatográficas.

Por fim, cabe salientar que este trabalho foi embasado nas atividades potenciais do piceatanol conforme relatado na literatura e que, para que o extrato de sementes de maracujá aqui proposto se torne um ativo cosmético, além das questões inerentes à sua produção e estabilização em formulação, é fundamental que se realizem estudos que corroborem a sua bioatividade *in vivo* e que atestem pela sua não toxicidade, não carcinogenicidade e não mutagenicidade, sozinho ou em combinação com o extrato das partes aéreas de jambu. A revisão de Medrano-Pardial et al. [111] sobre a avaliação toxicológica dos estilbenos atesta pela falta de reportes de genotoxicidade *in vitro* e toxicidade *in vivo* que corroborem a segurança desta classe de compostos, e esta seria mais uma vertente a se explorar para tornar o

extrato de sementes de maracujá um novo extrato bioativo com aplicação dermocosmética.

CONCLUSÃO

CONCLUSÃO

Com relação à difusão cutânea *in vitro* dos compostos fenólicos derivados de plantas, em geral, o CAPÍTULO 1 deste trabalho permitiu consolidar algumas características gerais por meio de dados da literatura. O estrato córneo e o sebo são fatores importantes de retenção destes compostos e a flexibilidade, o número de ligações de hidrogênio, o volume e o padrão de substituição são características que indicam a facilidade com que eles se translocam através da pele. A solubilidade do composto ou do extrato no veículo influencia o seu perfil de difusão, e a presença de um promotor de permeação não necessariamente o auxilia neste processo. A viscosidade do veículo e a micro ou nanoencapsulação dos extratos ou compostos isolados também influenciam os resultados, em geral oferecendo efeitos de liberação controlada e maior retenção cutânea. Ainda, o tipo de solvente presente no extrato também pode modular a forma com que seus compostos difundem pela pele. Desta forma, os testes de permeação cutânea *in vitro* são uma forma de triagem relevante no desenvolvimento de um produto envolvendo os fenólicos de origem vegetal.

Especificamente no que compete ao piceatanol e ao maracujá, destaca-se que a extração da torta desengordurada de sementes pela técnica de MAE permitiu, conforme indicado no CAPÍTULO 2, a obtenção de um extrato com características físico-químicas distintas das de um extrato preparado por refluxo. Além de uma coloração mais clara, o extrato preparado por MAE apresentou um teor mais elevado de piceatanol em menor tempo, bem como um perfil químico distinto do extrato obtido por refluxo como indicado na análise por infusão direta no espectrômetro de massas. Como MAE é uma técnica possivelmente escalonável, este trabalho abre caminhos para uma avaliação da viabilidade técnica-econômica-ambiental do processo de produção do extrato para se verificar a real possibilidade de sua implementação industrial com vistas a agregar valor à cadeia produtiva do maracujá por meio de um subproduto pouco explorado atualmente.

Apesar das características positivas do extrato, ele se mostrou instável quando incluído diretamente em uma formulação espessada com agente polimérico e tensoativo não iônico, mesmo nas presenças do extrato de jambu e dos filtros solares. Ambos os extratos, inclusive, foram totalmente incompatíveis com filtros solares inorgânicos. Neste sentido, para viabilizar o extrato deste trabalho como produto, é necessário considerar uma reformulação da base ou a encapsulação do ativo, de

modo que se alcance um produto com tempo de prateleira adequado. Abre-se, portanto, uma vertente farmacotécnica de trabalho sobre o extrato de maracujá obtido por MAE. Embora emulsões sejam uma das formas cosméticas mais comuns para produtos fotoprotetores, outras bases como os manteigas e bastões, ou mesmo o uso de outros componentes em uma emulsão, podem vir a constituir um produto viável.

Por fim, mesmo diante das instabilidades, este trabalho permitiu observar que o piceatanol na formulação base foi capaz de atingir o equivalente de derme na membrana Strat-M® e que, na presença do extrato de jambu ou dos filtros solares orgânicos, o ativo alcança camadas ainda mais profundas, mas não o suficiente para alcançar o líquido coletor da célula de Franz, corroborando o que foi observado por UHPLC-PAD e o predito *in silico*. O extrato de jambu, portanto, atuou como um promotor para o piceatanol na condição testada. Este trabalho trouxe as primeiras informações para eventuais futuros desenvolvimentos utilizando o extrato de semente de maracujá rico em piceatanol para fins dermocosméticos. Atenta-se que, respeitadas as legislações pertinentes e realizados os ensaios de eficácia e segurança necessários, este extrato segue com grande potencial de se tornar um novo ativo cosmético em consonância com as tendências de desenvolvimento de formulações com compostos naturais e com maior responsabilidade ambiental e social.

REFERÊNCIAS

REFERÊNCIAS

1. Mutha RE, Tatiya AU, and Surana SJ. Flavonoids as natural phenolic compounds and their role in therapeutics: an overview. Future Journal of Pharmaceutical Sciences 2021 7:1. 2021;7(1):1–13.

2. Dai J and Mumper RJ. Plant Phenolics: Extraction, Analysis and Their Antioxidant and Anticancer Properties. Molecules. 2010;15(10):7313.

3. Zhang Y, Cai P, Cheng G, and Zhang Y. A Brief Review of Phenolic Compounds Identified from Plants: Their Extraction, Analysis, and Biological Activity: https://doi.org/101177/1934578X211069721. 2022;17(1).

4. Ali Redha A. Review on Extraction of Phenolic Compounds from Natural Sources Using Green Deep Eutectic Solvents. J Agric Food Chem. 2021;69(3):878–912.

5. Schimek K, Hsu HH, Boehme M, Kornet JJ, Marx U, Lauster R, Pörtner R, and Lindner G. Bioengineering of a Full-Thickness Skin Equivalent in a 96-Well Insert Format for Substance Permeation Studies and Organ-On-A-Chip Applications. Bioengineering (Basel). 2018;5(2).

6. Aljuffali I, Hsu C-Y, Lin Y-K, and Fang J-Y. Cutaneous Delivery of Natural Antioxidants: The Enhancement Approaches. Curr Pharm Des. 2015;21(20):2745–57.

7. Cordova-Gomez M, Galano A, and Alvarez-Idaboy JR. Piceatannol, a better peroxyl radical scavenger than resveratrol. RSC Adv. 2013;3(43):20209–18.

8. Matsui Y, Sugiyama K, Kamei M, Takahashi T, Suzuki T, Katagata Y, and Ito T. Seeking a new anti-skin-aging material: Piceatannol and its derivatives from passion fruit (passiflora edulis) seed. *ACS Symposium Series*, Vol 1129. American Chemical Society; 2013.

9. Godic A, Poljšak B, Adamic M, and Dahmane R. The role of antioxidants in skin cancer prevention and treatment. Oxid Med Cell Longev. 2014;2014.

10. Papaccio F, D'arino A, Caputo S, and Bellei B. Focus on the Contribution of Oxidative Stress in Skin Aging. Antioxidants 2022, Vol 11, Page 1121. 2022;11(6):1121.

11. Zou W, Ramanathan R, Urban S, Sinclair C, King K, Tinker R, and Bansal V. Sunscreen testing: A critical perspective and future roadmap. TrAC Trends in Analytical Chemistry. 2022;157:116724.

12. Moniz T, Costa Lima SA, and Reis S. Human skin models: From healthy to disease-mimetic systems; characteristics and applications. Br J Pharmacol. 2020;177(19):4314–29.

13. Neupane R, Boddu SHS, Renukuntla J, Babu RJ, and Tiwari AK. Alternatives to Biological Skin in Permeation Studies: Current Trends and Possibilities. Pharmaceutics 2020, Vol 12, Page 152. 2020;12(2):152.

14. File:Skin layers.svg - Wikimedia Commons. Disponível em https://commons.wikimedia.org/wiki/File:Skin_layers.svg.

15. Brown TM and Krishnamurthy K. Histology, Dermis. StatPearls. 2022.

16. File:502 Layers of epidermis.jpg - Wikimedia Commons. Disponível em https://commons.wikimedia.org/wiki/File:502_Layers_of_epidermis.jpg.

17. Kolarsick PAJ, Kolarsick MA, and Goodwin C. Anatomy and Physiology of the Skin. J Dermatol Nurses Assoc. 2011;3(4):203–13.

18. Ministério da Saúde-MS Agência Nacional de Vigilância Sanitária-ANVISA.

19. DSM apresenta novo ingrediente de fotoproteção para o mercado brasileiro de filtros solares. Disponível em https://cosmeticinnovation.com.br/dsm-apresenta-novo-ingrediente-de-fotoprotecao-para-o-mercado-brasileiro-de-filtros-solares/.

20. TRIS-BIPHENYL TRIAZINE (NANO) – Ingredient - COSMILE Europe. Disponível em https://cosmileeurope.eu/inci/detail/17188/tris-biphenyl-triazine-nano/.

21. Stiefel C and Schwack W. Photoprotection in changing times - UV filter efficacy and safety, sensitization processes and regulatory aspects. Int J Cosmet Sci. 2015;37(1):2–30.

22. Teng H and Chen L. Polyphenols and bioavailability: an update. https://doi.org/101080/1040839820181437023. 2019;59(13):2040–51.

23. Eran Nagar E, Okun Z, and Shpigelman A. Digestive fate of polyphenols: updated view of the influence of chemical structure and the presence of cell wall material. Curr Opin Food Sci. 2020;31:38–46.

24. Catalkaya G, Venema K, Lucini L, Rocchetti G, Delmas D, Daglia M, De Filippis A, Xiao H, Quiles JL, Xiao J, *et al*. Interaction of dietary polyphenols and gut microbiota: Microbial metabolism of polyphenols, influence on the gut microbiota, and implications on host health. Food Front. 2020;1(2):109–33.

25. Sorrenti V, Fortinguerra S, Caudullo G, and Buriani A. Deciphering the Role of Polyphenols in Sports Performance: From Nutritional Genomics to the Gut Microbiota toward Phytonutritional Epigenomics. Nutrients 2020, Vol 12, Page 1265. 2020;12(5):1265.

26. Ashwin K, Pattanaik AK, and Howarth GS. Polyphenolic bioactives as an emerging group of nutraceuticals for promotion of gut health: A review. Food Biosci. 2021;44:101376.

27. Herranz-López M and Barrajón-Catalán E. Antioxidants and skin protection. Antioxidants. 2020;9(8):1–4.

28. Yang B, Dong Y, Wang F, and Zhang Y. Nanoformulations to Enhance the Bioavailability and Physiological Functions of Polyphenols. Molecules 2020, Vol 25, Page 4613. 2020;25(20):4613.

29. Vitorino C, Sousa J, and Pais A. Overcoming the Skin Permeation Barrier: Challenges and Opportunities. Curr Pharm Des. 2015;21(20):2698–712.

30. Silva G C. Identificação de flavonoides, quantificação de isovitexina e avaliação das atividades antioxidante e fotoprotetora *in vitro* dos extratos metanólico e glicólico de *Passiflora coccinea* (AUBL.). Dissertação de mestrado apresentada ao Instituto de Química da Unicamp para obtenção do título de mestra em Química na área de Química Analítica. 2012.

31. Gomes A, Aguiar L, Ferraz R, Teixeira C, and Gomes P. The Emerging Role of Ionic Liquid-Based Approaches for Enhanced Skin Permeation of Bioactive Molecules: A

Snapshot of the Past Couple of Years. International Journal of Molecular Sciences 2021, Vol 22, Page 11991. 2021;22(21):11991.

32. Rodrigues Leite-Silva V, Mandelli De Almeida M, Fradin A, Grice JE, and Roberts MS. Expert Review of Dermatology Delivery of drugs applied topically to the skin. 2014.doi:10.1586/edm.12.32

33. Anna Malinowska M, Billet K, Drouet S, Munsch T, Unlubayir M, Tungmunnithum D, Giglioli-Guivarc'h N, Hano C, and Lanoue A. Grape Cane Extracts as Multifunctional Rejuvenating Cosmetic Ingredient: Evaluation of Sirtuin Activity, Tyrosinase Inhibition and Bioavailability Potential. Molecules. 2020;25(9):2203.

34. Li N, Wu X, Jia W, Zhang MC, Tan F, and Zhang J. Effect of ionization and vehicle on skin absorption and penetration of azelaic acid. Drug Dev Ind Pharm. 2012;38(8):985–94.

35. Kurul E and Hekimoglu S. Skin permeation of two different benzophenone derivatives from various vehicles. Int J Cosmet Sci. 2001;23(4):211–8.

36. Wang S, Wang W, Gao Z, and Wang W. Theoretical study on the mechanism of reaction between piceatannol and hydroxyl radical. Gaodeng Xuexiao Huaxue Xuebao/Chemical Journal of Chinese Universities. 2015;36(8):1588–95.

37. Lu Y, Wang A, Shi P, Zhang H, and Li Z. Quantum Chemical Study on the Antioxidation Mechanism of Piceatannol and Isorhapontigenin toward Hydroxyl and Hydroperoxyl Radicals. PLoS One. 2015;10(7):e0133259.

38. Hosoda R, Hamada H, Uesugi D, Iwahara N, Nojima I, Horio Y, and Kuno A. Different antioxidative and antiapoptotic effects of piceatannol and resveratrol. Journal of Pharmacology and Experimental Therapeutics. 2021;376(3):385–96.

39. Matsui Y, Sugiyama K, Kamei M, Takahashi T, Suzuki T, Katagata Y, and Ito T. Extract of passion fruit (Passiflora edulis) seed containing high amounts of piceatannol inhibits melanogenesis and promotes collagen synthesis. J Agric Food Chem. 2010;58(20):11112–8.

40. Maruki-Uchida H, Kurita I, Sugiyama K, Sai M, Maeda K, and Ito T. The protective effects of piceatannol from passion fruit (Passiflora edulis) seeds in UVB-irradiated keratinocytes. Biol Pharm Bull. 2013;36(5):845–9.

41. Lee CH, Yang H, Park JHY, Kim JE, and Lee KW. Piceatannol, a metabolite of resveratrol, attenuates atopic dermatitis by targeting Janus kinase 1. Phytomedicine. 2022;99.

42. Piotrowska H, Kucinska M, and Murias M. Biological activity of piceatannol: Leaving the shadow of resveratrol. Mutation Research/Reviews in Mutation Research. 2012;750(1):60–82.

43. Arakaki DG, dos Santos VS, de Melo EP, Pereira H, Figueiredo PS, Cortês MR, Carollo CA, de Oliveira LCS, Tschinkel P, Reis F, *et al*. Canjiqueira Fruit: Are We Losing the Best of It? Foods. 2020;9(4).

44. Galeano E A V, Arantes S D, Padovan M P, da Costa A N, Vinagre D O V B, Dias, R Q Cadeia produtiva do Maracujá no Espírito Santo. Instituto Capixaba de Pesquisa, Assistência Técnica e Extensão Rural (INCAPER). Disponível em

https://biblioteca.incaper.es.gov.br/digital/bitstream/item/4436/1/Livro-cadeiaprodutivadomaracuja-Incaper.pdf.

45. Empresa Brasileira de Pesquisa Agropecuária (EMBRAPA). Cultivares de maracujá com alta produtividade e resistência a doenças e aproveitamento de resíduos da indústria atraem público nacional e estrangeiro - Portal Embrapa. Disponível em https://www.embrapa.br/busca-de-noticias/-/noticia/7223316/cultivares-de-maracuja-com-alta-produtividade-e-resistencia-a-doencas-e-aproveitamento-de-residuos-da-industria-atraem-publico-nacional-e-estrangeiro.

46. Empresa Brasileira de Pesquisa Agropecuária (EMBRAPA). Desempenho das exportações brasileiras. Disponível em http://www.cnpmf.embrapa.br/Base_de_Dados/index_pdf/dados/brasil/maracuja/b8_maracuja.pdf.

47. Linares-Devia N, Arrieta-Escobar J, Baena Y, Orjuela A, and Osorio C. Development and Characterization of Emulsions Containing Ground Seeds of Passiflora Species as Biobased Exfoliating Agents. Cosmetics 2022, Vol 9, Page 15. 2022;9(1):15.

48. Sebrae. O cultivo e o mercado do maracujá - Sebrae. Disponível em https://sebrae.com.br/sites/PortalSebrae/artigos/o-cultivo-e-o-mercado-do-maracuja,108da5d3902e2410VgnVCM100000b272010aRCRD.

49. Pan ZH, Ning DS, Fu YX, Li DP, Zou ZQ, Xie YC, Yu LL, and Li LC. Preparative Isolation of Piceatannol Derivatives from Passion Fruit (Passiflora edulis) Seeds by High-Speed Countercurrent Chromatography Combined with High-Performance Liquid Chromatography and Screening for α-Glucosidase Inhibitory Activities. J Agric Food Chem. 2020;68(6):1555–62.

50. Liu M, Li X, Liu Q, Xie S, Zhu F, and Chen X. Preparative isolation and purification of 12 main antioxidants from the roots of Polygonum multiflorum Thunb. using high-speed countercurrent chromatography and preparative HPLC guided by 1,1′-diphenyl-2-picrylhydrazyl-HPLC. J Sep Sci. 2020;43(8):1415–22.

51. Li H, Zhao Z, Xiouras C, Stefanidis GD, Li X, and Gao X. Fundamentals and applications of microwave heating to chemicals separation processes. Renewable and Sustainable Energy Reviews. 2019;114:109316.

52. Poole CF. Milestones in the development of liquid-phase extraction techniques. *Liquid-Phase Extraction*. Elsevier; 2020.

53. Chemat F, Rombaut N, Meullemiestre A, Turk M, Perino S, Fabiano-Tixier AS, and Abert-Vian M. Review of Green Food Processing techniques. Preservation, transformation, and extraction. Innovative Food Science and Emerging Technologies. 2017;41:357–77.

54. Petigny L, Périno S, Minuti M, Visinoni F, Wajsman J, and Chemat F. Simultaneous Microwave Extraction and Separation of Volatile and Non-Volatile Organic Compounds of Boldo Leaves. From Lab to Industrial Scale. Int J Mol Sci. 2014;15(5):7183–98.

55. Garcia-Garcia G, Rahimifard S, Matharu AS, and Dugmore TIJ. Life-Cycle Assessment of Microwave-Assisted Pectin Extraction at Pilot Scale. ACS Sustain Chem Eng. 2019;7(5):5167–75.

56. Radoiu M, Kaur H, Bakowska-Barczak A, and Splinter S. Microwave-Assisted Industrial Scale Cannabis Extraction. Technologies 2020, Vol 8, Page 45. 2020;8(3):45.

57. Kawakami S, Kinoshita Y, Maruki-Uchida H, Yanae K, Sai M, and Ito T. Piceatannol and its metabolite, isorhapontigenin, Induce SIRT1 expression in THP-1 human monocytic cell line. Nutrients. 2014;6(11):4794–804.

58. Uchida-Maruki H, Inagaki H, Ito R, Kurita I, Sai M, and Ito T. Piceatannol Lowers the Blood Glucose Level in Diabetic Mice. Biol Pharm Bull. 2015;38(4):629–33.

59. Sano S, Sugiyama K, Ito T, Katano Y, and Ishihata A. Identification of the strong vasorelaxing substance scirpusin B, a dimer of piceatannol, from passion fruit (Passiflora edulis) seeds. J Agric Food Chem. 2011;59(11):6209–13.

60. Lourith N and Kanlayavattanakul M. Antioxidant Activities and Phenolics of Passiflora edulis Seed Recovered from Juice Production Residue. J Oleo Sci. 2013;62(4):235–40.

61. da Silva MV, de Oliveira F dos S, Demczuk Junior B, Haminiuk CWI, and Visentainer JV. Hygroscopic equilibrium of microencapsulated extract of passion fruit seed and its effect on the antioxidant capacity. J Food Process Eng. 2018;41(1):e12597.

62. Oliveira DA, Angonese M, Ferreira SRS, and Gomes CL. Nanoencapsulation of passion fruit by-products extracts for enhanced antimicrobial activity. Food and Bioproducts Processing. 2017;104:137–46.

63. Oliveira DA, Angonese M, Gomes C, and Ferreira SRS. Valorization of passion fruit (Passiflora edulis sp.) by-products: Sustainable recovery and biological activities. Journal of Supercritical Fluids. 2016;111:55–62.

64. Viganó J, Zabot GL, and Martínez J. Supercritical fluid and pressurized liquid extractions of phytonutrients from passion fruit by-products: Economic evaluation of sequential multi-stage and single-stage processes. Journal of Supercritical Fluids. 2017;122:88–98.

65. de Santana FC, de Oliveira Torres LR, Shinagawa FB, de Oliveira e Silva AM, Yoshime LT, de Melo ILP, Marcellini PS, and Mancini-Filho J. Optimization of the antioxidant polyphenolic compounds extraction of yellow passion fruit seeds (Passiflora edulis Sims) by response surface methodology. J Food Sci Technol. 2017;54(11):3552–61.

66. Maruki-Uchida H, Morita M, Yonei Y, and Sai M. *Effect of Passion Fruit Seed Extract Rich in Piceatannol on the Skin of Women: A Randomized, Placebo-Controlled, Double-Blind Trial*. Vol 64 2018.

67. Setoguchi Y, Oritani Y, Ito R, Inagaki H, Maruki-Uchida H, Ichiyanagi T, and Ito T. Absorption and metabolism of piceatannol in rats. J Agric Food Chem. 2014;62(12):2541–8.

68. Jarosova V, Vesely O, Marsik P, Jaimes JD, Smejkal K, Kloucek P, and Havlik J. Metabolism of stilbenoids by human faecal microbiota. Molecules. 2019;24(6).

69. Dai Y, Lim JX, Yeo SCM, Xiang X, Tan KS, Fu JH, Huang L, and Lin HS. Biotransformation of Piceatannol, a Dietary Resveratrol Derivative: Promises to Human Health. Mol Nutr Food Res. 2020;64(2).

70. Jusuf NK, Putra IB, and Dewi NK. Antibacterial Activity of Passion Fruit Purple Variant (Passiflora edulis Sims var. edulis) Seeds Extract Against Propionibacterium acnes . Clin Cosmet Investig Dermatol. 2020;Volume 13:99–104.

71. Zhu T, Fang F, Sun D, Yang S, Zhang X, Yu X, and Yang L. Piceatannol Inhibits P. acnes–Induced Keratinocyte Proliferation and Migration by Downregulating Oxidative Stress and the Inflammatory Response. Inflammation. 2020;43(1):347–57.

72. Hung C-F, Lin Y-K, Huang Z-R, and Fang J-Y. Delivery of Resveratrol, a Red Wine Polyphenol, from Solutions and Hydrogels in the Skin. Biol Pharm Bull. 2008;31(5):955–62.

73. Eskandari M, Rembiesa J, Startaitė L, Holefors A, Valančiūtė A, Faridbod F, Ganjali MR, Engblom J, and Ruzgas T. Polyphenol-hydrogen peroxide reactions in skin: *In vitro* model relevant to study ROS reactions at inflammation. Anal Chim Acta. 2019;1075:91–7.

74. Gupta R, Dwadasi BS, Rai B, and Mitragotri S. Effect of Chemical Permeation Enhancers on Skin Permeability: In silico screening using Molecular Dynamics simulations. Scientific Reports 2019 9:1. 2019;9(1):1–11.

75. Carpentieri-Rodrigues LN, Zanluchi JM, and Grebogi IH. Percutaneous absorption enhancers: mechanisms and potential. Brazilian Archives of Biology and Technology. 2007;50(6):949–61.

76. File:Acmella Oleracea - പല്ലുവേദനച്ചെടി.JPG - Wikimedia Commons. Disponível em https://commons.wikimedia.org/wiki/File:Acmella_Oleracea_-_%E0%B4%AA%E0%B4%B2%E0%B5%8D%E0%B4%B2%E0%B5%81%E0%B4%B5%E0%B5%87%E0%B4%A6%E0%B4%A8%E0%B4%9A%E0%B5%8D%E0%B4%9A%E0%B5%86%E0%B4%9F%E0%B4%BF.JPG.

77. Barbosa AF, de Carvalho MG, Smith RE, and Sabaa-Srur AUO. Spilanthol: Occurrence, extraction, chemistry and biological activities. Brazilian Journal of Pharmacognosy. 2016;26(1):128–33.

78. Stepniowska, A; Cieplinska, P; Fac, W; Gorska J. Review Article: Selected Alkaloids Used in the Cosmetics Industry. 2021;72(2).

79. Savic S, Petrovic S, Savic S, and Cekic N. Identification and photostability of N-alkylamides from Acmella oleracea extract. J Pharm Biomed Anal. 2021;195.

80. Ye Y, Li Y, Bi T, and Jiang L. Improvement of urban eye skin in Chinese female by supramolecular retinol plus acmella oleracea extract-containing product. J Cosmet Dermatol. 2021.doi:10.1111/JOCD.14621

81. Wu LC, Fan NC, Lin MH, Chu IR, Huang SJ, Hu CY, and Han SY. Anti-inflammatory effect of spilanthol from Spilanthes acmella on murine macrophage by down-regulating LPS-induced inflammatory mediators. J Agric Food Chem. 2008;56(7):2341–9.

82. Abeysiri GRPI, Dharmadasa RM, Abeysinghe DC, and Samarasinghe K. Screening of phytochemical, physico-chemical and bioactivity of different parts of Acmella oleraceae Murr. (Asteraceae), a natural remedy for toothache. Ind Crops Prod. 2013;50:852–6.

83. Abeysinghe DC, Wijerathne SMNK, and Dharmadasa RM. Secondary Metabolites Contents and Antioxidant Capacities of Acmella Oleracea Grown under Different Growing Systems. World J Agric Res. 2014;2(4):163–7.

84. Paulraj J, Govindarajan R, and Palpu P. The Genus Spilanthes Ethnopharmacology, Phytochemistry, and Pharmacological Properties: A Review. Adv Pharmacol Sci. 2013;2013:22.

85. Moro SD de S, de Oliveira Fujii L, Teodoro LFR, Frauz K, Mazoni AF, Esquisatto MAM, Rodrigues RAF, Pimentel ER, and de Aro AA. Acmella oleracea extract increases collagen content and organization in partially transected tendons. Microsc Res Tech. 2021.doi:10.1002/jemt.23809

86. Stein R, Berger M, Santana de Cecco B, Mallmann LP, Terraciano PB, Driemeier D, Rodrigues E, Beys-da-Silva WO, and Konrath EL. Chymase inhibition: A key factor in the anti-inflammatory activity of ethanolic extracts and spilanthol isolated from Acmella oleracea. J Ethnopharmacol. 2021;270:113610.

87. De Spiegeleer B, Boonen J, Malysheva S V., Mavungu JD Di, De Saeger S, Roche N, Blondeel P, Taevernier L, and Veryser L. Skin penetration enhancing properties of the plant N-alkylamide spilanthol. J Ethnopharmacol. 2013;148(1):117–25.

88. Formulações Cosméticas: tendências, desafios e inovação. Disponível em https://www.talkscience.com.br/industria-cosmetica/formulacoes-cosmeticas-tendencias-desafios-e-inovacao.

89. Sunscreen: How to Help Protect Your Skin from the Sun | FDA. Disponível em https://www.fda.gov/drugs/understanding-over-counter-medicines/sunscreen-how-help-protect-your-skin-sun.

90. BRASIL. Agência Nacional de Vigilância Sanitária (ANVISA). Guia de estabilidade de produtos cosméticos. Disponível em http://portal.anvisa.gov.br/documents/106351/107910/Guia+de+Estabilidade+de+Produtos+Cosm%C3%A9ticos/49cdf34c-b697-4af3-8647-dcb600f753e2.

91. Cosmetic Toiletry and Fragrance Association (CTFA), COLIPA. Cosmetics Europe: guidelines on stability testing of cosmetic products. 2004.

92. A Indústria de Higiene Pessoal, Perfumaria e Cosméticos Essencial para o Brasil FEV 2023.

93. Bom S, Jorge J, Ribeiro HM, and Marto J. A step forward on sustainability in the cosmetics industry: A review. J Clean Prod. 2019;225:270–90.

94. Dini I and Laneri S. The New Challenge of Green Cosmetics: Natural Food Ingredients for Cosmetic Formulations. Molecules 2021, Vol 26, Page 3921. 2021;26(13):3921.

95. BRASIL. Ministério da Agricultura e Pecuária (MAPA). O que são Produtos Orgânicos? Disponível em https://www.gov.br/agricultura/pt-br/assuntos/sustentabilidade/organicos/o-que-sao-produtos-organicos.

96. Bagade SB and Patil M. Recent Advances in Microwave Assisted Extraction of Bioactive Compounds from Complex Herbal Samples: A Review. https://doi.org/101080/1040834720191686966. 2019;51(2):138–49.

97. Li Y, Radoiu M, Fabiano-Tixier AS, and Chemat F. From laboratory to industry: Scale-up, quality, and safety consideration for microwave-assisted extraction. Food Engineering Series. 2013;207–29.

98. Ciriminna R, Carnaroglio D, Delisi R, Arvati S, Tamburino A, and Pagliaro M. Industrial Feasibility of Natural Products Extraction with Microwave Technology. ChemistrySelect. 2016;1(3):549–55.

99. Radoiu M and Mello A. Technical advances, barriers, and solutions in microwave—assisted technology for industrial processing. Chemical Engineering Research and Design. 2022;181:331–42.

100. BRASIL. Agência Nacional de Vigilância Sanitária (ANVISA). Formulário de Fitoterápicos 2ª EDIÇÃO. 2021.

101. Navarro-Orcajada S, Conesa I, Vidal-Sánchez FJ, Matencio A, Albaladejo-Maricó L, García-Carmona F, and López-Nicolás JM. Stilbenes: Characterization, bioactivity, encapsulation and structural modifications. A review of their current limitations and promising approaches. Crit Rev Food Sci Nutr. 2022.doi:10.1080/10408398.2022.2045558

102. Latva-Mäenpää H, Wufu R, Mulat D, Sarjala T, Saranpää P, and Wähälä K. Stability and photoisomerization of stilbenes isolated from the bark of norway spruce roots. Molecules. 2021;26(4):1036.

103. Savic S, Petrovic S, Savic S, and Cekic N. Identification and photostability of N-alkylamides from Acmella oleracea extract. J Pharm Biomed Anal. 2021;195:113819.

104. Hoang HT, Moon JY, and Lee YC. Natural Antioxidants from Plant Extracts in Skincare Cosmetics: Recent Applications, Challenges and Perspectives. Cosmetics 2021, Vol 8, Page 106. 2021;8(4):106.

105. Taofiq O, Heleno SA, Calhelha RC, Fernandes IP, Alves MJ, Barros L, González-Paramás AM, Ferreira ICFR, and Barreiro MF. Phenolic acids, cinnamic acid, and ergosterol as cosmeceutical ingredients: Stabilization by microencapsulation to ensure sustained bioactivity. Microchemical Journal. 2019;147:469–77.

106. Bazana MT, Codevilla CF, and de Menezes CR. Nanoencapsulation of bioactive compounds: challenges and perspectives. Curr Opin Food Sci. 2019;26:47–56.

107. Katakam LNR, Dongala T, and Ettaboina SK. Novel stability indicating UHPLC method development and validation for simultaneous quantification of hydrocortisone acetate, pramoxine hydrochloride, potassium sorbate and sorbic acid in topical cream formulation. Talanta Open. 2020;1:100004.

108. Papageorgiou S, Varvaresou A, Panderi I, Giannakou M, Spiliopoulou C, and Athanaselis S. Development and validation of a reversed-phase high-performance liquid chromatographic method for the quantitation and stability of α-lipoic acid in cosmetic creams. Int J Cosmet Sci. 2020;42(3):221–8.

109. Arce FJ, Asano N, See GL, Itakura S, Todo H, and Sugibayashi K. Usefulness of Artificial Membrane, Strat-M®, in the Assessment of Drug Permeation from Complex Vehicles in Finite Dose Conditions. Pharmaceutics. 2020;12(2).

110. Haq A, Goodyear B, Ameen D, Joshi V, and Michniak-Kohn B. Strat-M® synthetic membrane: Permeability comparison to human cadaver skin. Int J Pharm. 2018;547(1–2):432–7.

111. Medrano-padial C, Prieto AI, Puerto M, and Pichardo S. Toxicological Evaluation of Piceatannol, Pterostilbene, and ε-Viniferin for Their Potential Use in the Food Industry: A Review. Foods. 2021;10(3).

ANEXOS

ANEXO I

Permissões para reprodução de figuras e tabelas

ACS Publications
Most Trusted. Most Cited. Most Read.

Review on Extraction of Phenolic Compounds from Natural Sources Using Green Deep Eutectic Solvents

Author: Ali Ali Redha
Publication: Journal of Agricultural and Food Chemistry
Publisher: American Chemical Society
Date: Jan 1, 2021

PERMISSION/LICENSE IS GRANTED FOR YOUR ORDER AT NO CHARGE

This type of permission/license, instead of the standard Terms and Conditions, is sent to you because no fee is being charged for your order. Please note the following:

- Permission is granted for your request in both print and electronic formats, and translations.
- If figures and/or tables were requested, they may be adapted or used in part.
- Please print this page for your records and send a copy of it to your publisher/graduate school.
- Appropriate credit for the requested material should be given as follows: "Reprinted (adapted) with permission from {COMPLETE REFERENCE CITATION}. Copyright {YEAR} American Chemical Society." Insert appropriate information in place of the capitalized words.
- One-time permission is granted only for the use specified in your RightsLink request. No additional uses are granted (such as derivative works or other editions). For any uses, please submit a new request.

If credit is given to another source for the material you requested from RightsLink, permission must be obtained from that source.

BACK CLOSE WINDOW

Sunscreen testing: A critical perspective and future roadmap

Author: Wenyue Zou,Rajesh Ramanathan,Sylvia Urban,Craig Sinclair,Kerryn King,Rick Tinker,Vipul Bansal
Publication: TrAC Trends in Analytical Chemistry
Publisher: Elsevier
Date: December 2022

JOHN WILEY AND SONS LICENSE
TERMS AND CONDITIONS

Aug 04, 2023

This Agreement between Unicamp -- Gisláine Silva ("You") and John Wiley and Sons ("John Wiley and Sons") consists of your license details and the terms and conditions provided by John Wiley and Sons and Copyright Clearance Center.

License Number	5602120451336
License date	Aug 04, 2023
Licensed Content Publisher	John Wiley and Sons
Licensed Content Publication	International Journal of Cosmetic Science
Licensed Content Title	Photoprotection in changing times – UV filter efficacy and safety, sensitization processes and regulatory aspects
Licensed Content Author	C. Stiefel, W. Schwack
Licensed Content Date	Oct 28, 2014
Licensed Content Volume	37
Licensed Content Issue	1
Licensed Content Pages	29
Type of use	Dissertation/Thesis
Requestor type	University/Academic

Format	Print and electronic
Portion	Figure/table
Number of figures/tables	1
Will you be translating?	No
Title	ESTUDO DA INTERAÇÃO ENTRE OS EXTRATOS DA SEMENTE DO MARACUJÁ (PASSIFLORA EDULIS) E DAS PARTES AÉREAS DE JAMBU (SPILANTHES ACMELLA) EM FORMULAÇÕES FOTOPROTETORAS TÓPICAS: ESTABILIDADE E PERMEAÇÃO CUTÂNEA
Institution name	Unicamp
Expected presentation date	Oct 2023
Order reference number	0001
Portions	Table 1
Requestor Location	Unicamp Rua Eng Augusto Figueiredo 437 Campinas, SP 13045603 Brazil Attn: Unicamp
Publisher Tax ID	EU826007151
Total	0.00 USD

Terms and Conditions

TERMS AND CONDITIONS

This copyrighted material is owned by or exclusively licensed to John Wiley & Sons, Inc. or one of its group companies (each a"Wiley Company") or handled on behalf of a society with which a Wiley Company has exclusive publishing rights in relation to a particular work (collectively "WILEY"). By clicking "accept" in connection with completing this licensing transaction, you agree that the following terms and conditions apply to this transaction (along with the billing and payment terms and conditions established by the Copyright Clearance Center Inc., ("CCC's Billing and Payment terms and conditions"), at the time that you opened your RightsLink account (these are available at any time at http://myaccount.copyright.com).

Terms and Conditions

- The materials you have requested permission to reproduce or reuse (the "Wiley Materials") are protected by copyright.
- You are hereby granted a personal, non-exclusive, non-sub licensable (on a stand-alone basis), non-transferable, worldwide, limited license to reproduce the Wiley Materials for the purpose specified in the licensing process. This license, **and any CONTENT (PDF or image file) purchased as part of your order,** is for a one-time use only and limited to any maximum distribution number specified in the license. The first instance of republication or reuse granted by this license must be completed within two years of the date of the grant of this license (although copies prepared before the end date may be distributed thereafter). The Wiley Materials shall not be used in any other manner or for any other purpose, beyond what is granted in the license. Permission is granted subject to an appropriate acknowledgement given to the author, title of the material/book/journal and the publisher. You shall also duplicate the copyright notice that appears in the Wiley publication in your use of the Wiley Material. Permission is also granted on the understanding that nowhere in the text is a previously published source acknowledged for all or part of this Wiley Material. Any third party content is expressly excluded from this permission.
- With respect to the Wiley Materials, all rights are reserved. Except as expressly granted by the terms of the license, no part of the Wiley Materials may be copied, modified, adapted (except for minor reformatting required by the new Publication), translated, reproduced, transferred or distributed, in any form or by any means, and no derivative works may be made based on the Wiley Materials without the prior permission of the respective copyright owner.**For STM Signatory Publishers clearing permission under the terms of the STM Permissions Guidelines only, the terms of the license are extended to include subsequent editions and for editions in other languages, provided such editions are for the work as a whole in situ and does not involve the separate exploitation of the permitted figures or extracts,** You may not alter, remove or suppress in any manner any copyright, trademark or other notices displayed by the Wiley Materials. You may not license, rent, sell, loan, lease, pledge, offer as security, transfer or assign the Wiley Materials on a stand-alone basis, or any of the rights granted to you hereunder to any other person.
- The Wiley Materials and all of the intellectual property rights therein shall at all times remain the exclusive property of John Wiley & Sons Inc, the Wiley Companies, or their respective licensors, and your interest therein is only that of having possession of and the right to reproduce the Wiley Materials pursuant to Section 2 herein during the continuance of this Agreement. You agree that you own no right, title or interest in or to the Wiley Materials or any of the intellectual property rights therein. You shall have no rights hereunder other than the license as provided for above in Section 2. No right, license or interest to any trademark, trade name, service mark or other branding ("Marks") of WILEY or its licensors is granted hereunder, and you agree that you shall not assert any such right, license or interest with respect thereto

- NEITHER WILEY NOR ITS LICENSORS MAKES ANY WARRANTY OR REPRESENTATION OF ANY KIND TO YOU OR ANY THIRD PARTY, EXPRESS, IMPLIED OR STATUTORY, WITH RESPECT TO THE MATERIALS OR THE ACCURACY OF ANY INFORMATION CONTAINED IN THE MATERIALS, INCLUDING, WITHOUT LIMITATION, ANY IMPLIED WARRANTY OF MERCHANTABILITY, ACCURACY, SATISFACTORY QUALITY, FITNESS FOR A PARTICULAR PURPOSE, USABILITY, INTEGRATION OR NON-INFRINGEMENT AND ALL SUCH WARRANTIES ARE HEREBY EXCLUDED BY WILEY AND ITS LICENSORS AND WAIVED BY YOU.
- WILEY shall have the right to terminate this Agreement immediately upon breach of this Agreement by you.
- You shall indemnify, defend and hold harmless WILEY, its Licensors and their respective directors, officers, agents and employees, from and against any actual or threatened claims, demands, causes of action or proceedings arising from any breach of this Agreement by you.
- IN NO EVENT SHALL WILEY OR ITS LICENSORS BE LIABLE TO YOU OR ANY OTHER PARTY OR ANY OTHER PERSON OR ENTITY FOR ANY SPECIAL, CONSEQUENTIAL, INCIDENTAL, INDIRECT, EXEMPLARY OR PUNITIVE DAMAGES, HOWEVER CAUSED, ARISING OUT OF OR IN CONNECTION WITH THE DOWNLOADING, PROVISIONING, VIEWING OR USE OF THE MATERIALS REGARDLESS OF THE FORM OF ACTION, WHETHER FOR BREACH OF CONTRACT, BREACH OF WARRANTY, TORT, NEGLIGENCE, INFRINGEMENT OR OTHERWISE (INCLUDING, WITHOUT LIMITATION, DAMAGES BASED ON LOSS OF PROFITS, DATA, FILES, USE, BUSINESS OPPORTUNITY OR CLAIMS OF THIRD PARTIES), AND WHETHER OR NOT THE PARTY HAS BEEN ADVISED OF THE POSSIBILITY OF SUCH DAMAGES. THIS LIMITATION SHALL APPLY NOTWITHSTANDING ANY FAILURE OF ESSENTIAL PURPOSE OF ANY LIMITED REMEDY PROVIDED HEREIN.
- Should any provision of this Agreement be held by a court of competent jurisdiction to be illegal, invalid, or unenforceable, that provision shall be deemed amended to achieve as nearly as possible the same economic effect as the original provision, and the legality, validity and enforceability of the remaining provisions of this Agreement shall not be affected or impaired thereby.
- The failure of either party to enforce any term or condition of this Agreement shall not constitute a waiver of either party's right to enforce each and every term and condition of this Agreement. No breach under this agreement shall be deemed waived or excused by either party unless such waiver or consent is in writing signed by the party granting such waiver or consent. The waiver by or consent of a party to a breach of any provision of this Agreement shall not operate or be construed as a waiver of or consent to any other or subsequent breach by such other party.
- This Agreement may not be assigned (including by operation of law or otherwise) by you without WILEY's prior written consent.
- Any fee required for this permission shall be non-refundable after thirty (30) days from receipt by the CCC.
- These terms and conditions together with CCC's Billing and Payment terms and conditions (which are incorporated herein) form the entire agreement between you and WILEY concerning this licensing transaction and (in the absence of fraud) supersedes all prior agreements and representations of the parties, oral or written. This Agreement may not be amended except in writing signed by both parties. This Agreement shall be

ANEXO II

Comprovante de cadastro da pesquisa no sistema de gestão do patrimônio genético (SisGen) permitindo acesso às sementes de maracujá para fins de pesquisa

Ministério do Meio Ambiente
CONSELHO DE GESTÃO DO PATRIMÔNIO GENÉTICO
SISTEMA NACIONAL DE GESTÃO DO PATRIMÔNIO GENÉTICO E DO CONHECIMENTO TRADICIONAL ASSOCIADO

Comprovante de Cadastro de Acesso
Cadastro nº AE5774B

A atividade de acesso ao Patrimônio Genético, nos termos abaixo resumida, foi cadastrada no SisGen, em atendimento ao previsto na Lei nº 13.123/2015 e seus regulamentos.

Número do cadastro:	**AE5774B**
Usuário:	**UNICAMP**
CPF/CNPJ:	**46.068.425/0001-33**
Objeto do Acesso:	**Patrimônio Genético**
Finalidade do Acesso:	**Pesquisa**

Espécie

Passiflora edulis

Título da Atividade:	**Extratos de maracujá**

Equipe

Gislaine Correa da Silva	**UNICAMP**
Carla Beatriz Grespan Bottoli	**UNICAMP**

Data do Cadastro:	**07/04/2020 16:33:24**
Situação do Cadastro:	**Concluído**

Conselho de Gestão do Patrimônio Genético
Situação cadastral conforme consulta ao SisGen em **16:33** de **07/04/2020**.

SISTEMA NACIONAL DE GESTÃO DO PATRIMÔNIO GENÉTICO E DO CONHECIMENTO TRADICIONAL ASSOCIADO - SISGEN

ANEXO III

Comprovante de cadastro da pesquisa no sistema de gestão do patrimônio genético (SisGen) permitindo acesso às partes aéreas de jambu para fins de pesquisa

Ministério do Meio Ambiente
CONSELHO DE GESTÃO DO PATRIMÔNIO GENÉTICO
SISTEMA NACIONAL DE GESTÃO DO PATRIMÔNIO GENÉTICO E DO CONHECIMENTO TRADICIONAL ASSOCIADO

Comprovante de Cadastro de Acesso
Cadastro nº AE903BD

A atividade de acesso ao Patrimônio Genético, nos termos abaixo resumida, foi cadastrada no SisGen, em atendimento ao previsto na Lei nº 13.123/2015 e seus regulamentos.

Número do cadastro:	**AE903BD**
Usuário:	**UNICAMP**
CPF/CNPJ:	**46.068.425/0001-33**
Objeto do Acesso:	**Patrimônio Genético**
Finalidade do Acesso:	

☑ **Pesquisa Científica** ☐ **Bioprospecção** ☐ **Desenvolvimento Tecnológico**

Espécie
Achyrocline satureioides
Cordia verbenacea
Acmella oleracea

Título da Atividade: **Avaliação da atividade de extratos vegetais nativos**

Equipe	
Rodney Alexandre Ferreira Rodrigues	**UNICAMP**
José Cláudio Klier Monteiro Filho	**unicamp**
Carla Beatriz Grespan Bottoli	**unicamp**
Gisláine Correa da Silva	**unicamp**

Data do Cadastro: **12/09/2018 10:42:28**
Situação do Cadastro: **Concluído**

Conselho de Gestão do Patrimônio Genético
Situação cadastral conforme consulta ao SisGen em **10:51** de **13/09/2018**.

SISTEMA NACIONAL DE GESTÃO DO PATRIMÔNIO GENÉTICO E DO CONHECIMENTO TRADICIONAL ASSOCIADO - SISGEN

ANEXO IV

Autorização para republicação do artigo Passion fruit seed extract enriched in piceatannol nesta tese (Capítulo 2)

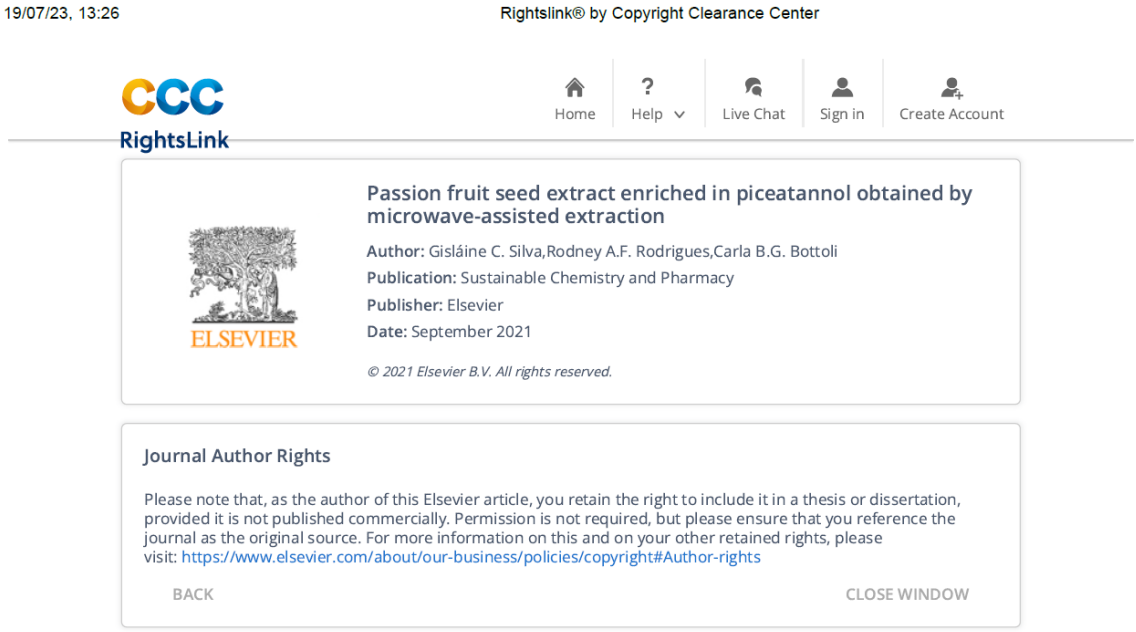

19/07/23, 13:26 Rightslink® by Copyright Clearance Center

CCC RightsLink

Home | Help | Live Chat | Sign in | Create Account

ELSEVIER

Passion fruit seed extract enriched in piceatannol obtained by microwave-assisted extraction

Author: Gisláine C. Silva,Rodney A.F. Rodrigues,Carla B.G. Bottoli

Publication: Sustainable Chemistry and Pharmacy

Publisher: Elsevier

Date: September 2021

© 2021 Elsevier B.V. All rights reserved.

Journal Author Rights

Please note that, as the author of this Elsevier article, you retain the right to include it in a thesis or dissertation, provided it is not published commercially. Permission is not required, but please ensure that you reference the journal as the original source. For more information on this and on your other retained rights, please visit: https://www.elsevier.com/about/our-business/policies/copyright#Author-rights

BACK CLOSE WINDOW

ANEXO V

DECLARAÇÃO

As cópias dos documentos de minha autoria ou de minha coautoria, já publicados ou submetidos para publicação em revistas científicas ou anais de congressos sujeitos a arbitragem, que constam da minha Dissertação/Tese de Mestrado/Doutorado, intitulada "ESTUDO DA INTERAÇÃO ENTRE OS EXTRATOS DA SEMENTE DO MARACUJÁ (*PASSIFLORA EDULIS*) E DAS PARTES AÉREAS DE JAMBU (*SPILANTHES ACMELLA*) EM FORMULAÇÕES FOTOPROTETORAS TÓPICAS: ESTABILIDADE E PERMEAÇÃO CUTÂNEA" não infringem os dispositivos da Lei nº 9.610/98, nem o direito autoral de qualquer editora.

Campinas, 05 de outubro de 2023

Gisláine Correa da Silva
R.G. nº 43.574.661-3 SSP/SP

Carla Beatriz Grespan Bottoli
RG nº 5.977.307- 0 SSP/PR